NASA TECHNICAL REPORT

NASA TR R-309

NASA TR R-309

PARAMETRIC ANALYSIS OF MICROWAVE AND LASER SYSTEMS FOR COMMUNICATION AND TRACKING—A SUMMARY

by F. Kalil

Goddard Space Flight Center
Greenbelt, Md.

NATIONAL AERONAUTICS AND SPACE ADMINISTRATION • WASHINGTON, D. C. • APRIL 1969

PARAMETRIC ANALYSIS OF MICROWAVE AND LASER SYSTEMS FOR COMMUNICATION AND TRACKING—A SUMMARY

By F. Kalil

Goddard Space Flight Center
Greenbelt, Md.

NATIONAL AERONAUTICS AND SPACE ADMINISTRATION

For sale by the Clearinghouse for Federal Scientific and Technical Information
Springfield, Virginia 22151 – CFSTI price $3.00

ABSTRACT

This document, a condensed and modified version of a contractor study (Reference 1), is a comparative analysis of laser and microwave telecommunication systems for space applications. Parametric families of curves are presented that give the weights and telecommunications capabilities of spaceborne communication systems. These curves permit the mission planner and designer to compare various systems and select the one that best meets their requirements. A sample case demonstrates the use of these curves. The sample calculation and concluding remarks point out the advantages of a computerized method that uses the calculus of maxima and minima for selecting the optimum spaceborne communication system configuration that can provide the specified information rate for the least spaceborne weight penalty and/or cost. Reference 1 presents detailed information and supporting data that have been used to draw the parametric graphs in the report. In addition, Reference 1 contains the details, and demonstrates the use of, the method previously mentioned.

CONTENTS

PARAMETRIC ANALYSIS OF MICROWAVE AND LASER SYSTEMS FOR COMMUNICATION AND TRACKING—A SUMMARY

by
F. Kalil
Goddard Space Flight Center

INTRODUCTION

Present NASA space vehicles employ radio frequencies almost exclusively—especially in the VHF, UHF, and S-band spectra—for telecommunications with the earth. In addition, the C-band is used to a large extent for tracking. In some rare cases (e.g., Beacon Explorers B, C, GEOS A, GEOS B, D1-C, and D1-D), ground laser beams are reflected from spaceborne corner reflectors to determine the range of the spacecraft. Rapid advances in the laser state of the art and growing demands for larger communication rates have stimulated interest in the feasibility of CW laser telecommunications for other space applications. Hence, in August 1965, a study began involving a comparative analysis of microwave and laser space telecommunication systems. A fundamental objective of the study was to provide the mission planner and designer with reference data (weight, volume, reliability, and costs), supplementary material, and a method for selecting the system (microwave or optical) which best suits his requirements.

The mission planner and designer frequently must make trade-offs among such spacecraft parameters as power consumption, transmitter power output, antenna size, overall spaceborne communication system weight, and downlink communication rate. Generally, it is desirable to have the lightest spaceborne communication system practicable for a given downlink communication rate. Some other factors that are beyond the scope of this report but which the mission planner and designer must consider are

1. Booster availability, payload, capability, and costs;
2. Type and amount of spaceborne experimental equipment; and
3. Tracking and communications requirements.

In the case of tracking and communication requirements, relevant or related considerations include

1. Availability and/or costs of ground support facilities,
2. Availability, reliability, weight, and size of qualified spaceborne components, subsystems, and systems; and
3. Mission coverage, i.e., the amount of time that the spacecraft can make contact with the ground station.

Furthermore the designer must be aware that much work must be done to make the optical systems operational, particularly in developing space-qualified hardware, improving the lifetime expectancy of the lasers, solving the problem of acquisition and tracking associated with the very narrow laser beams, and gaining a better understanding of atmospheric effects and statistical cloud distribution.

This report presents, in a readily usable and primarily graphical form, two of the more important parameters of interest to the mission planner and designer: the spaceborne weight and the operational capabilities (bandwidths and signal-to-noise ratios) of the more promising systems for communicating high data rates to the ground. The uplink is not considered because, theoretically, ground stations are not hampered by limitations on transmitter power, weight, and volume; hence they can transmit whatever power is necessary. However, the spacecraft, which has constraints on payload weight, volume, and power, frequently must transmit large amounts of experimental data in a relatively short time—as in the case of the Lunar Orbiters, with their downlink RF bandwidths of 3 MHz and a baseband of 310 kHz. The four "most promising" carrier frequencies considered in this report are

1. S-band ($f = 2.3$ GHz, $\lambda = 13$ cm),
2. X-band ($f = 10$ GHz, $\lambda = 3$ cm),
3. Infrared ($f = 2.83 \times 10^{13}$ Hz, $\lambda = 10.6\mu$),
4. Visible ($f = 5.66 \times 10^{14}$ Hz, $\lambda = 0.53\mu$).

These were chosen on the basis of practical considerations such as sky noise; system noise temperature; antenna size, tolerance, and gain as a function of carrier frequency; atmospheric attenuation; coherence length of the atmosphere; and the availability of laser oscillators. For these frequencies, the overall spaceborne communication system weight (less the power supply weight, which is tabulated independently) is plotted against the communication system capability for various power supply output power, communication ranges (distances), transmitter aperture (antenna) diameters, and ground system characteristics.

In this report, the communication system capability is taken to be the product of signal quality (generally, available signal-power-to-noise-power ratio) and signal quantity (bandwidth or bit rate) because this permits subsequent trade-offs between signal quality and signal quantity. Separate graphs give the bit error probability

as a function of signal quality for both RF and optical systems, and for various types of modulation. Also, separate graphs are used to compare the signal quality, after conversion from digital to analog form, for various types of modulation and analog source signal sampling rates. This is done in order to make this report as versatile and useful as possible for selecting a system for a given purpose.

The communication ranges selected in this report are 10^8 to 10^{10} km, which is characteristic of planetary distances, and 10^4 to 10^6 km, which is characteristic of earth-synchronous orbits and lunar distances. The choices of communication ranges, carrier frequencies, and ground facilities are summarized in Table 1.

In summary, the parametric families of curves and tables presented in this report permit the mission planner and designer to make a quick evaluation of the capabilities, size, power requirements, and spaceborne weights of several types of communication systems (S-band, X-band, IR, and visible) for earth-moon and planetary missions. These curves also allow the designer to make trade-offs among such parameters as

1. Spaceborne communication system weight,
2. Downlink signal quality such as analog $(S/N)_{out}$ or bit error probability for various types of modulation,
3. Downlink signal quantity such as base bandwidth or bit rate,
4. Spaceborne transmitter antenna or aperture size, and
5. Power supply requirements (power output, dimensions, and weight).

The report also briefly summarizes some existing and some projected space programs and goals in order to give the reader a broader perspective regarding space telecommunications requirements. Detailed supporting information (including theory and references) is given in Reference 1.

SPACE PROGRAM GOALS AND TELECOMMUNICATIONS SYSTEM REQUIREMENTS

Mission objectives directly influence the selection of the spaceborne communication system and its subsystems. For instance, the mission duration, including flight times, has a direct bearing on the system and subsystem lifetime requirements. Also, the distance from the sun largely dictates the type of power supply to be used. When this distance is too large, the solar panels become relatively ineffective, and other types of power sources, such as nuclear power supplies must be considered.

Table 1

Summary of Communication Ranges, Carrier Frequencies, and Ground Facilities Selected for this Study.

Communication Range	Carrier Frequency	Ground Facility	
		Type of Equipment	Comments or Reason for Choice
Planetary distances, 10^8 to 10^{10} km	S-band (2.3 GHz)	210-ft (64m) diam antenna, DSIF	Best available, i.e., highest gain at S-band and lowest system noise temperature
	X-band (10 GHz)	120-ft (36.5m) haystack antenna	Best available; highest gain at X-band
	Infrared (λ = 10.6μ)	4m receiver aperture diam with heterodyne detection	Not available, but best or largest feasible for heterodyne detection, because max coherence length of atmosphere is estimated to be ~4m at this wavelength.* Also, heterodyne detection is best because no suitable detectors with gain are available.
	Visible (λ = 0.53μ)	10m, effective receiver aperture diam with direct detection	Not available; proposed Aricebo-type photon "bucket" for direct detection. Heterodyne detection is not practical because coherence length of atmosphere is only about 0.03m at this wavelength.
Earth synchronous orbit and lunar distances	S-band and X-band (2.3 GHz and 10 GHz)	30-ft and 85-ft MSFN or STADAN facilities	Available for S-band; may need some modifications for X-band; larger gain antennas not necessary at these distances
	Infrared (λ = 10.6μ)	1m receiver aperture diam with heterodyne detection	A good, practical size, available, reflective type telescope; larger sizes not necessary
	Visible (λ = 0.53μ)	1m receiver aperture diam with direct detection	A good, practical size, available, reflective or refractive type telescope; larger sizes not necessary

*Under ideal conditions (see Reference 1). Recently some measurements are being undertaken at Mt. Palomar by Mr. J. Westphal of Cal. Tech. (Reference: Private correspondence with N. McAvoy, GSFC, and M. Shumate, JPL). Also NBS, Boulder, Colorado, is undertaking some measurements. Preliminary results seem to verify this estimate.

Technology Growth to Date

Figure 1 shows the projected growth of technology in some of the areas that pertain to manned space flight.

Communication Rate Requirements

Data transmission requirements depend on the number and type of experiments, the time interval during which information must be returned, and the information storage capacity. Typical instrument payloads for an unmanned planetary flyby spacecraft and their associated data outputs are listed in Table 2. The optimum

Table 2

Data Requirements for Planetary Flyby Scientific Payload.

Measurement	Sample Rate Per Hour	Bits Per Sample	Totals	
			Bits	Measurement Time Assumed
Interplanetary Measurements				
Solar magnetic field	2	32	5.6×10^5	1 yr
Solar wind	1	200	17.5×10^5	1 yr
Cosmic dust	1	100	8.8×10^5	1 yr
Lyman α line intensity	1	8	0.7×10^5	1 yr
X-ray flux	1	24	2.1×10^5	1 yr
Cosmic-ray flux	3	72	18.9×10^5	1 yr
Solar flare proton flux	1	24	2.1×10^5	1 yr
			55.7×10^5	
Planetary Flyby Measurements				
Magnetic field	60	16	1.0×10^4	10 hr
Trapped radiation	66	56	3.7×10^4	10 hr
Atmospheric composition	612	256	1.6×10^4	0.1 hr
Surface features	300	2.5×10^6	1.5×10^8	0.2 hr
			1.5×10^8	

transmission rate for returning these data must be determined by a trade-off among transmitter power, transmitting and receiving aperture size, information storage capacity, and reliability. Typical maximum data rate requirements for various types of information are listed in Table 3. Real-time television data rate requirements are plotted against bandwidth in Figure 2, with resolution as a parameter.

Table 3

Typical (PCM) Data Rate Requirements.

Type	Source Signal Bandwidth, f_m (i.e., baseband)	Representation, Bits/Sample n	Maximum Bit Rate ($B_{if} \doteq 2nf_m = R_B$)	Tolerable Error Rate
Scientific data	0 to 1 kHz	9	18 kbps	10^{-2}
Engineering data	0 to 1 kHz	7	14 kbps	10^{-2}
Command data			50 bps	10^{-5}
Teletype			75 bps	10^{-5}
Speech	0 to 4 kHz	5	40 kbps	10^{-3}
Real-time television (500 × 500-element picture)	15 Hz to 4 MHz	6	48 Mbps	10^{-3}
Picture transmission (500 × 500-element picture in 12.5 sec)	15 Hz to 10 kHz	6	120 kbps	10^{-3}

Flight Times and Mission Duration

Figure 3 depicts a typical earth-Mars trajectory with flight times. The total flight time from an earth-parking orbit to Mars intercept is 200 days. Table 4 gives a more detailed time history for this trajectory, which is a quick-look (patched conic) rather than an accurate, integrated trajectory. The symbols used in Table 4 are defined in Figure 4. Typical flight times to planets beyond Mars are shown in Figures 5 and 6.

Table 4

Earth-Mars Trajectory Data.

INJECTION: JUNE 11, 1971 JULIAN DATE: 2441114.2530768
MARS INTERCEPT: DEC. 28, 1971 JULIAN DATE: 2441314.25307083

D	H	M	V (km/sec)	γ (deg)	$\dot{r}$ (km/sec)	$\dot{r}$ (fps)	RFS (km)	RFE (km)	RFT (km)	RVE (deg)	RVS (deg)	RVT (deg)	ESVA (deg)
0	0	19.5	11.43	0	0	0	151,910,000	6,560	89,559,090	90.0	174.98	57.24	.0000057
0	12	19.5	3.65	83.76	3.6	11,800	152,200,000	188,980	88,893,130	126.4	174.88	57.39	0.055
1	0	19.5	3.386	86.26	3.3	10,850	152,120,000	339,360	88,272,720	123.56	174.74	57.55	0.104
5	0	0	3.154	89.26	3.1	10,200	152,830,000	1,440,290	83,508,450	120.62	172.34	58.68	0.437
10	0	0	3.157	89.47	3.1	10,200	153,880,000	2,802,310	77,769,030	120.51	167.97	59.94	0.793
20	0	0	3.264	87.10	3.2	10,500	156,470,000	5,565,43	67,092,870	121.59	158.46	61.88	1.281
30	0	0	3.514	84.51	3.5	11,500	159,630,000	8,472,660	57,583,510	123.29	148.99	62.94	1.415
40	0	0	4.027	82.59	4.0	13,100	163,270,000	11,685,300	49,313,550	125.398	139.85	63.04	1.141
50	0	0	4.803	83.47	4.8	15,800	167,260,000	15,456,000	42,301,130	127.38	131.08	62.14	0.4666
60	0	0	5.751	86.03	5.7	18.700	171,490,000	19,983,000	36,504,510	128.69	122.72	60.29	0.8095
70	0	0	6.899	88.76	6.8	22,400	175,870,000	25,429,000	31,818,830	129.15	114.76	57.69	2.394
80	0	0	8.164	85.21	8.1	26,700	180,300,000	31,923,000	28,079,890	128.62	107.19	54.61	4.429
90	0	0	9.492	80.72	9.3	30,600	184,710,000	39,483,000	25,070,110	127.12	99.98	51.42	6.873
100	0	0	10.93	76.23	10.6	35,000	189,020,000	48,118,000	22,596,590	124.82	93.10	48.44	9.707
110	0	0	12.39	71.72	11.8	38,800	193,190,000	57,797,000	20,421,790	121.81	86.52	45.90	12.899
120	0	0	13.88	67.57	12.8	42,100	197,160,000	68,426,000	18,386,490	118.22	80.22	43.90	16.42
130	0	0	15.42	63.54	13.6	44,700	200,898,000	79,940,000	16,369,220	114.18	74.15	42.45	20.24
140	0	0	16.94	59.59	14.5	47,600	204,360,000	92,220,000	14,294,380	109.76	68.31	41.49	24.33
150	0	0	18.46	55.90	15.3	50,300	207,530,000	105,150,000	12,124,180	105.02	62.65	40.94	28.66
160	0	0	20.01	52.29	15.9	52,300	210,380,000	118,600,000	9,848,820	100.04	57.15	40.68	33.20
170	0	0	21.52	48.73	16.0	52,500	212,899,000	132,440,000	7,477,420	94.85	51.80	40.62	37.93
180	0	0	23.01	45.36	16.4	54,000	215,060,000	146,510,000	5,030,370	89.48	46.57	40.63	42.80
190	0	0	24.50	45.03	16.3	53,600	216,870,000	160,680,000	2,533,420	83.96	41.44	40.54	47.81
200	0	0	24.74	39.69	15.7	51,700	218,290,000	174,810,000	12,831	78.31	36.40	56.06	52.90

Tables 5 and 6 summarize the sun, moon, and planet dimensions that are useful for quick-look mission analysis and for determining communication ranges. Table 6 also gives the semimajor axes of the planet orbits, which is the same as their mean distance from the sun.

Payload Weight Restrictions (Booster Capability)

Permissible payload for a given mission is dictated by launch vehicle capability; the allocation of that payload is determined by mission objectives. The fractional part of the payload comprised by the communication system will vary, depending on the required data rates and transmission range. Payload capabilities of present and projected launch vehicles are depicted in Figure 7.

Table 5

Sun, Moon, and Planet Constants.[1]

Body	Symbol	Radius (km)	Mass Ratio (planet to sun)[2]	Surface Gravity, earth = 1	Sidereal Rotation Period (mean solar time)	Inclination of Equator to Orbit
Sun	☉	696,000	1		$24^d.7$	
Mercury	☿	2,495	1.7×10^{-7}	0.37	88^d	?
Venus	♀	6,200	2.45×10^{-6}	0.87	30^d ?	32°
Earth	⊕	6,378 Eq. 6,357 Pol.	2.999×10^{-6}	1.00	$23^h 56^m 04^s$	23° 27′
Moon	☾	1,738	3.6822×10^{-8}	0.17	$27^d.32166$	6° 41′
Mars	♂	3,400	3.2326×10^{-7}	0.38	$24^h 37^m 23^s$	23° 59′
Jupiter	♃	71,350 Eq. 66,600 Pol.	9.5479×10^{-4}	2.72	$9^h 50^m 30^s$	3° 04′
Saturn	♄	60,400 Eq. 54,050 Pol.	2.8558×10^{-4}	1.19	$10^h 14^m$	26° 44′
Uranus	♅	~24,850	4.373×10^{-5}	~0.97	$10^h 49^m$	97° 55′
Neptune	♆	~26,500	5.1773×10^{-5}	~1.0 to 1.4	$\sim 14^h$	28° 48′
Pluto	♇	7,000?	3.03×10^{-7} ?	0.08?	$6^d.39$?	?

[1]Based on data given by: W. M. Smart, "Spherical Astronomy," Cambridge University Press, 1962, R. H. Battin, "Astronautical Guidance," McGraw-Hill Book Co., N. Y., 1964, C. W. Allen, "Astrophysical Quantities," 2nd Ed., Univ. of London, Athlone Press, 1963.

[2]Mass of sun = 1.99×10^{30} kg.

Table 6[6]

Elements of the Planetary Orbits for the Epoch 1960 January 1 G.M. Noon

Name	Semimajor Axis a (in astronomical units)	Eccentricity e	Sidereal Period (in tropical years)	Sidereal Mean Daily Motion, n	Synodic Period (in days)	Mean Orbital Speed (km/sec)
Mercury	0.387 099	0.205 627	0.240 85	4°.092 339	115.88	47.8
Venus	0.723 332	0.006 793	0.615 21	1.602 131	583.92	35.0
Earth	1.000 000	0.016 726	1.000 04	0.985 609	—	29.8
Mars	1.523 691	0.093 368	1.880 89	0.524 033	779.94	24.2
Jupiter	5.202 803	0.048 435	11.862 23	0.083 091	398.88	13.1
Saturn	9.538 843	0.055 682	29.457 72	0.033 460	378.09	9.7
Uranus	19.181 951	0.047 209	84.013 31	0.011 732	369.66	6.8
Neptune	30.057 779	0.008 575	164.793 45	0.005 981	367.48	5.4
Pluto	39.438 71	0.250 236	247.686	0.003 979	366.72	4.7

Name	Inclination i	Mean Longitude		
		Ascending Node θ	Perihelion ω	Epoch ϵ
Mercury	7°.003 99	47°.857 14	76°.833 09	222°.621 65
Venus	3.394 23	76.319 72	131.008 31	174.294 31
Earth	0.0	0.0	102.252 53	100.158 15
Mars	1.849 91	49.249 03	335.322 69	258.767 29
Jupiter	1.305 36	100.044 44	13.678 23	259.831 12
Saturn	2.489 91	113.307 47	92.264 47	280.671 35
Uranus	0.773 06	73.796 30	170.010 83	141.304 96
Neptune	1.773 75	131.339 80	44.273 95	216.940 90
Pluto	17.169 9	109.885 62	224.160 24	181.646 32

1. Mean distance from sun = semi-major axis
2. 1 A.U. = 149.59900 km
   1.852 km = 1 n. mi. (exact)
3. 1 tropical year = 365.2422 mean solar days
   1 sidereal year = 365.2564 mean solar days
   1 Julian year = 365.25 mean solar days
   1 mean solar day = 24 hrs. mean solar time (exact)
   = $24^h\ 3^m\ 56^s.556$ sidereal time
   1 sidereal day = $23^h\ 56^m\ 4^s.091$ mean solar time
4. Sidereal period = time interval between two successive returns of a planet to the same point among the stars as viewed from the sun.
5. Synodic period = interval between two successive times at which the heliocentric longitudes of the planet and earth are the same.
6. Based on data given by: W.M. Smart, "Spherical Astronomy," Cambridge University Press, 1962, R.H. Battin, "Astronautical Guidance," McGraw-Hill Book Co., N.Y., 1964, C.W. Allen, "Astrophysical Quantities," 2nd Ed., Univ. of London, Athlone Press, 1963.

Power Supplies

Tables 7 and 8 show the weights, dimensions, mission durations, and ratings at end of mission (power supply capabilities deteriorate in time). Typical mission durations, at the end of which the power supply ratings are referred, are included in these tables. The reasons for deterioration are beyond the scope of this report. Typically, however, solar panel degradation is largely caused by radiation and particle bombardment. The degradation of reactor and radioisotope thermoelectric supplies is caused in primarily by the thermal effects on the solid-state thermocouples (thermal-to-electric energy converters). Although this information is repeated later, it is included here because the choice of power supply is so closely linked with mission duration, distance from the sun, and payload weight restrictions.

SUMMARY OF SPACEBORNE COMMUNICATIONS SYSTEM – WEIGHTS AND CAPABILITIES

This section presents a parametric family of curves and tables that enables the mission planner and designer to make a quick evaluation of the capabilities, size, power requirements, and weights of the "most promising" types of spaceborne communication systems (S-band, X-band, IR, and visible) for earth-moon and planetary missions. For a given application (i.e., downlink communication rate, distance, and mission duration), these data (curves and tables) will allow the designer to make trade-offs among the following parameters:

1. Carrier frequency, ground system, and type of detection;
2. Spaceborne communication system weight;
3. Downlink signal quality such as analog signal $(S/N)_{out}$, or digital signal bit error probability for various types of modulation;
4. Downlink information rate such as basebandwidth or bit rate;
5. Spaceborne transmitter antenna or aperture size; and
6. Power supply requirements—power output, dimensions, and weight.

The communication ranges chosen are 10^8 to 10^{10} km and 10^4 to 10^6 km.

Choice of Carrier Frequency

The selection of carrier frequency is based on practical considerations of

1. Sky noise (background radiation),
2. System noise,
3. Antennas (ground and spaceborne)—practical sizes, tolerances, and gains as a function of carrier frequency,

Table 7

Electrical Power Supplies and Their Weights.

Probe Near:	Mercury				Venus				Earth				Mars				Jupiter		
Distance from Sun (km)	57.7×10^6				108×10^6				149×10^6				227×10^6				775×10^6		
Expected Communication Distance from Earth (km)	115 to 190×10^6 (1968)				40 to 190×10^6 (1970)				10^4				90 to 310×10^6 (1973)				600 to 890×10^6 (1973)		
Mission Duration (days)	82 to 152				72 to 210				30				118 to 260				450 to 1200+		
Power System Type / Power Output at End of Mission (watts)	Solar Photovoltaic	Solar Thermionic	Reactor Thermoelectric	Radioisotope Thermoelectric	Solar Photovoltaic	Solar Thermionic	Reactor Thermoelectric	Radioisotope Thermoelectric	Solar Photovoltaic	Fuel Cell	Reactor Thermoelectric	Radioisotope Thermoelectric	Solar Photovoltaic	Reactor Thermoelectric	Radioisotope Thermoelectric	Solar Photovoltaic	Reactor Thermoelectric	Radioisotope Thermoelectric
	Total Power System Weight (kilograms)																	
10	0.181	0.363		2.27	0.177	0.272		2.25	0.227	4.44		2.25	0.5		2.25	5.8		2.25
25	0.454	0.953		5.67	0.434	0.643		5.67	5.67	11.1		5.67	1.22		5.67	14.4		5.67
50	0.909	1.86		11.3	0.84	1.28		11.3	1.13	22.2		11.3	2.4		11.3	28.9		11.3
100	1.81	3.72		22.7	1.77	2.56		22.7	2.27	44.4		22.7	4.81		22.7	57.8		22.7
250	4.54	9.30		56.7	4.43	6.43		56.7	5.67	111		56.7	12.0		56.7	144		56.7
500	9.09	18.6	311	117.0	8.4	12.8	310	117.0	11.7	222	310	117.0	24.0	310	117.0	289	310	117.0
1000	18.1	37.2	375	227	17.7	25.6	376	227	22.7	444	376	227	48.1	375	227	577	375	227
2000	36.3	74.4	488		35.4	51.3	488		45.4	890	437		96.2	488		1155	488	
5000	90.9	186	1080		84	127	1075		113.2	2220	1080		240	1085		2880	1085	
7500	136.0	279	1625		133	193	1625		170	3330	1625		356	1625		4330	1625	
10000	181.0	372	1665		177	256	1665		227	4440	1665		481	1665		5790	1665	

Notes: 1. Assumes no batteries.
2. Power conditioning losses and weights not included.

Table 8

Electrical Power Supplies and Their Volume or Area.

Probe Near:	Mercury				Venus				Earth				Mars			Jupiter		
Distance from Sun (km)	57.7×10^6				108×10^6				149×10^6				227×10^6			775×10^6		
Expected Communication Distance from Earth (km)	115 to 190×10^6 (1968)				40 to 190×10^6 (1970)				10^4				90 to 310×10^6 (1973)			600 to 890×10^6 (1973)		
Mission Duration (days)	82 to 152				72 to 210				30				118 to 260			450 to 1200+		
Power System Type / Power Output at End of Mission (watts)	Solar Photovoltaic (area, cm^2)	Solar Thermionic (area, cm^2)	Reactor Thermoelectric (volume, cm^3)	Radioisotope Thermoelectric (volume, cm^3)	Solar Photovoltaic (area, cm^2)	Solar Thermionic (area, cm^2)	Reactor Thermoelectric (volume, cm^3)	Radioisotope Thermoelectric (volume, cm^3)	Solar Photovoltaic (area, cm^2)	Fuel Cell (volume, cm^3)	Reactor Thermoelectric (volume, cm^3)	Radioisotope Thermoelectric (volume, cm^3)	Solar Photovoltaic (area, cm^2)	Reactor Thermoelectric (volume, cm^3)	Radioisotope Thermoelectric (volume, cm^3)	Solar Photovoltaic (area, cm^2)	Reactor Thermoelectric (volume, cm^3)	Radioisotope Thermoelectric (volume, cm^3)
	Total Power System Volume (cm^3) or Area (cm^2)																	
10	559			0.858 $\times 10^4$	0.465 $\times 10^3$			0.858 $\times 10^4$	0.65 $\times 10^3$			0.858 $\times 10^4$	1.39 $\times 10^3$		0.858 $\times 10^4$	16.85 $\times 10^3$		0.858 $\times 10^4$
25	1400			2.28 $\times 10^4$	1.21 $\times 10^3$			2.28 $\times 10^4$	1.675 $\times 10^3$			2.28 $\times 10^4$	3.53 $\times 10^3$		2.28 $\times 10^4$	42.1 $\times 10^3$		2.28 $\times 10^4$
50	2700	837		4.56 $\times 10^4$	2.42 $\times 10^3$	2.42 $\times 10^3$		4.56 $\times 10^4$	3.35 $\times 10^3$			4.56 $\times 10^4$	6.98 $\times 10^3$		4.56 $\times 10^4$	84.1 $\times 10^3$		9.56 $\times 10^4$
100	5400	1580		9.13 $\times 10^4$	4.75 $\times 10^3$	4.82 $\times 10^3$		9.13 $\times 10^4$	6.63 $\times 10^3$			9.13 $\times 10^4$	13.95 $\times 10^3$		9.13 $\times 10^4$	168.5 $\times 10^3$		9.13 $\times 10^4$
250	13.4 $\times 10^3$	4000		22.7 $\times 10^4$	12 $\times 10^3$	12.1 $\times 10^3$		22.7 $\times 10^4$	16.55 $\times 10^3$			22.7 $\times 10^4$	34.8 $\times 10^3$		22.7 $\times 10^4$	421 $\times 10^3$		22.7 $\times 10^4$
500	26.8 $\times 10^3$	7.9 $\times 10^3$	45.8 $\times 10^4$	45.2 $\times 10^4$	23.9 $\times 10^3$	24.2 $\times 10^3$	45.8 $\times 10^4$	45.2 $\times 10^4$	33 $\times 10^3$		45.8 $\times 10^4$	45.2 $\times 10^4$	69.7 $\times 10^3$	45.8 $\times 10^4$	45.2 $\times 10^4$	841 $\times 10^3$	45.8 $\times 10^4$	45.2 $\times 10^4$
1000	53.5 $\times 10^3$	15.7 $\times 10^3$	92.5 $\times 10^4$	90.4 $\times 10^4$	47.6 $\times 10^3$	48.2 $\times 10^3$	92.5 $\times 10^4$	90.4 $\times 10^4$	66 $\times 10^3$		92.5 $\times 10^4$	90.4 $\times 10^4$	139.5 $\times 10^3$	92.5 $\times 10^4$	90.4 $\times 10^4$	1685 $\times 10^3$	92.5 $\times 10^4$	90.4 $\times 10^4$
2000	107.1 $\times 10^3$	31.4 $\times 10^3$	236 $\times 10^4$		95.6 $\times 10^3$	96.8 $\times 10^3$	236 $\times 10^4$		132 $\times 10^3$		236 $\times 10^4$		279 $\times 10^3$	236 $\times 10^4$		3370 $\times 10^3$	236 $\times 10^4$	
5000	268 $\times 10^3$	78.7 $\times 10^3$	790 $\times 10^4$		23.9 $\times 10^3$	242 $\times 10^3$	790 $\times 10^4$		330 $\times 10^3$		790 $\times 10^4$		699 $\times 10^3$	790 $\times 10^4$		8420 $\times 10^3$	790 $\times 10^4$	
7500	401 $\times 10^3$	118 $\times 10^3$	1450 $\times 10^4$		45.2 $\times 10^3$	363 $\times 10^3$	1450 $\times 10^4$		496 $\times 10^3$		1450 $\times 10^4$		1045 $\times 10^3$	1450 $\times 10^4$		12600 $\times 10^3$	1450 $\times 10^4$	
10000	535 $\times 10^3$	157 $\times 10^3$	2340 $\times 10^4$		477 $\times 10^3$	482 $\times 10^3$	2340 $\times 10^4$		660 $\times 10^3$		2340 $\times 10^4$		1395 $\times 10^3$	2340 $\times 10^4$		16850 $\times 10^3$	2340 $\times 10^4$	

Notes: 1. Assumes no batteries.
2. Power conditioning losses and volumes not included.

4. Atmospheric attenuation,
5. Coherence length of the atmosphere, and
6. Availability, power output, and efficiencies of transmitting sources (oscillators, power amplifiers, and lasers).

The most promising carrier frequencies presently are

1. S-band (f = 2.3 GHz, λ = 13 cm),
2. X-band (f = 10 GHz, λ = 3 cm),
3. Infrared (f = 2.83×10^{13} Hz, λ = 10.6μ, CO_2 laser), and
4. Visible (f = 5.66×10^{14} Hz, λ = 0.53μ, Nd^{3+} YAG laser with a lithium niobate frequency doubler).

For these carrier frequencies, Table 9 lists transmitter sources and some of their characteristics as used in the subsequent parametric analyses.

Choice of Ground Facilities and Type of Detection

Ground facilities for the microwave systems were chosen on the basis of the best available or most practical, whereas the optical systems were chosen on the basis of what is theoretically feasible and practically achievable. Table 1 summarizes the choice of ground facilities with comments and reasons for the choices. The "best" type of detection for the optical systems are also shown. Since heterodyne detection with a phase-lock loop to track the carrier is used commonly with microwave systems, it is not shown in the table.

Spaceborne Communications Systems – Weights and Capabilities

This portion of the report presents a condensed version of such parameters as spaceborne communication system weight, power supply requirements, antenna diameter, and capabilities of the most promising systems for communicating high information rates to the ground. In the graphs presented, the spaceborne communication system capability is the product of signal quality and signal quantity. For example, the signal quality might be the ratio of available signal power-to-noise power or the signal energy-to-noise power spectral density. The signal quantity (information rate) might be the bandwidth or the bit rate. In this part of the report, in which bandwidth is used in lieu of bit rate, the equivalent noise bandwidth of the receiver's IF stage is used. How this IF bandwidth relates to the basebandwidth, i.e., the frequency band occupied by the transmitted signal when first used to modulate a carrier, depends on the type of modulation used.

Table 9

Carrier Frequency, Spaceborne Transmitter Sources,[1] and Their Characteristics.

Carrier		Wave-length, λ	Type Osc.	Frequency Multiplication	Type of Power Amplifier	Power[2] Output (watts)	Efficiency (percent)	Band-width (percent)	Avail-able
Band	Frequency, f								
S-band	2.3 GHz	13 cm	Crystal	Yes	Solid-state	≤ 0.3	5 to 7	>10	Yes
				(probably solid state)	TWT	3	25 to 35	>10	Yes
						30	25 to 35		Yes
						300	estimated 30		No
X-band	10 GHz	3 cm	Crystal	Yes	Solid-state	≤ 0.3	estimated 3	>10	Yes
					TWT	3	25 to 35	>10	Yes
						30	25 to 35		Yes
						300	estimated 30		No
IR	2.83×10^{13} Hz	10.6μ	CO_2 laser	Not needed	Laser[3]	≤ 0.1	≥ 10		Yes
						1			Yes
						10			Yes
						100			Yes
Visible	5.66×10^{14} Hz	0.53μ	Nd^{3+} YAG	Lithium niobate frequency doubler	Laser[3]	≤ 0.01	~1		Yes
						0.1			Yes
						1			Yes
						10			Yes

[1] See Chapter 5, Reference 1, for further details on these and other transmitter sources. The sources listed here and their characteristics are limited to what was used herein in the analyses for the parametric curves.

[2] Characteristics of output power used in subsequent parametric analysis.

[3] Frequently for a space application the laser oscillator could provide adequate power without power amplification over the power ranges considered here.

The communication range equation used to compute the ratio C/N, received carrier-to-noise ratio (average power ratio), depends on the system, carrier frequency, and type of detection. These range equations and their limitations are summarized in Table 10 along with appropriate constants such as atmospheric transmissivity. Symbols are defined in Appendix A.

On the basis of these range equations and the subsystem weights given in Appendix B, the spaceborne communication system weight (less the power supply weight, which is tabulated independently—Table 7 versus the communications capability is depicted graphically in Figures 8a through 15d for the following cases.

1. Planetary missions

   a. Communication range (R) = 10^8 to 10^{10} km
   b. Power supply output (P_{BB}) = 1, 10, 100, and 1000w

2. Lunar and earth-synchronous orbital missions

   a. Communication range (R) = 10^4 to 10^6 km
   b. Power supply output = 10 mw, 100 mw, 1w, 10w

By interpolating between these graphs, the user can select the best system for his needs by trading off such factors as the following.

1. Signal quality,

$$\left(\frac{S}{N}\right)_{IF} \simeq \frac{E}{N_0} \begin{cases} \text{obtainable when matched-filter} \\ \text{detection is employed} \end{cases}$$

2. Signal quantity, $B_{IF} \simeq R_B$
3. Spaceborne communication system weight

This will be illustrated later by means of a sample calculation.

It should be pointed out that the system weights given in Figures 8a through 15d are assessments based on the best current knowledge (see Reference 1). For instance, the Surveyor and Lunar Orbiter spaceborne communication system weights and system capabilities correspond with the data shown. However, these curves must be updated as the state of the art progresses; for lightweight, low power, short range systems, the asymptotic limits of these curves have a larger percentage error. Also, when designing communications links between earth-orbiting satellites, a large disparity in Doppler shift, acquisition time, tracking rates, and solar background will affect the predicted system parameters and weights significantly.

Table 10

Communication Range Equations Used.[1]

Carrier	Range Equation and Comments
S-band (2.3 GHz)	$\frac{C}{N} \cdot B_{IF} = \frac{\pi^2}{16} \frac{P_T\, d_T^2\, d_R^2\, \eta_{a,T}\, \eta_{a,R}}{\lambda^2 R^2 k T\, L_T L_R} \tau_{atm}$, standard one-way range equation
X-band (10 GHz)	Same as above
IR ($\lambda = 10.6\mu$)	$\frac{C}{N} \cdot B_{IF} = \frac{\pi^2}{64} \frac{P_T\, d_T^2\, d_R^2}{R^2 \lambda h c} \tau_T \tau_R \tau_{atm} \eta_q$, heterodyne detection, where local oscillator power is large enough to swamp out (1) all quantum noise (shot noise) caused by signal, background, and dark current from photodetector which acts as a mixer, and (2) thermal noise. Note: This equation is equivalent to the above, except that $\eta_{a,T} \doteq \eta_{a,R} \doteq \frac{1}{2}$; $\tau_T = \frac{1}{L_T}$; $\tau_R = \frac{1}{L_R}$; while the noise power spectral density is hf_c, and the detector efficiency (η_q) is added.
Visible ($\lambda = 0.53\mu$)	$\mu_{S,B} = \frac{\eta_q P_c}{h f_c R_b}$ (signal photons/bit) out of photomultiplier. $\mu_{N,B} = \frac{\eta_q P_B}{h f_c R_B}$ (background noise photons/bit) out of photomultiplier. $P_c = \frac{\pi^2 P_T\, d_T^2\, d_{R,eff}^2\, \tau_T \tau_R \tau_a}{16 R^2 \lambda^2}$ {total signal power received on photomultiplier cathode. $P_B = \tau_a \tau_R \lambda_i \pi^2 \frac{d_R^2}{16} \theta_R^2 Q_B h f_c$ {background radiation power received on photomultiplier cathode.

[1] For definition of symbols, see Appendix A.

Table 10 (Continued)

Carrier	Range Equation and Comments
	$\left[\frac{C}{N}\right]_{\text{into } 2^{nd} \text{ det.}} = \frac{1}{2}\left[\frac{\mu_{S,B}}{1 + \frac{\mu_{N,B}}{\mu_{S,B}}}\right]$, for the case of direct detection using a cooled photomultiplier with large gain (i.e., thermal noise and photomultiplier dark current are negligible). $Q_B \tilde{=} 10^{16}$ photons - $sec^{-1}cm^{-2}$-micron-$steradian^{-1}$, = background photon spectral radiance at $\lambda = 0.53\mu$.

Notes: $\frac{C}{N} \doteq \frac{E}{N_0}$, when using a matched-filter receiver.

In practice, a 1-db degradation can be expected when nonideal matched filter receivers are used.

$B_{IF} = \frac{1}{\tau}$, required IF bandwidth,

τ = bit width in seconds,

$R_B = \frac{1}{\tau}$, bit rate in bps.

The spaceborne communication system weight given in Figures 8a through 15d include all subsystems weights except the power supply; they include the weights of the following:

1. Transmitter, including signal conditioner,
2. Modulator,
3. Antenna or telescope (structure, gimbals, driver motors, wiring, etc.),
4. Pointing or acquisition and tracking subsystem, and
5. Heat rejection system.

Modulation Systems Capabilities

This part of the report describes the capabilities of modulation systems and techniques in sufficient detail to enable the designer or mission planner to make a

choice of the modulation technique that best suits his requirements. Herein, the capability of a modulation technique is considered to be:

1. For digital systems—the probability (P_e) that there will be an erroneous bit at the output of the detector (demodulator) as a function of the predetection E/N_0 into the second detector, where E is the signal energy per bit, and N_0 is the noise power spectral density (one sided).
2. For analog systems—the enhancement factor, the factor relating the output S/N in the baseband to the predetection C/N.

Table 11 summarizes the probability of error expressions for various types of modulation techniques used in both optical and RF systems, and Figures 16 through 19 graphically depict how the P_e varies with:

1. E/N_0 in the case of RF and optical heterodyne detection systems.
2. $\mu_{s,b}$ and $\mu_{n,b}$, the average number of signal and noise photoelectrons per bit emitted by the photodetector in the case of a direct-detection optical system.

Table 12 provides expressions that show the bandwidth requirements and how the intelligence signal-to-noise power ratio at the receiver output is affected by the type of modulation for both the analog/uncoded and the digital/coded systems. The expressions are presented two ways:

1. In terms of the total signal-to-noise input power ratios and
2. In terms of the sideband signal-to-noise input power ratios.

This facilitates a comparison of the modulation techniques from the viewpoint of total received power requirements and signal-to-noise improvement with bandwidth. The expressions for the various modulation techniques are presented in the order of system effectiveness from the viewpoint of how effectively an increase in bandwidth improves the intelligence signal-to-noise power ratio out of the system. The PCM systems are the best from this viewpoint, although the wideband frequency modulation (WBFM) system is the best of the continuous (i.e., nonpulsed and noncoded) systems.

Figure 20 compares the FM analog modulation system with the PCM/PM (or PSK) digital systems on the basis of output $(S/N)_{out}$ versus the input $(C/N)_{IF}$, where

$\left(\frac{S}{N}\right)_{out}$ = average power ratio of the analog signal-to-noise ratio out of the receiver (after digital-to-analog conversion in the case of the digital system), and

Table 11

Probability of Error Expressions.

System	Detection Statistics	Expression
Optical PCM/IM (threshold detection)	Poisson	$P_e = \frac{1}{2}\left(1 + P_N^B - P_{SN}^B\right)$, where $P_N^B = \sum_{k\ N_t^B}^{\infty} \frac{\left(\frac{\mu_{N,B}}{L}\right)^k \exp\left[\left(\frac{\mu_{N,B}}{L}\right)\right]}{k!}$; $P_{SN}^B = \sum_{k\ N_t^B}^{\infty} \frac{(\mu_{S,B} + \mu_{N,B})^k \exp\left[-(\mu_{S,B} + \mu_{N,B})\right]}{k!}$, where N_t^B greatest integer value of k_t^B; $k_t^B = \frac{\mu_{S,B}}{\ln\left(1 + \frac{\mu_{S,B}}{\mu_{N,B}}\right)}$.
Radio PCM/AM (on-off key) (noncoherent detection) For optimum threshold setting	Gaussian	$P_e = \frac{1}{2}\left[1 - Q\left(\sqrt{\frac{2E}{N_0}}, b_0\right) + e^{-b_0^2/2}\right]$, where $Q(\cdot,\cdot)$ is the Marcum Q function, and $b_0 \simeq \sqrt{2 + \frac{E}{2N_0}}$ is the optimum threshold setting.
Radio PCM/AM (on-off key) (coherent detection)	Gaussian	$P_e = \frac{1}{2}\left(1 - \operatorname{erf}\sqrt{\frac{E}{4N_0}}\right)$
Optical PCM/PL	Poisson	$P_e = 1 - \exp\left[(\mu_{S,B} + \mu_{N,B})\right] \sum_{j=1}^{\infty}\left(\frac{2\mu_{S,B} + \frac{\mu_{N,B}}{2}}{\mu_{N,B}}\right)^{j/2} I_j\left[\sqrt{2\left(\mu_{S,B} + \frac{\mu_{N,B}}{2}\right)\mu_{N,B}}\right] + \frac{1}{2} I_0\left[\sqrt{2\left(m_{S,B} + \frac{\mu_{N,B}}{2}\right)\mu_{N,B}}\right]$.
Optical PCM/FM (heterodyne detection)	Gaussian	$P_e = \frac{1}{2}\exp\left[-\frac{1}{2}\left(\frac{S}{N}\right)_{IF}\right]$
Radio PCM/FM (FSK) (noncoherent detection)	Gaussian	$P_e = \frac{1}{2}\exp\left(-\frac{E}{2N_0}\right)$
Radio PCM/FM (CFSK) (coherent detection)	Gaussian	$P_e = \frac{1}{2}\left(1 - \operatorname{erf}\sqrt{\frac{E}{2N_0}}\right)$

Table 11 (Continued)

System	Detection Statistics	Expression
Radio PCM/PM (PSK) (coherent detection)	Gaussian	$P_e = \frac{1}{2}\left(1 - \text{erf}\sqrt{\frac{E}{N_0}}\right)$
Radio PCM/PM (ΔPSK) (differentially coherent detection)	Gaussian	$P_e = \frac{1}{2}\exp\left(-\frac{E}{N_0}\right)$
Optical PPM (threshold detection)	Poisson	$P_E' = \left(1 - \frac{P_{SN}^P}{LP_N^P}\right) + \left[\frac{\left(1 - P_N^P\right)^{L-1}}{LP_N^P}\right]\left(P_{SN}^P - P_N^P\right)$ where $P_N^P = \sum_{k=N_t}^{\infty} \frac{\left(\frac{\mu_{N,P}}{L}\right)^k \exp\left[-\left(\frac{\mu_{N,P}}{L}\right)\right]}{k!}$ $P_{SN}^P = \sum_{k=N_t^P}^{\infty} \frac{\left(\mu_{S,P} + \frac{\mu_{N,P}}{L}\right)^k \exp\left[-\left(\mu_{S,P} + \frac{\mu_{N,P}}{L}\right)\right]}{k!}$ N_t^P = greatest integer value of k_T^P $k_t^P = \frac{\mu_{S,P} + \ell n\,(L-1)}{\ell n\left(1 + \frac{L\mu_{S,P}}{\mu_{N,P}}\right)}$ L = no. of time slots in which signal photons are transmitted

$\left(\frac{C}{N}\right)_{IF}$ = average power ratio of the total input signal-to-noise ratio within the IF bandwidth, sometimes given as $(S/N)_{IF}$.

Figure 20 shows the effect of the FM modulation index (m_f) in the WBFM system, and the effect of n, the number of digital bits per sample, for the PCM/PM systems.

The FM analog and PCM/PM digital systems were chosen for Figure 20 because they are the best of the analog and digital coherent detection systems. For optical systems, in which the coherence length of the atmosphere precludes a large receiver aperture for coherent detection, thus necessitating direct detection, the PCM/PL system appears best (see the bit-error probability curves, Figures 16 through 19).

Table 12

Signal-to-Noise Ratios and Bandwidth Requirements.

System	Relation Between Input and Output S/N	IF Bandwidth Required, in Hz
Analog/uncoded systems AM-DSB	$(S/N)_{out} = \frac{m_a^2}{1 + \frac{m_a^2}{2}} \left(\frac{S_{in,\,total}}{N_0 B_{IF}}\right) = 2\left(\frac{S_{in,\,sidebands}}{N_0 B_{IF}}\right)$	$B_{IF} = 2f_m$, f_m = maximum signal frequency or basebandwidth $0 \le m_a \le 1$
AM-DSB/SC	$(S/N)_{out} = 2\left(\frac{S_{in,\,total}}{N_0 B_{IF}}\right) = 2\left(\frac{S_{in,\,sidebands}}{N_0 B_{IF}}\right)$	B_{IF} $2f_m$
AM-SSB/SC	$(S/N)_{out} = \left(\frac{S_{in,\,total}}{N_0 B_{IF}}\right) = \left(\frac{S_{in,\,sidebands}}{N_0 B_{IF}}\right)$	$B_{IF} = f_m$
NBFM	$(S/N)_{out} \cong 3m_f^2 \left(\frac{S_{in,\,total}}{N_0 B_{IF}}\right) \cong 6\left(\frac{S_{in,\,sidebands}}{N_0 B_{IF}}\right)$ for large $S/N \gtrsim 10$, i.e. above threshold	$B_{IF} \cong 2f_m$ $m_f \lesssim 0.6$
WBFM	$(S/N)_{out} = 3m_f^2 (m_f + 1)\left(\frac{S_{in,\,total}}{N_0 B_{IF}}\right) \cong \frac{3m_f^2 (m_f + 1)}{[1 - J_0^2(m_f)]}\left(\frac{S_{in,\,sidebands}}{N_0 B_{IF}}\right)$ for large $S/N \gtrsim 10$, i.e., above threshold	$B_{IF} \cong 2f_m (m_f + 1)$, Carson's Rule $m_f > 5$
PAM/AM	$(S/N)_{out} = m_a^2 \left(\frac{S_{in,\,total}}{N_0 B_{IF}}\right)$	B_{IF} $2f_m$ · (no. of channels)
PDM/AM or PPM/AM	$(S/N)_{out}$ $2m_a^2 t_0^2 B_{IF}^2 \left(\frac{S_{in\ total}}{N_0 B_{IF}}\right)$	B_{IF} $\frac{1}{t_r}$, t_r pulse rise time t_0 max. spacing between pulses.
All Coded/digital systems, such as PCM/AM, PCM/FM, PCM/PM, or PCM/PL	$(S/N_Q)_{out} = 2^{2n} - 1$ $(S/N_E)_{out} = \frac{1}{4P_e Q_e}$ - 1, $P_e = Q_e = 1$ $(S/N_R)_{out} = \frac{1}{\left(\frac{N_Q}{S}\right)_{out} + \left(\frac{N_E}{S}\right)_{out}} \quad \frac{S_{out}}{N_Q + N_E}$ } after digital-to-analog conversion	$B_{IF} = \frac{1}{\tau} \cdot R_B$, τ pulse width R_B bit rate, bps $R_B > 2nf_m$, n no of bits digital word N_Q quantization noise N_R resultant output noise caused by quantization and bit error noise N_E bit error noise P_E probability of a bit being interpreted incorrectly, P_e function of $(S/N)_{IF} = E_b/N_0$ and depends on type of modulation (see Table 14) Q_E probability of a bit being interpreted correctly

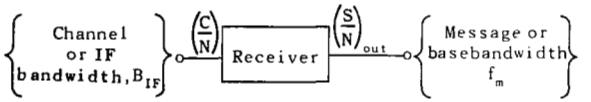

$\frac{C}{N} = \frac{S_{in,\,total}}{N_0 B_{IF}} = \left(\frac{S}{N}\right)_{IF}$

N_0 = noise power spectral density

$C = S_{in,\,total}$ = total received power (carrier plus sudebands) in the IF equivalent noise bandwidth, B_{IF}

C = unmodulated carrier power

Figure 21 (after J. W. Whelan, Reference 2) compares the FM analog and PCM/PM digital systems by presenting the ratio of the FM-to-PCM average transmitter powers required to provide a given output S/N ratio at threshold, for each of the threshold definitions. This figure also shows the ratio of the analog-to-digital system's required transmission bandwidths as a function of the output S/N ratio, as given by

$$\frac{BW_{FM}}{BW_{PCM}} = \frac{2f_m\left(m_f + 1\right)}{2f_m n} = \frac{m_f + 1}{n} .$$

These are the minimum bandwidths required to pass the significant carrier sidebands. In practice, wider bandwidths are required to allow for frequency instabilities such as Doppler shift and oscillator drift and to reduce distortion (see also S. C. Plotkin, Reference 3, who discusses this latter point in detail).

From Figure 21 it can be seen that the FM and PSK systems are quite comparable in terms of required transmission power in the range of output S/N ratios from about 15 to 40 db. Only at very high or very low output S/N ratios do the PSK and ΔPSK digital systems show a substantial power saving over the FM analog system. From the viewpoint of bandwidth requirements, the FM analog and PCM digital systems are quite comparable for output S/N ratios between 10 and 35 db, with the FM analog system having a slight advantage. However, for operation outside this range, the PCM digital systems have a considerable advantage because of the more efficient trade-off between S/N ratio and bandwidth in the PCM system as greater accuracy is demanded.

Figures 22, 23, and 24 show fundamental block diagrams for the following types of communication systems, including transmitter and receiver:

1. RF analog with heterodyne detection,
2. RF and/or optical digital with heterodyne detection,
3. Optical analog with heterodyne detection, and
4. Optical digital with direct detection.

Figure 23 shows how corrections for Doppler shifts can be made by means of a simple feedback circuit to control the local oscillator so as to have a constant IF carrier or center frequency and thus minimize the required IF bandwidth. Otherwise the IF bandwidth must be broadened to accept both the desired sideband signals and the Doppler shift. In this case, more noise $\left(N = N_0 B_{IF}\right)$ would be permitted to pass through the IF stage with a commensurate decrease in total signal

power-to-noise power ratio. The one-way Doppler shift is

$$\Delta f_{Doppler} = f_c \frac{\dot{r}}{c},$$

where $\dot{r}$ is the radial speed of the transmitter relative to the receiver, f_c is the carrier frequency, and c is the speed of light ($c = 3 \times 10^5$ km/sec). For planetary missions, for instance, the $\dot{r}$ could vary from 0 to 16 km/sec depending on what part of the trajectory the vehicle is in (see Table 4), so that

$\Delta f_{Doppler}$	Carrier
0 to $\sim 10^5$ Hz	S-band (f_c = 2.3 GHz)
0 to $\sim 5 \times 10^5$ Hz	X-band (f_c = 10 GHz)
0 to $\sim 1.6 \times 10^9$ Hz	IR ($\lambda_c = 10.6\mu$)
0 to $\sim 3 \times 10^{10}$ Hz	Visible ($\lambda_c = 0.53\mu$)

Thus, the advantage is apparent for using a local voltage-controlled oscillator to correct for Doppler shifts in a heterodyne detection system. Although this is difficult in an optical system, a frequency-modulated CW CO_2 laser system using a heterodyne receiver has been demonstrated. The transmitter and receiver were mounted on hilltops approximately 12 miles (~19 km) apart. At 4-MHz baseband-width, analog/uncoded, on a 30-MHz subcarrier, TV communication was demonstrated. The receiving aperture was an 8-inch mirror.

Figure 22 also shows a receiver preamplifier commonly used in RF systems and located as near the antenna feeds as practical to minimize receiver line losses. Because of their low noise figure, cooled parametric amplifiers or masers are commonly used as preamplifiers. Furthermore, the receiver lines from the antenna feed to the preamplifier may be cooled to reduce the effective system noise temperature.

Sample Calculation

Problem

Consider the following problem in which a Mars mission is being planned. The program manager specifies that real-time television (approximate commercial standard or 4-MHz source bandwidth—see Figure 2) is required in order to survey

the Mars surface with a Mars orbiter spacecraft. The mission and spacecraft are to be analogous to the Lunar Orbiter. Other data required are scientific and engineering type data (~2 kHz source bandwidth; see Table 3 for example). The spacecraft is payload-weight limited. To conserve payload weight, the overall spaceborne communication system weight is to be kept to a minimum. It will be assumed for this example that the following ground systems (Table 1 summarized here for convenience) be available to facilitate the selection of the lightest-weight communication system possible.

Carrier	Ground facility
S-band (f_c = 2.3 GHz)	210-ft (64m) antenna, DSIF
X-band (f_c = 10 GHz)	120-ft (36.5m) haystack antenna (MIT)
IR (λ_c = 10.6μ)	4m telescope, heterodyne detection rcvr
Visible (λ_c = 0.53μ)	10m, effective diameter "photon bucket" with direct detection rcvr

Solution

As stated earlier, the most efficient modulation techniques are FM for analog signal transmission, and PSK for digital signal transmission. Furthermore, as shown in Figure 23, the PSK system is comparable to the FM system at output S/N ratios between ~15 and 40 db, but that outside this range the PSK system is superior. It should be reemphasized that these comments pertain only to the case wherein the input $(C/N)_{IF}$ is above threshold for both definitions, and heterodyne detection is used. This applies to both optical and RF systems. However, in the case of laser/optical systems wherein the signal must traverse the atmosphere and the small coherence length of the atmosphere precludes the use of large receiver apertures with coherent detection, then direct detection with PCM/PL modulation is more desirable. With the best modulation technique(s) having been established, the required spaceborne communication system weight will now be examined.

At Mars distances, $R \cong 2 \times 10^8$ km, and based on the given requirements, the basebandwidth $f_m = 4 \times 10^6$ Hz. For the PCM system

$$R_B = 2n f_m = 48 \times 10^6 \text{ bps}, \quad \text{for} \quad n = 6,$$

and

$$B_{IF} \cong \frac{1}{\tau} = R_B = 48 \times 10^6 \text{ Hz}.$$

For the FM analog system,

$$B_{IF} \cong 2f_m\left(m_f + 1\right) = 48 \times 10^6 \text{ Hz} , \quad \text{for} \quad m_f = 5 .$$

Assuming threshold conditions,

$$\left(\frac{C}{N}\right)_{IF} = 10 \quad \text{or} \quad 10 \text{ db} ;$$

$$\therefore \left(\frac{C}{N}\right)_{IF} \times B_{IF} = 4.8 \times 10^8 \text{ Hz} ,$$

which is quite high. However, this is only a sample calculation; when the experimenter or program manager sees the impact of the requirement that has been imposed on the communication system, they may reconsider.

Continuing with the analysis, a solar panel power supply with the necessary peripheral distribution system, etc., will be assumed since solar panels are the best power supplies available from the viewpoint of power output per unit weight at Mars distances. Furthermore, their lifetime makes them well suited for a Mars mission. Tables 7 and 8 give the weights and solar panel area requirements as a function of power output.

On the basis of the foregoing requirements and considerations and Figures 8, 9, 10, and 11, the resulting spaceborne communication system parameters (such as P_T, d_T, weight) and trade-offs are summarized in Table 13.

Concluding Remarks

From Table 13 it can be seen that the two lightest-weight systems that meet the foregoing requirements are the 100-watt CO_2 laser and the 1-watt Nd^{3+} YAG laser. Furthermore, in the case of the Nd^{3+} YAG laser, the required spaceborne communication system weight is higher at both the lower power and higher power outputs. This shows that there is some optimum sizing and corresponding weight distribution that result in a minimum weight system. For this reason, a computerized method using the calculus of maxima and minima was developed (Reference 1). The method determines the optimum selection of communication systems parameters for any specified mission, application, or requirements. The optimization criteria are minimum weight and minimum cost. These criteria permit the selection of that

Table 13

Spaceborne Communications System Requirements and Trade-offs for Mars Mission with Real-Time, Commercial-Quality TV (See Table 12 for Ground Systems Used).

- $R \cong 2 \times 10^8$ km
- $\left(\frac{C}{N}\right)_{IF} = 10$
- $f_m = 4 \times 10^6$ Hz
- $n = 6$
- $B_{IF} = 2nf_m = 48 \times 10^6$ Hz
- $\left(\frac{C}{N}\right)_{IF} \times B_{IF} = 4.8 \times 10^8$ Hz
- or $\mu_{S,B} \cdot R_B = 4.8 \times 10^8$ signal photoelectrons/sec

Carrier	P_{bb} (w)	P_T (w)	d_τ, (m)	d_τ, (ft)	Spaceborne System (From Figures 9 to 12) Comm. Sys. (lb)	Spaceborne System (From Tables 9 and 10) Power Supply [1] (ft^2)	Spaceborne System (From Tables 9 and 10) Power Supply [1] (lb)	Comments
S-band (f = 2.3 GHz)	1000	300	30	~98[2]	7000	15.4	10.6	Not competitive. Too large an antenna. Will probably be better to go to higher P_{BB}.
X-band (f = 10 GHz)	1000	300	18	60	2000	15.4	10.6	Could be competitive if a higher P_{BB} results in a lower weight system
	100	30	~30	~100[2]	~8000	15.4	10.6	Not competitive
CO_2 laser, IR ($\lambda = 10.6\mu$)	1000	100	~0.6	2	500	15.4	10.6	Competitive; has a higher beamwidth (18μ rad) and a smaller, less-difficult ground aperture to build than Nd^{3+} YAG.
	100	10	2	6.6	1500	15.4	10.6	Not competitive
Nd^{3+} YAG, Visible ($\lambda = 0.53\mu$)	1000	10	~0.3	1	950	15.4	10.6	Not competitive
	100	1	1	3.3	470	15.4	10.6	Competitive, but has a narrow beamwidth of 0.5μ rad and a more difficult ground system to build
	10	0.1	~2.8	9.2 [2]	2500	1.5	1.1	Not competitive

[1] Power supply needed to feed spaceborne communication system only (from Tables 7, 8).
[2] Antenna too large.

set of system parameters, such as spaceborne transmitter power output and antenna diameters, that result in a minimum overall weight or cost for the spaceborne communication system for any given signal-to-noise ratio, bandwidth, carrier frequency, and ground system characteristics. The method is versatile in that, with the cost optimization, (fixed and/or variable) costs either of the ground systems or of the booster or both may be taken into consideration if desired.

It should be pointed out that cloud cover and bad weather are factors that must be considered when choosing a laser system. However, this topic is discussed elsewhere (e.g., see References 1, 4, 5, and 6) and hence is not discussed here, except to say that there are locations on the earth which have an approximate 95 percent probability of clear weather (References 1, 4).

ACKNOWLEDGMENTS

The author gratefully acknowledges the comments and suggestions of L. Stokes, K. Brinkman, Neil Birch, B. Kruger, N. McAvoy, H. Plotkin, J. Miller, J. P. Shaughnessy, and W. P. Varson.

Goddard Space Flight Center
National Aeronautics and Space Administration
Greenbelt, Maryland, December 1967
311-02-01-01-51

REFERENCES

1. "Reference Data for Advanced Space Communication and Tracking Systems," Hughes Aircraft Company, Aerospace Group, Culver City, California, for GSFC, Contract No. NAS 5-9637, NASA Technical Information Facility Accession Nos. N67-32164, N67-32165, N67-32166, N67-32167, N67-31303.

2. Whelan, J. W., "Analog-FM vs. Digital PSK Transmission," *IEEE Transactions on Communication Technology,* Vol. Com-14, No. 3, pp. 275-282, June 1966.

3. Plotkin, S. C., "FM Bandwidth as a Function of Distortion and Modulation Index," *IEEE Transactions on Communication Technology, Concise Papers,* pp. 467-470, June 1967.

4. Kalil, F., "Optical and Microwave Communications—A Comparison," NASA Technical Note D-3984, May 1968.

5. Deirinendjian, D., "Scattering and Polarization Properties of Water Clouds and Hazes in the Visible and Infrared," *Appl. Opt.*, Vol. 3, pp. 187-196, Feb. 1964.

6. Sherr, P. E., "World Wide Cloud Coverage Study," Allied Research Associates, Inc., Concord, Mass., for Marshall Space Flight Center, Huntsville, Alabama, Contract No. NAS 8-21040, monthly progress reports, beginning Feb. 1967.

BIBLIOGRAPHY

Allen, C. W., "Astrophysical Quantities," Second Ed., London: Univ. of London, Athlone Press, 1963.

Barton, D. K., "Radar Systems Analysis," Englewood Cliffs, New Jersey: Prentiss-Hall, Inc., 1965.

Battin, R. H., "Astronautical Guidance," New York: McGraw-Hill Book Co., Inc., 1964.

Black, H. S., "Modulation Theory," New York: D. Van Nostrand Co., Inc., 1953.

Davenport, W. B. and Root, W. L., "An Introduction to the Theory of Random Signals and Noise," New York: McGraw-Hill Book Co., Inc., 1958.

Fagot, J. and Magne, P., "Frequency Modulation Theory," New York: Pergamon Press, 1961.

Hancock, J. C., "An Introduction to the Principles of Communication Theory," New York: McGraw-Hill Book Co., Inc., 1961.

Panter, P. F., "Modulation, Noise, and Spectral Analysis," New York: McGraw-Hill Book Co., Inc., 1965.

Skolnik, M. I., "Introduction to Radar Systems," New York: McGraw-Hill Book Co., Inc., 1962.

Smart, W. M., "Spherical Astronomy," Cambridge: Cambridge University Press, 1962.

Schwartz, M., "Information Transmission, Modulation and Noise," New York: McGraw-Hill Book Co., Inc., 1959.

Schwartz, M., Bennet, W. R., and Stein, S., "Communication Systems and Techniques," New York: McGraw-Hill Book Co., Inc., 1966.

Appendix A

List of Symbols and Modulation Nomenclature

Symbols

$\left(\frac{S}{N}\right)_{out}$ = analog intelligence average signal power to average noise power ratio

d_R = ground receiver antenna/aperture diameter, meters

G_R = ground receiver antenna/aperture gain, dimensionless

R_B = downlink bit rate, bits/per sec

d_T = spaceborne antenna/aperture diameter

P_{BB} = power supply output power

R = range/distance, meters

E/N_0 = predetection signal energy in each bit/noise power spectral density

$\left(\frac{S}{N}\right)_{IF}$ or $\left(\frac{C}{N}\right)_{IF}$ = total receiver signal-to-noise power within the IF bandwidth (B_{IF}); with matched filter receiver $(S/N)_{IF} = E/N_0$. In practice, with nonideal, matched-filter receiver, a 1-db degradation may be experienced.

B_{IF} = equivalent noise bandwidth of the IF stage. The maximum $R_B = B_{IF}$.

N_0 = noise power spectral density

N or N_T = thermal noise power in the IF bandwidth B_{IF}; i.e., $N_T = N_0 B_{IF}$

$N_0 = \begin{cases} kT_e, \text{ for RF systems} \\ hf_c, \text{ for optical heterodyne detection systems} \end{cases}$

$k = 1.38047 \times 10^{-23}$ Joules per degree Kelvin, Boltzmann's constant

$h = 6.624 \times 10^{-34}$ Joule-sec, Plank's constant

N_e or N_E = bit error noise, i.e., the noise in the signal out of a digital receiver, after digital-to-analog conversion, caused by a received bit being interpreted incorrectly.

N_Q = quantization noise, i.e., the noise in the signal out of a digital receiver, after digital-to-analog conversion, caused by the original source signal having been quantized in the analog-to-digital analog conversion process

N_R = resultant noise in the analog signal out of a PCM system caused by both quantization and bit error noises

P_E or P_e = probability of a detected bit being in error, sometimes called error rate

Q_E or Q_e = probability of a detected bit being correct

$P_e + Q_e = 1$

P_T = transmitter power output at the transmitter output terminals

P_R = total received signal power—carrier plus sidebands; it is very nearly equal to C, the total carrier plus sideband power contained in the equivalent IF bandwidth. If P_R is referred to the input to the receiver preamplifier, then the total effective system noise temperature (T_e) for signal-to-noise ratio calculations must also be referred to this point.

$T_e = \frac{T_a}{L_R} + T_0 \left(F_0 - 1\right) + T_L \left(1 - \frac{1}{L_R}\right)$ = total effective system noise temperature referred to the preamplifier input

T_a = antenna noise temperature caused by background radiation (galactic noise, planetary noise, solar noise), side-lobe noise, back-lobe noise in the case of a mesh-type antenna, spillover (noise that gets into the antenna feed via optical paths other than side or back lobes), and atmospheric absorption with its ensuing reradiation

T_0 = 290°K, standard reference temperature

F_0 = receiver noise referred to the preamplifier input

In general, for N cascaded networks,

$$F_0 = F_1 + \frac{F_2 - 1}{G} , + \frac{F_3 - 1}{G_1 G_2} + \cdots + \frac{F_n - 1}{G_1 G_2 \cdots G_{n-1}}$$

F_n = the noise figure on the N^{th} network in the cascade, etc., $F = \frac{(S/N)_{out}}{(S/N)_{in}}$

G_n = the gain of the N^{th} network in the cascade, etc., G = signal voltage out/signal voltage in. Similarly, the effective system noise temperature of N networks in cascade is

$$T_{e,network} = T_1 + \frac{T_2}{G_1} + \frac{T_3}{G_1 G_2} + \cdots + \frac{T_n}{G_1 G_2 \cdots G_{n-1}}$$

$$T_{e,network} = T_0 (F_0 - 1)$$

T_n = $T_0 (F_n - 1)$, effective system temperature of the N^{th} network in the cascade

$1/L_R$ = receiver line losses; sometimes denoted as τ_R, the receiver transmissivity

T_L = receiver line temperature

NOTE: For ultimate performance and very low system noise temperatures, the receiver preamplifier is as near to the antenna input terminals or feed as is practical to minimize receiver line losses. Also, the lines and the preamplifier are cooled to reduce the system noise.

$1/L_T$ = transmitter line losses, sometimes denoted as τ_T, the transmitter transmissivity

τ_a = transmissivity of the atmosphere

t_0 = maximum displacement in time between pulses in the case of pulse-position modulation

t_r = pulse rise-time in pulse modulation systems

n = number of bits per digital word

m_a = amplitude modulation index

m_f = frequency modulation index

$\mu_{s,B}$ = average number of signal photoelectrons per bit out of the photodetector of a direct-detection optical receiver; in the case where a photomultiplier is used, the photodetector is considered to be the photomultiplier cathode

$$\mu_{s,B} = \frac{\eta_q P_c}{h f_c R_B}$$

$\mu_{N,B}$ = average number of background radiation photoelectrons per bit out of the photodetector of a direct-detection receiver; in the case where a photomultiplier is used, the photodetector is considered to be the photomultiplier cathode

$$\mu_{N,B} = \frac{\eta_q P_B}{h f_c R_B}$$

η_q = photodetector quantum efficiency, i.e., the ratio of the average number of photoelectrons out of the photodetector to the average number of photons impinging onto the photodetector surface

f_c = carrier frequency, Hz

λ_c = carrier wavelength, meters

$c = \lambda_c f_c$ = speed of light = 3×10^8 meters per second

P_B = background radiation power at the input to the optical receiver photodetector

$$P_B = \begin{cases} \tau_a \tau_R \lambda_i \dfrac{\pi d_R^2}{4} H_{B,\lambda}, & \text{point sources} \\ \tau_a \tau_R \lambda_i \pi d_{source}^2 \dfrac{d_R^2}{16R^2} W_\lambda, & \text{plane source that does not cover receiver full field of view} \\ \tau_a \tau_R \lambda_i \pi^2 \dfrac{d_R^2}{16} \theta_{R,FOV}^2 N_{B,\lambda}, & \text{infinite plane source} \end{cases}$$

λ_i = bandpass of receiver spectral filter; practical limits of $1\text{Å} \lesssim \lambda_i \lesssim 10\text{Å}$

$H_{B,\lambda}$ = background spectral irradiance, watts/cm^2 - μ

W_λ = background spectral radiant emittance, watts/cm^2 - μ

$N_{B,\lambda}$ = background spectral radiance, watts/cm^2 - μ - sr

$W_{B,\lambda} = \pi N_{B,\lambda}$ for a Lambertian radiator

d_{source} = diameter of background radiating source

$\theta_{R,FOV}$ = receiver field-of-view

$Q_{B,\lambda} = \dfrac{N_{B,\lambda}}{hc/\lambda_c}$, background spectral radiance in photons/sec-cm^2-μ-sr (See Tables A1 and A2)

Table A1

Background Spectral Radiance at the Transmission Wavelengths.

Background Spectral Radiance Photons	Wavelength				
Sec-cm^2-μ-sr	0.51μ	0.63μ	0.84μ	3.39μ	10.6μ
Q_B	$1.0 \times 10^{+16}$	5.0×10^{15}	4.0×10^{15}	1.7×10^{14}	5.6×10^{15}

Table A2

Typical Atmospheric Attenuation at the Transmission Wavelengths.

Atmospheric Transmissivity (dimensionless)	Wavelength				
	0.51μ	0.63μ	0.84μ	3.39μ	10.6μ
τ_a	0.75	0.82	0.70	0.87	0.80

Modulation Nomenclature

Analog Communication Systems

AM-DSB = amplitude modulation-double sideband

AM-DSB/SC = amplitude modulation-double sideband with suppressed carrier

AM-SSB/SC = amplitude modulation-single sideband with suppressed carrier

NB FM = narrow-band frequency modulation

Uncoded Pulse Systems

PAM/AM = pulse amplitude modulation/amplitude modulation; i.e., the carrier is amplitude-modulated with pulses whose amplitude varies as the amplitude of the source signal.

PDM/AM = pulse duration modulation/amplitude modulation; i.e., the carrier is amplitude-modulated with constant-amplitude pulses whose duration varies as the amplitude of the source signal.

PPM/AM = pulse position modulation/amplitude modulation; i.e., the carrier is amplitude-modulated with pulses of constant width and height but whose spacing between them varies as the rate of the source signal.

Coded/Digital Systems

PCM/PM = PSK = pulse code modulation/phase modulation, or phase shift keying; i.e., the phase of the carrier is shift-keyed in a coded

manner by pulses. In a binary digital system, these pulses are called bits that represent the digit 1 or the digit 0.

PCM/FM = FSK = pulse code modulation/frequency modulation or frequency shift keying; i.e., the frequency of the carrier is shift-keyed in a coded manner.

PCM/PL = pulse code modulation, in which the polarization of the carrier is shift-keyed in a coded manner; used in optical systems where the carrier polarization can be shifted at a rapid rate.

PCM/AM = pulse code modulation, in which the amplitude of the carrier is shift-keyed in a coded manner.

PCM/IM = pulse code modulation, in which the intensity of the carrier (usually optical frequencies) is shift-keyed in a coded manner; analogous to PCM/AM, except that in optical systems the carrier amplitude cannot be modulated directly as in RF systems.

Appendix B

Subsystem Weights for a Spaceborne Communication System

This appendix presents the subsystem weights of the spaceborne communication system. The total spaceborne communication system is divided into the following subsystem weights (see also Figure B1):

1. Transmitter, including oscillator, power amplifier and/or laser, and voltage converter to convert the power supply voltage to the desired value,
2. Modulator, including data conditioner such as digitizer and encoder,
3. Antenna or aperture, including mounts and wiring, but not including gimbals that are considered part of the acquisition and tracking subsystem,
4. Acquisition and tracking, i.e., the pointing subsystem, including gimbals, drive motors, servoelectronics, and wiring, and
5. Heat dissipation system.

In the following figures, which are self-explanatory and taken from Reference 1, the subsystem weights are plotted as a function of the following parameters when applicable:

1. Transmitter power output,
2. Antenna or aperture diameter, and
3. Amount of wasted power that generates undesirable heat that must be dissipated. The heat dissipation subsystem is in essence a cooling subsystem, which may be nothing more than radiation fins; or it may require coolants, plumbing, pumps, and/or heat exchangers, depending on how much heat must be dissipated.

Using these subsystem weights as presented in Figures B2 through B10, the following sample calculation presented in Table B1 demonstrates how the parametric curves given in the report were derived.

Table B1

Sample Calculation – Spaceborne Communication System Weight and Capability

Parameter Description	Dimension	Signal Calculation	Subsystem Weight	
			lb	kg
Communication range, R	0.54×10^8 nm or 10^8 km			
Carrier frequency	2.3×10^9 Hz			
Carrier wavelength	13 cm (0.428 ft)			
Power supply output, P_{BB}	100w			
Transmitter				
Power output, P_T	30w	14.7 dbw		
Antenna diameter, d_T	3m (10 ft)			
Antenna gain, G_T		35 db	40	18.2
Wasted power to be dissipated	70w			
Heat dissipater subsystem			5	2.3
Transmitter weight (oscillator, modulator, TWT, encoder, A-to-D converter, wiring)			8	3.6
Acquisition and tracking subsystem			37	16.8
Transmitter line loss, $1/L_T$		$\sim$ -1 db		
Atmospheric attenuation		$\sim$ - 1 db		
Space loss $(\lambda/4\pi R)^2$		-259.7 db		
Receiver				
Antenna diam, d_R	210 ft (64m)			
Antenna gain, G_R		61.4 db		
Line loss, $1/L_R$		$\sim$ -1 db		
Effective system noise temp, T_e	27°K			
$1/KT_e$		+214.3 db Hz/w		
Max $E/N_0 \cdot R_B$		62.7 db Hz or 1.9×10^6 bps		
Total spaceborne communication system weight (less power supply weight)			90	41

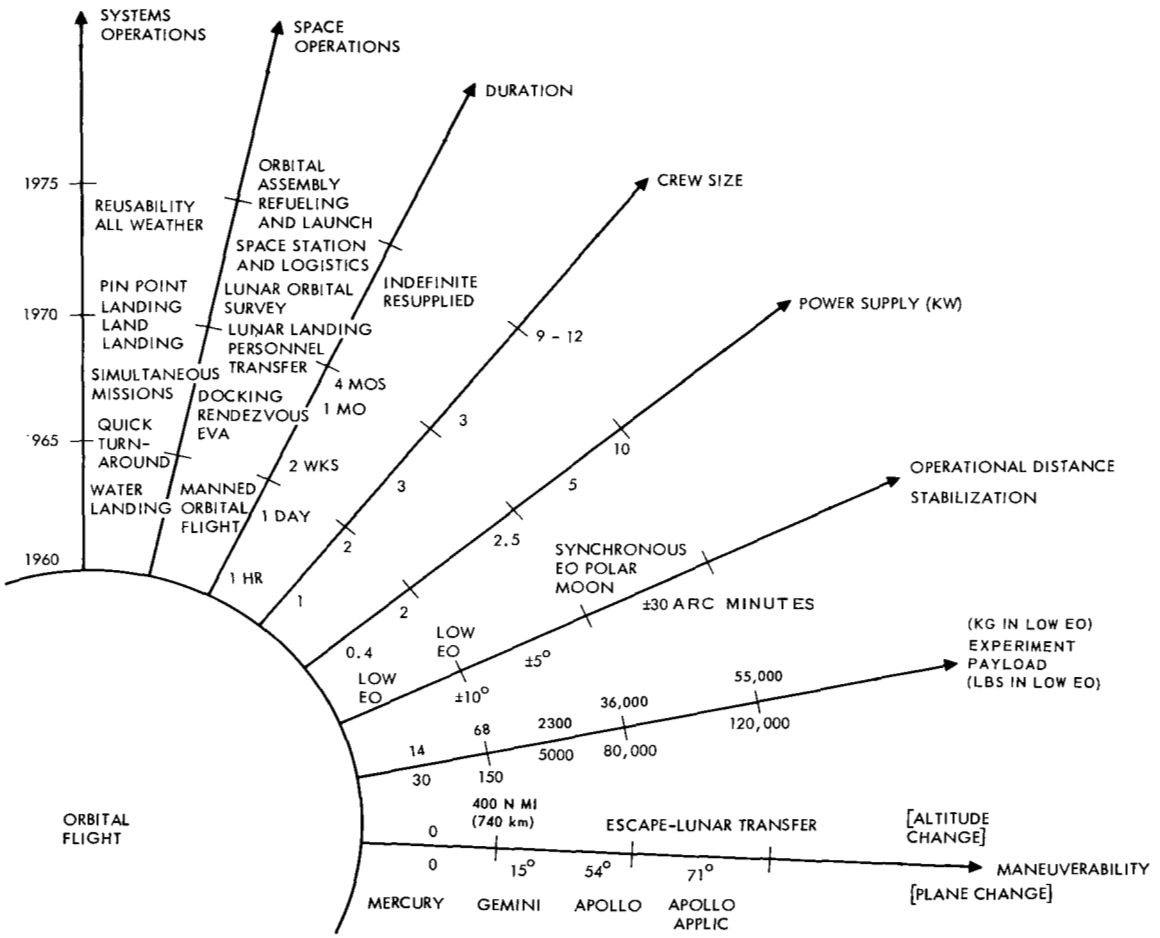

Figure 1–Technology growth in areas critical to manned space flight, based on past, present, and approved programs.

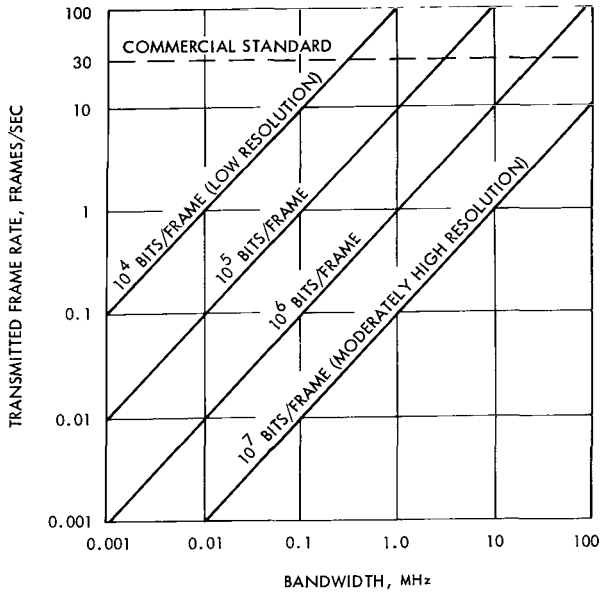

BANDWIDTH REQUIREMENTS CAN BE REDUCED MOST HANDILY BY STRETCHING THE SIGNAL IN TIME (THAT IS, REDUCING THE NUMBER OF FRAMES TRANSMITTED PER SECOND), AS THIS GRAPH SHOWS. HOWEVER, THE NATURE OF THE ANALOG SIGNAL PUTS AN EFFECTIVE LOWER LIMIT ON FRAME RATE.

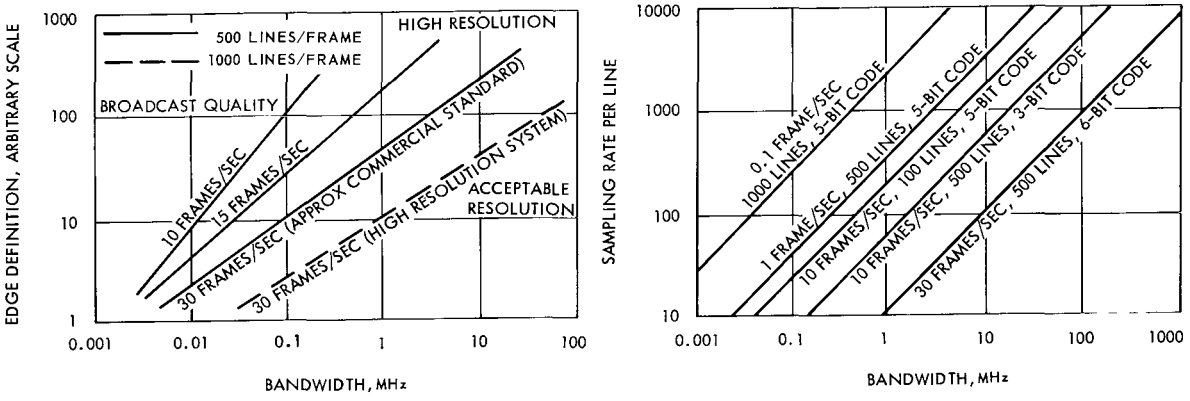

REAL-TIME TRANSMISSION OF NARROW-BANDWIDTH SIGNALS IMPOSES LIMITATIONS ON BOTH ANALOG AND DIGITAL SYSTEMS. IN ANALOG (RIGHT), IT RESULTS IN PICTURES OF LOW CONTRAST, INDICATED HERE IN TERMS OF EDGE DEFINITION. IN DIGITAL (LEFT), IT FORCES A LOW SAMPLING RATE.

Figure 2–Television bandwidth requirements.

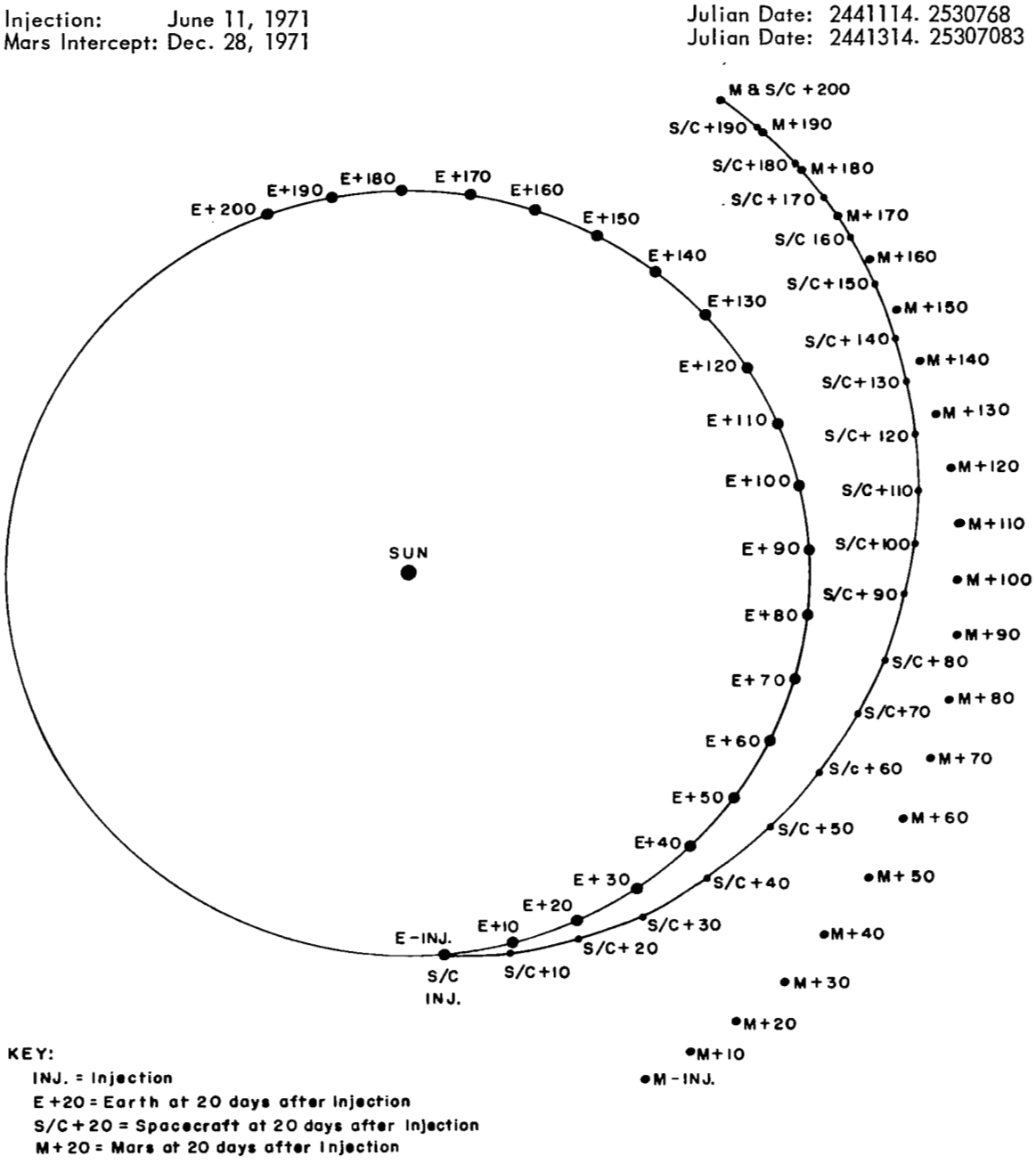

Figure 3–Earth-Mars trajectory.

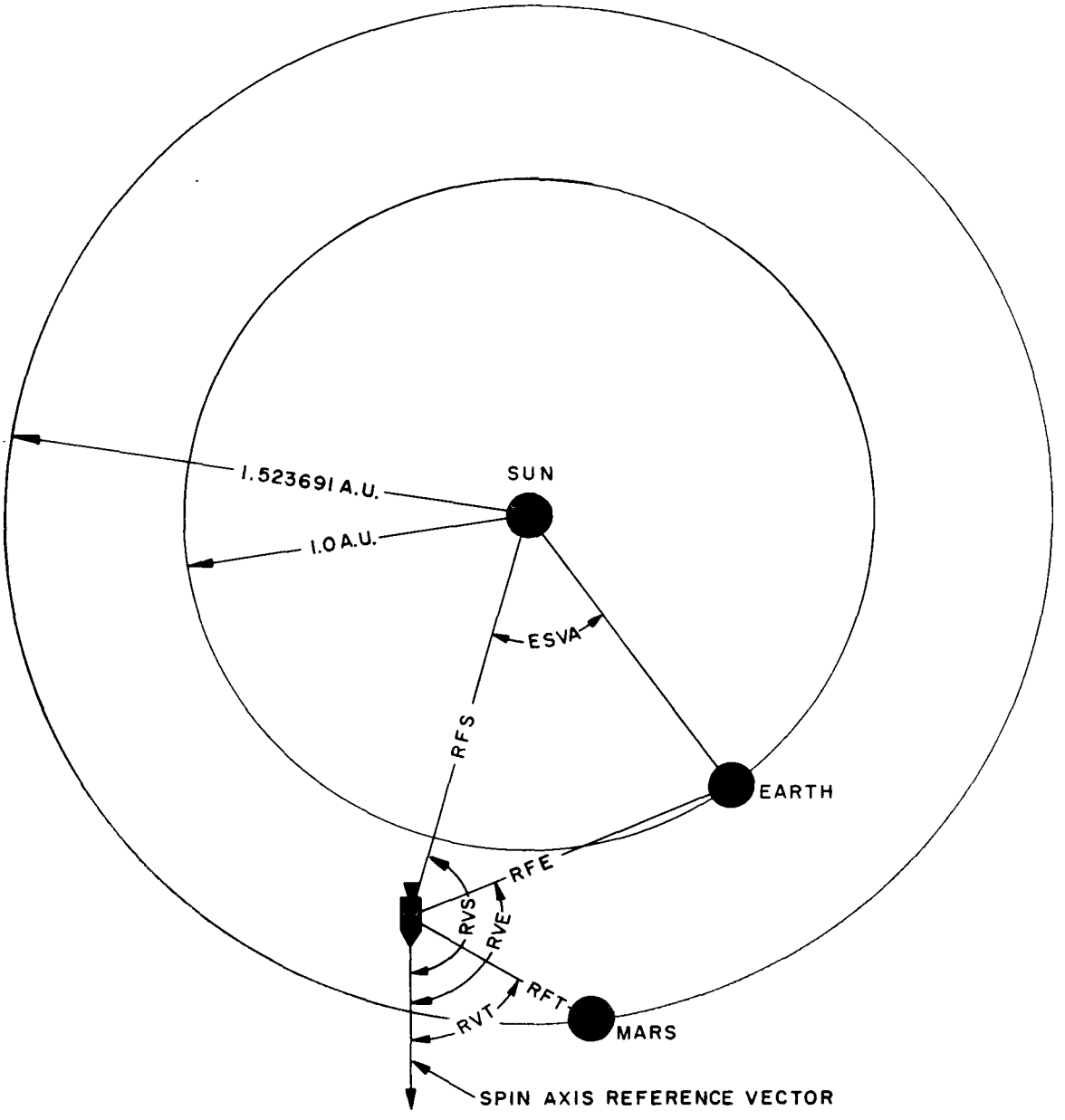

Figure 4–Earth-Mars trajectory geometry, pictorially defining symbols used in Table 6.

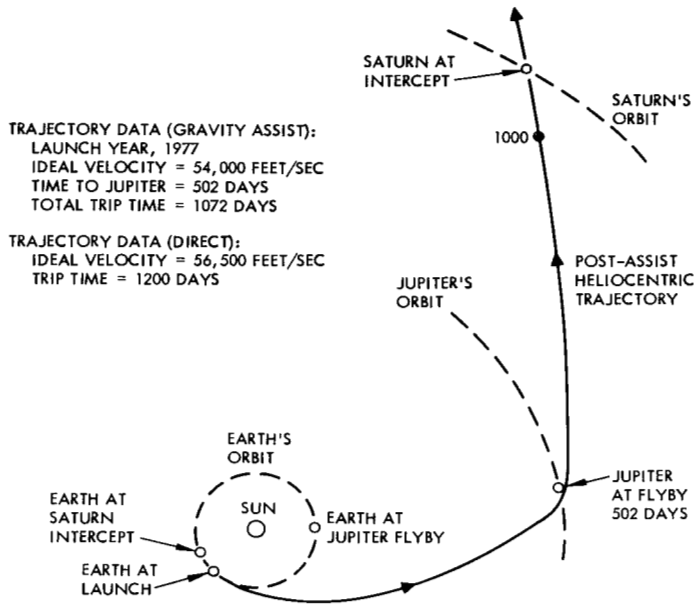

Figure 5–Jupiter gravity-assisted saturn flyby mission.

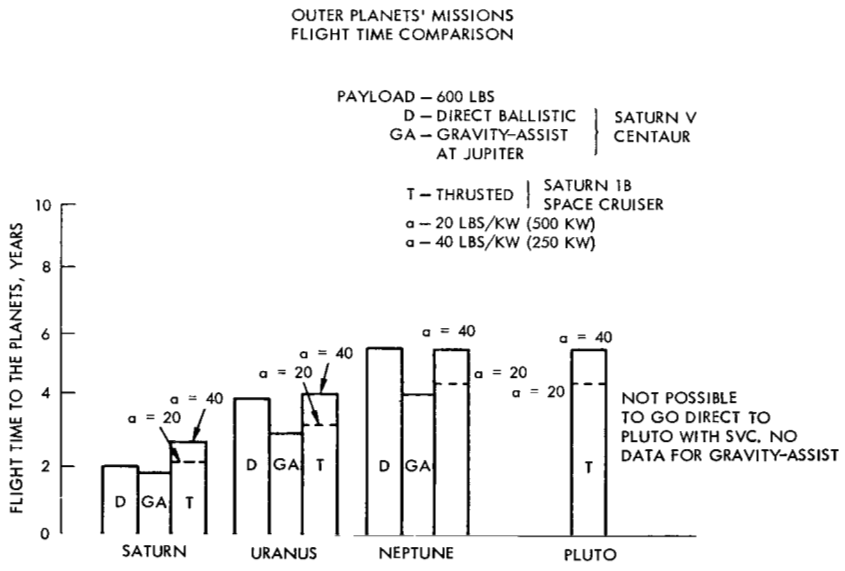

Figure 6–Comparison of one-way flight times to the outer planets using ballistic, gravity-assisted, and thrusted trajectories.

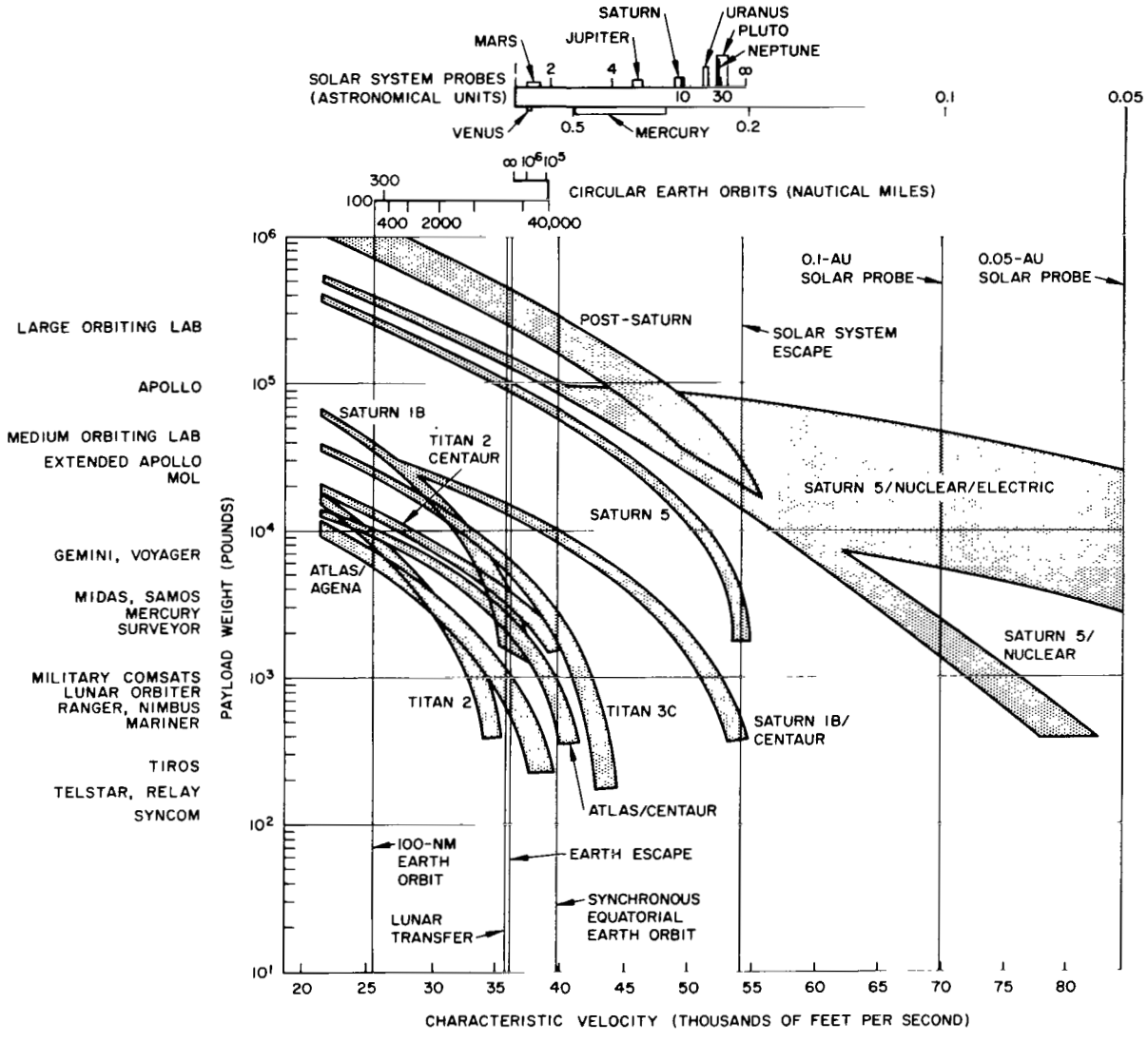

Figure 7–Launch vehicle capabilities–payloads and destination.

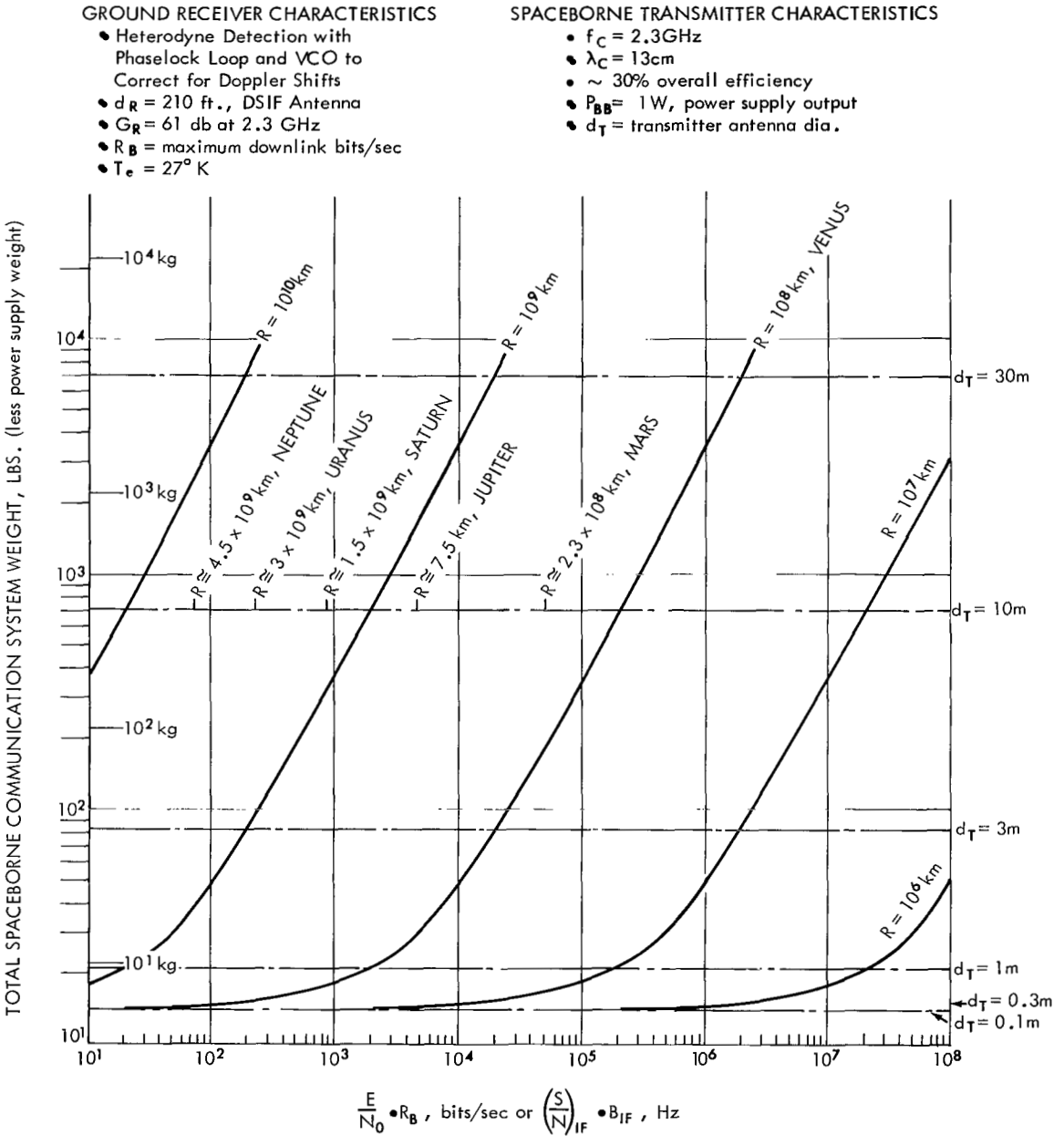

Figure 8a–S-band (f = 2.3 GHz) spaceborne communication system weight versus downlink performance capability–a parametric analysis for planetary missions, for a power supply output of 1 watt.

GROUND RECEIVER CHARACTERISTICS

- Heterodyne Detection with Phaselock Loop and VCO to Correct for Doppler Shifts
- d_R = 210 ft., DSIF Antenna
- G_R = 61 db at 2.3 GHz
- R_B = maximum downlink bits/sec
- T_e = 27° K

SPACEBORNE TRANSMITTER CHARACTERISTICS

- f_C = 2.3GHz
- λ_C = 13cm
- ~ 30% overall efficiency
- P_{BB} = 10W, power supply output
- d_T = transmitter antenna dia.

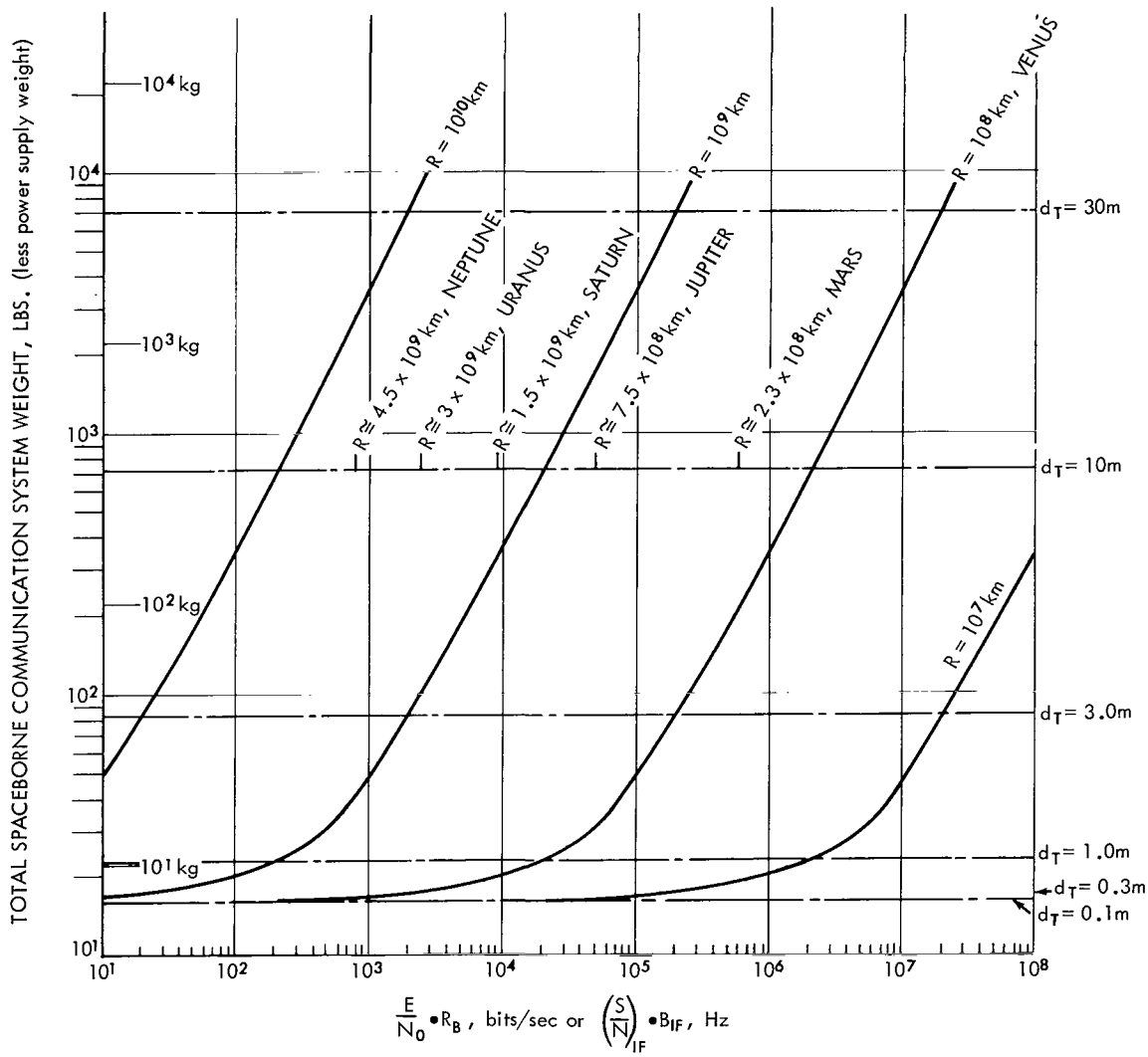

Figure 8b–S-band (f = 2.3 GHz) spaceborne communication system weight versus downlink performance capability–a parametric analysis for planetary missions, for a power supply output of 10 watts.

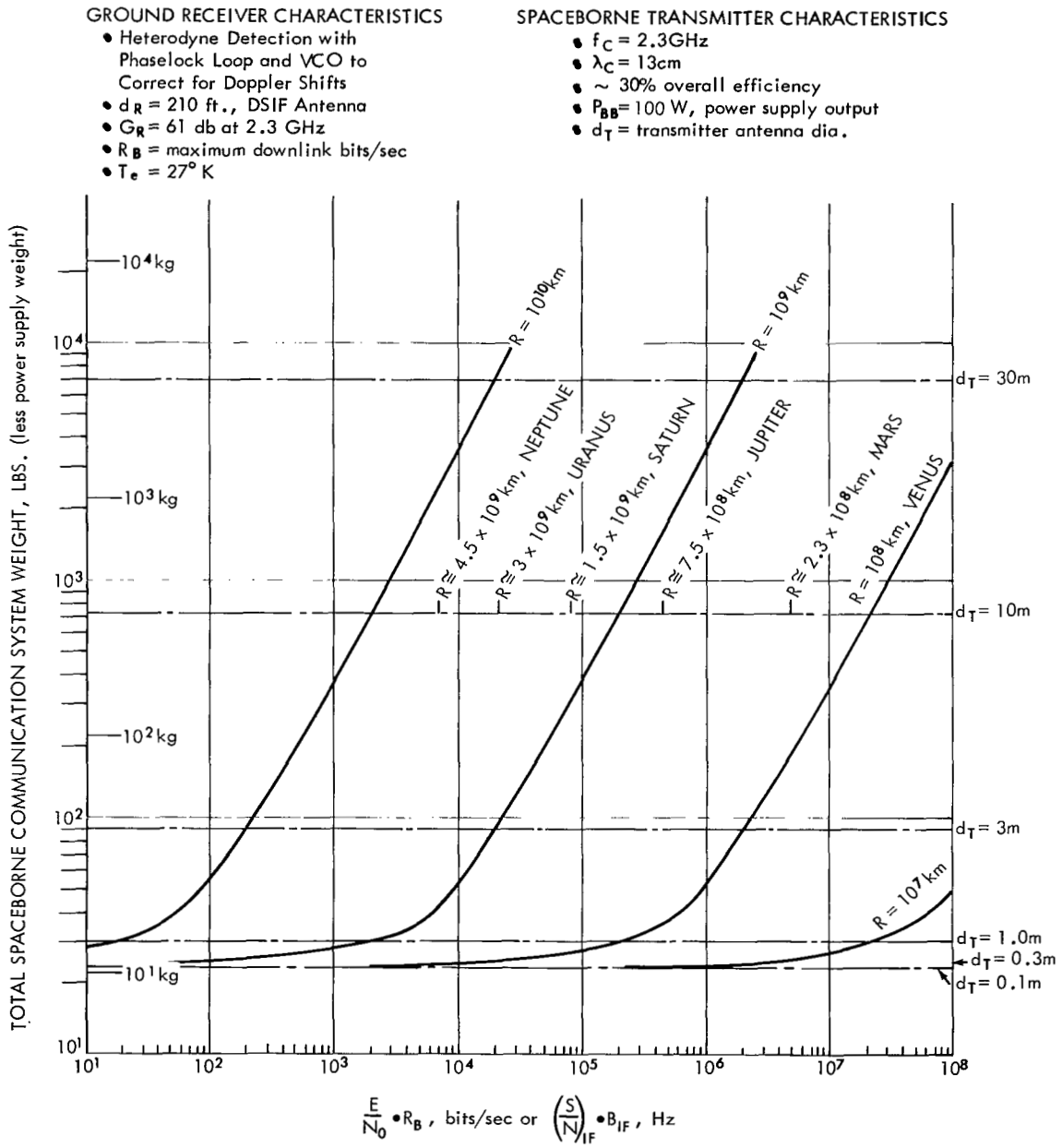

Figure 8c–S-band (f = 2.3 GHz) spaceborne communication system weight versus downlink performance capability–a parametric analysis for planetary missions, for a power supply output of 100 watts.

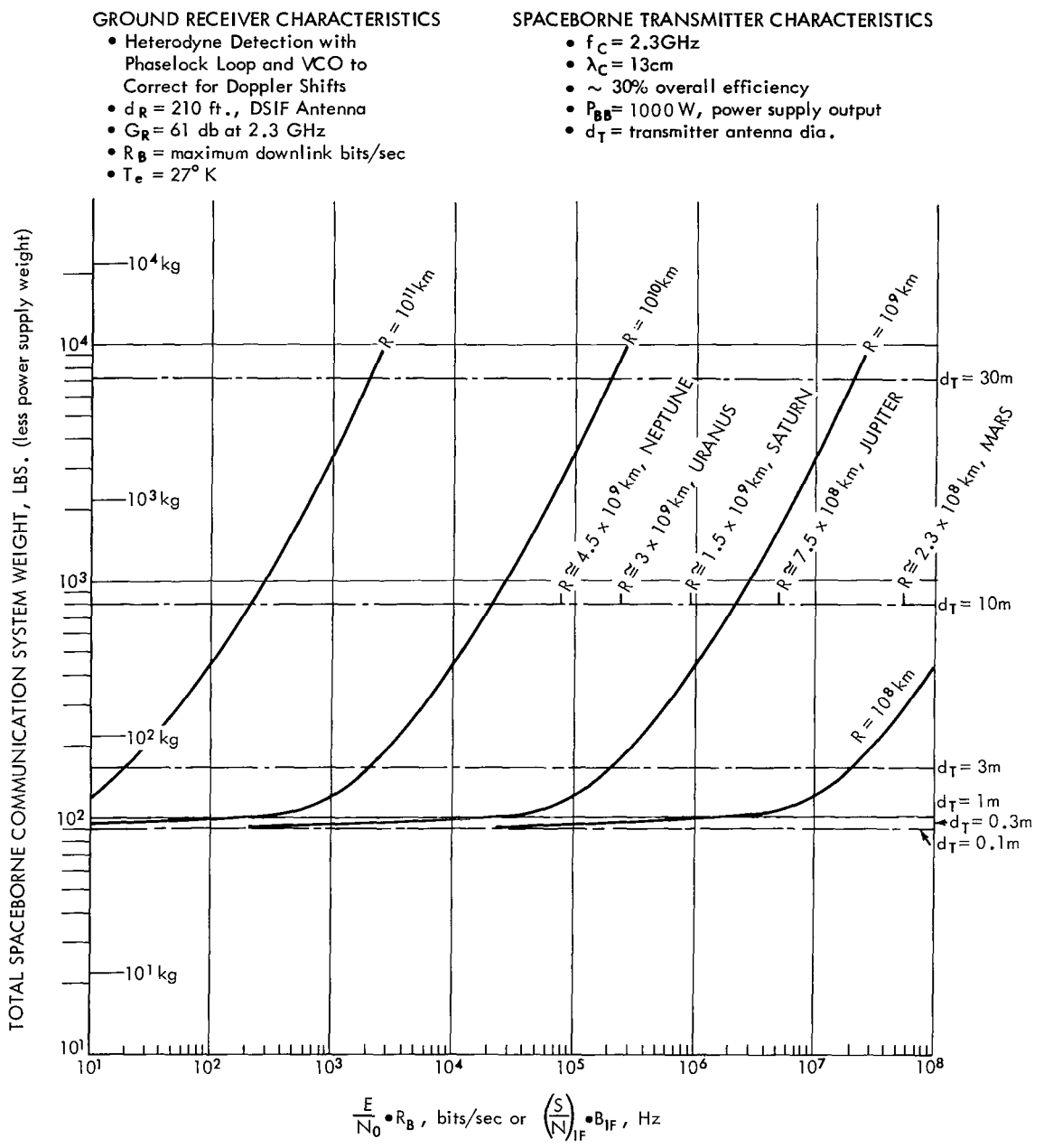

Figure 8d–S-band (f = 2.3 GHz) spaceborne communication system weight versus downlink performance capability–a parametric analysis for planetary missions, for a power supply output of 1000 watts.

GROUND RECEIVER CHARACTERISTICS

- Heterodyne Detection with Phaselock loop and VCO to Correct for Doppler Shifts
- d_R = 120 ft., Haystack Antenna
- G_R = 67db at 10GHz
- R_B = maximum downlink bits/sec
- T_e = 60° K

SPACEBORNE TRANSMITTER CHARACTERISTICS

- f_C = 10GHz
- λ_C = 3cm
- ~30% overall efficiency
- P_{BB} = 1W, power supply output
- d_T = transmitter antenna dia.

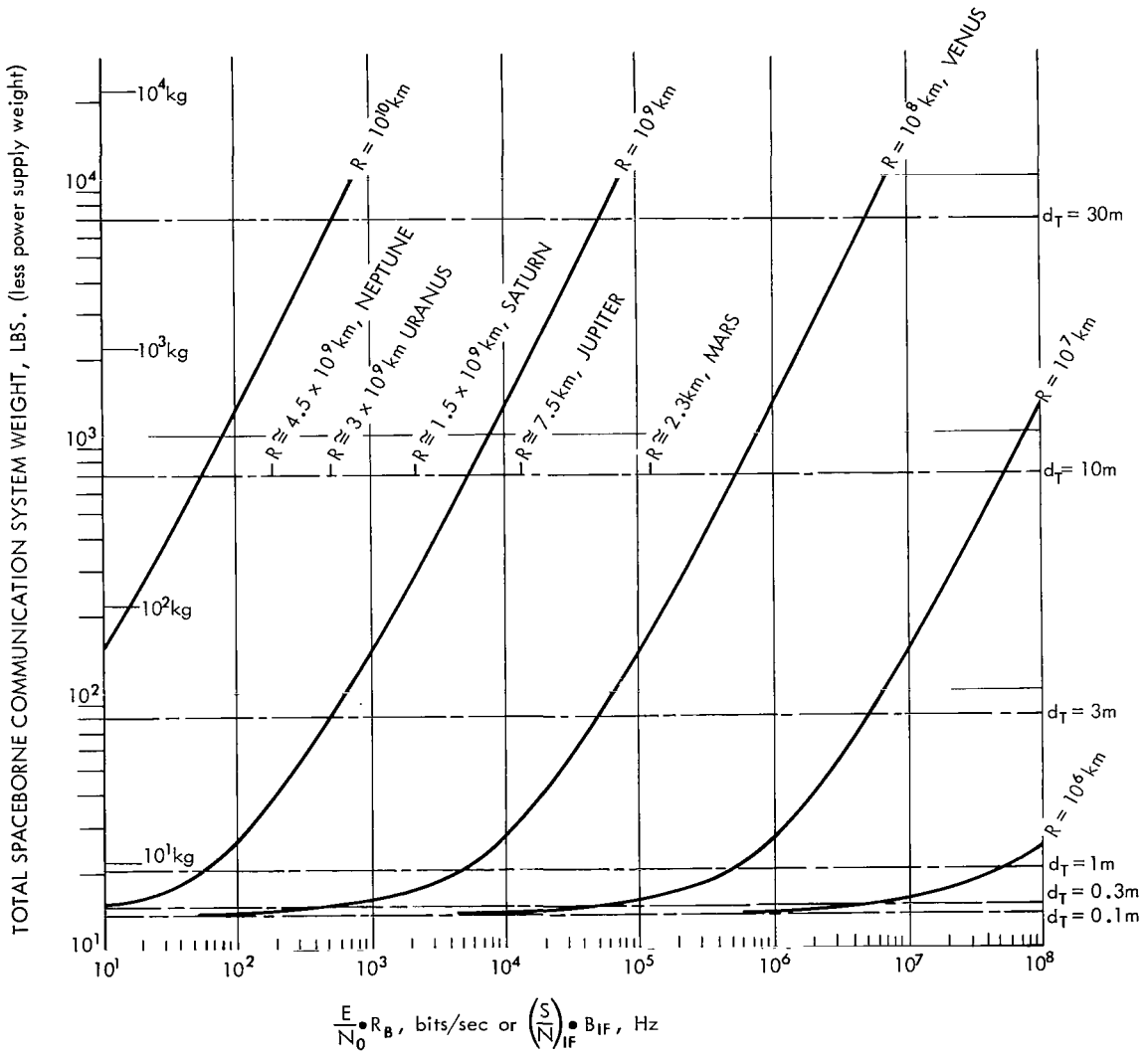

Figure 9a–X-band (f = 10 GHz) spaceborne communication system weight versus downlink performance capability–a parametric analysis for planetary missions, for a power supply output of 1 watt.

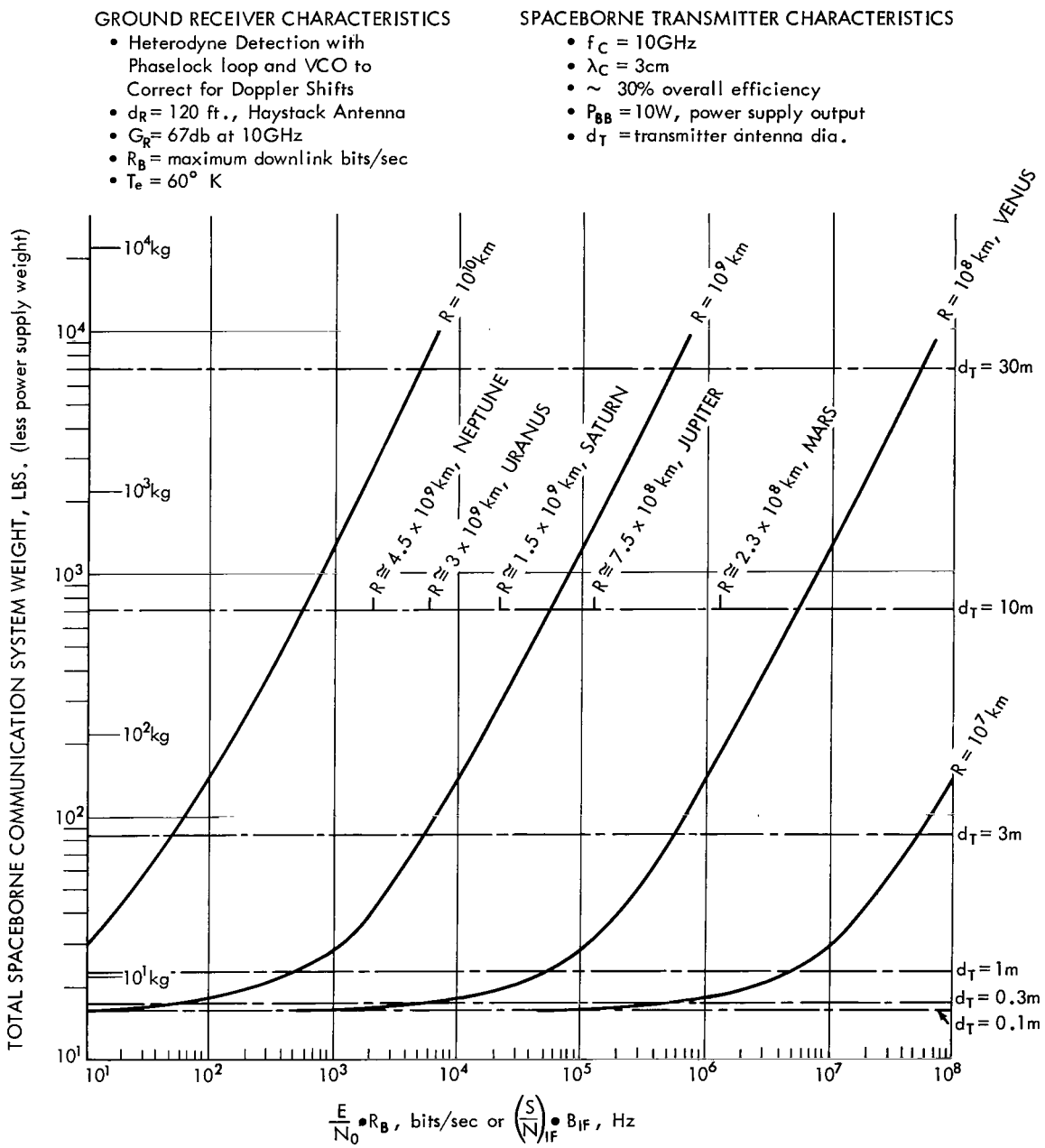

Figure 9b–X-band (f = 10 GHz) spaceborne communication system weight versus downlink performance capability–a parametric analysis for planetary missions, for a power supply output of 10 watts.

GROUND RECEIVER CHARACTERISTICS

- Heterodyne Detection with Phaselock loop and VCO to Correct for Doppler Shifts
- d_R = 120 ft., Haystack Antenna
- G_R = 67db at 10GHz
- R_B = maximum downlink bits/sec
- T_e = 60° K

SPACEBORNE TRANSMITTER CHARACTERISTICS

- f_C = 10GHz
- λ_C = 3cm
- ~30% overall efficiency
- P_{BB} = 100W, power supply output
- d_T = transmitter antenna dia.

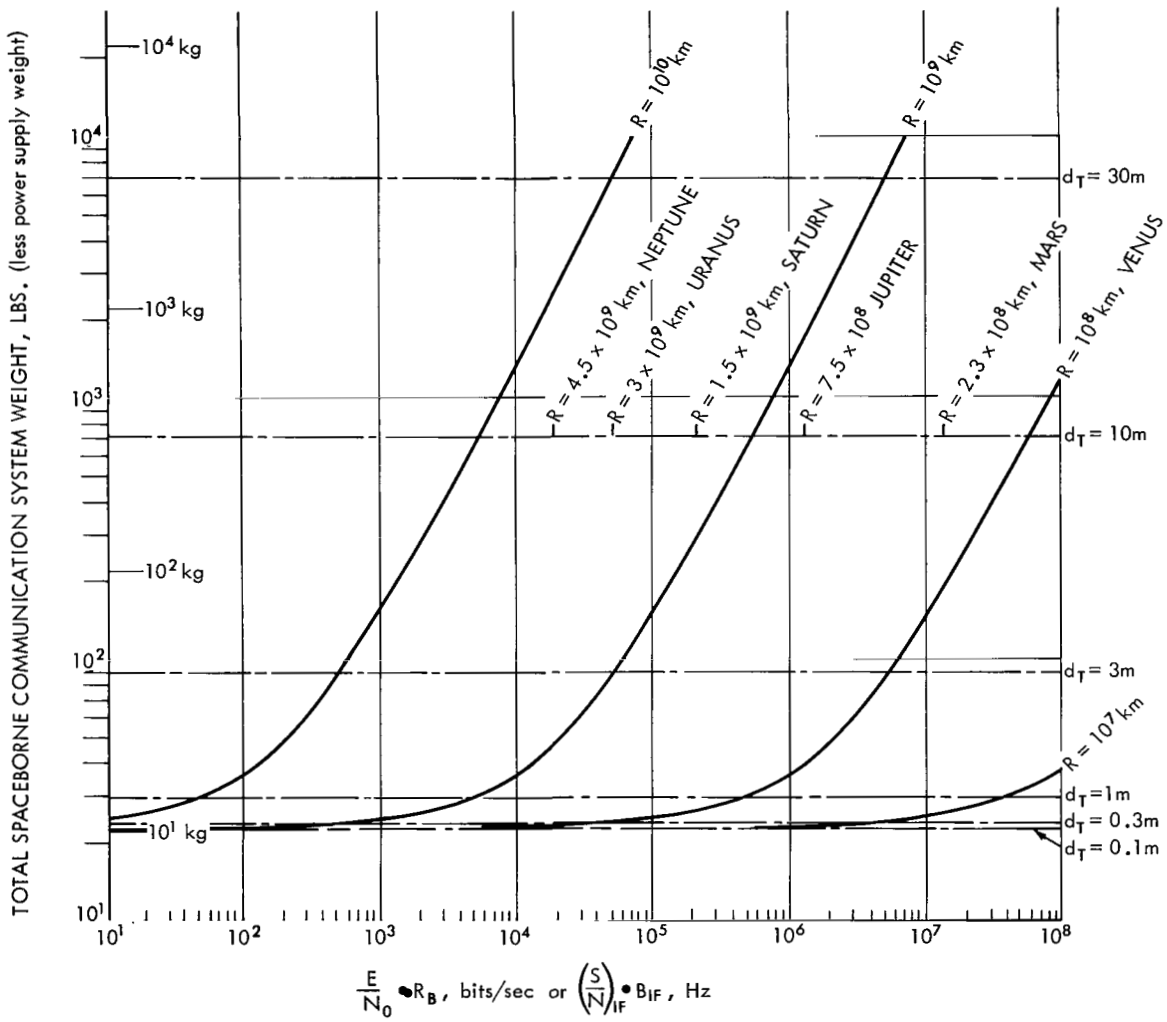

Figure 9c–X-band (f = 10 GHz) spaceborne communication system weight versus downlink performance capability–a parametric analysis for planetary missions, for a power supply output of 100 watts.

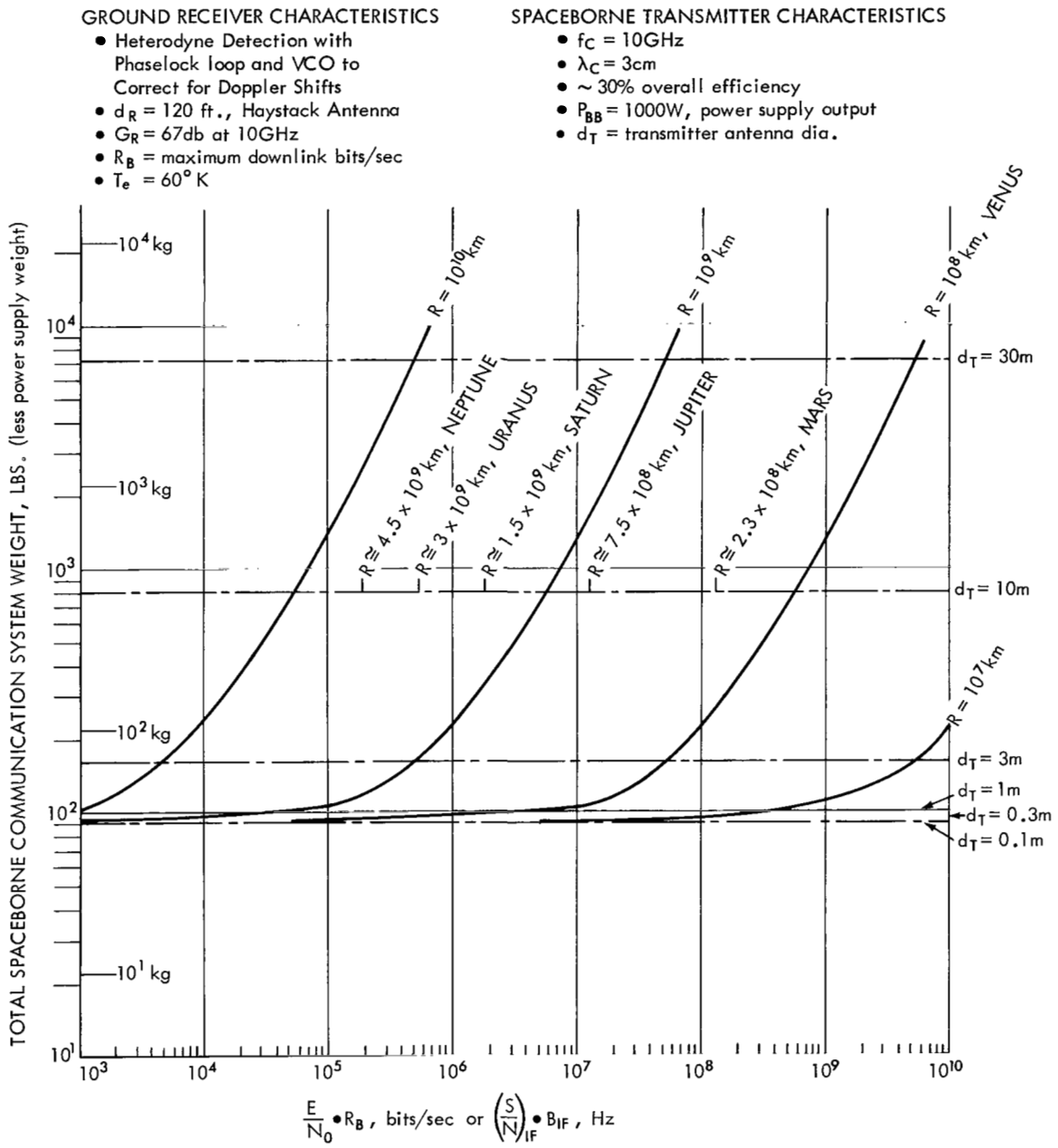

Figure 9d–X-band (f = 10 GHz) spaceborne communication system weight versus downlink performance capability–a parametric analysis for planetary missions, for a power supply output of 1000 watts.

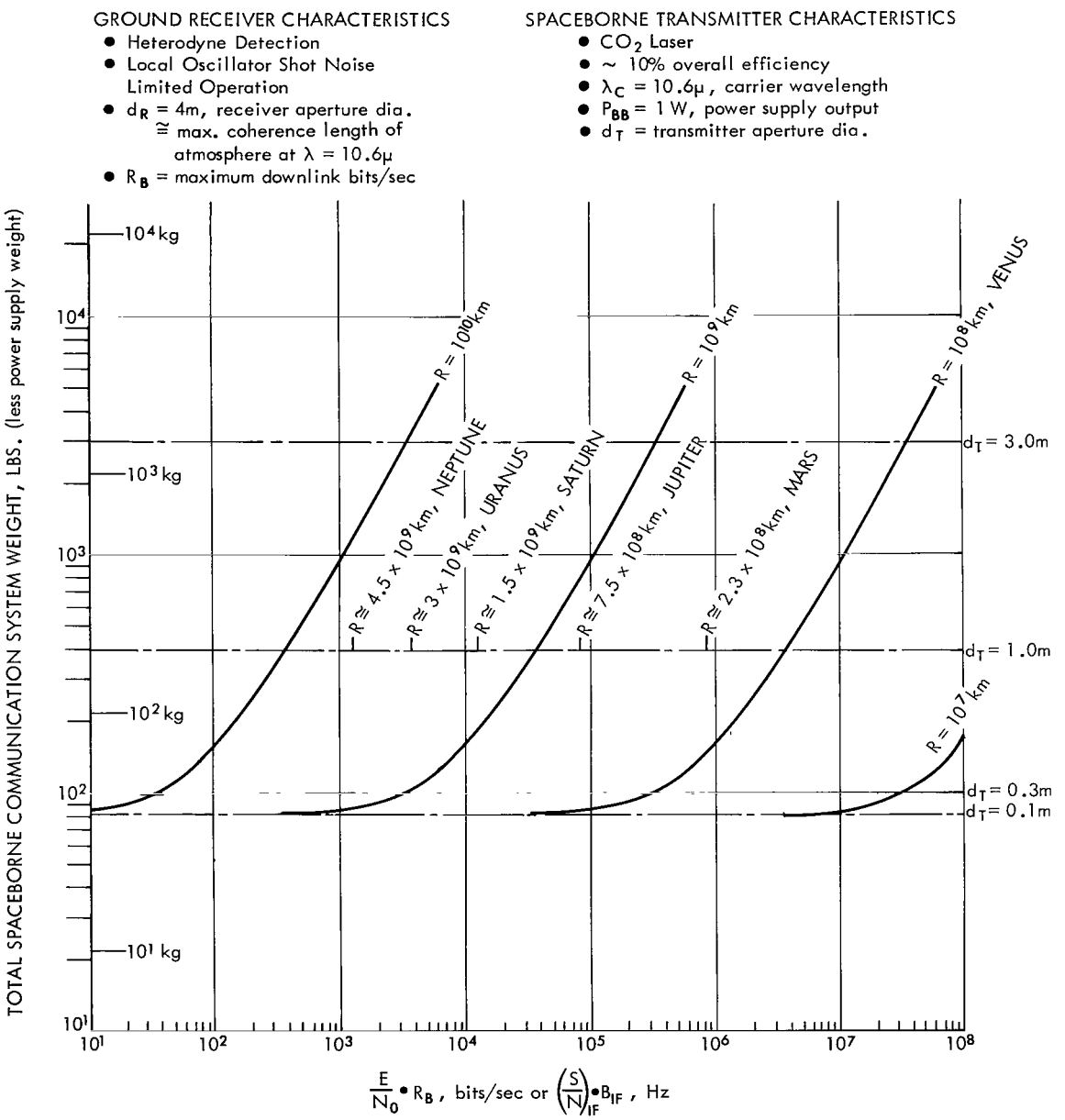

Figure 10a–Optical (IR, $\lambda = 10.6\mu$) spaceborne communication system weight versus downlink performance capability–a parametric analysis for planetary missions, for a power supply output of 1 watt.

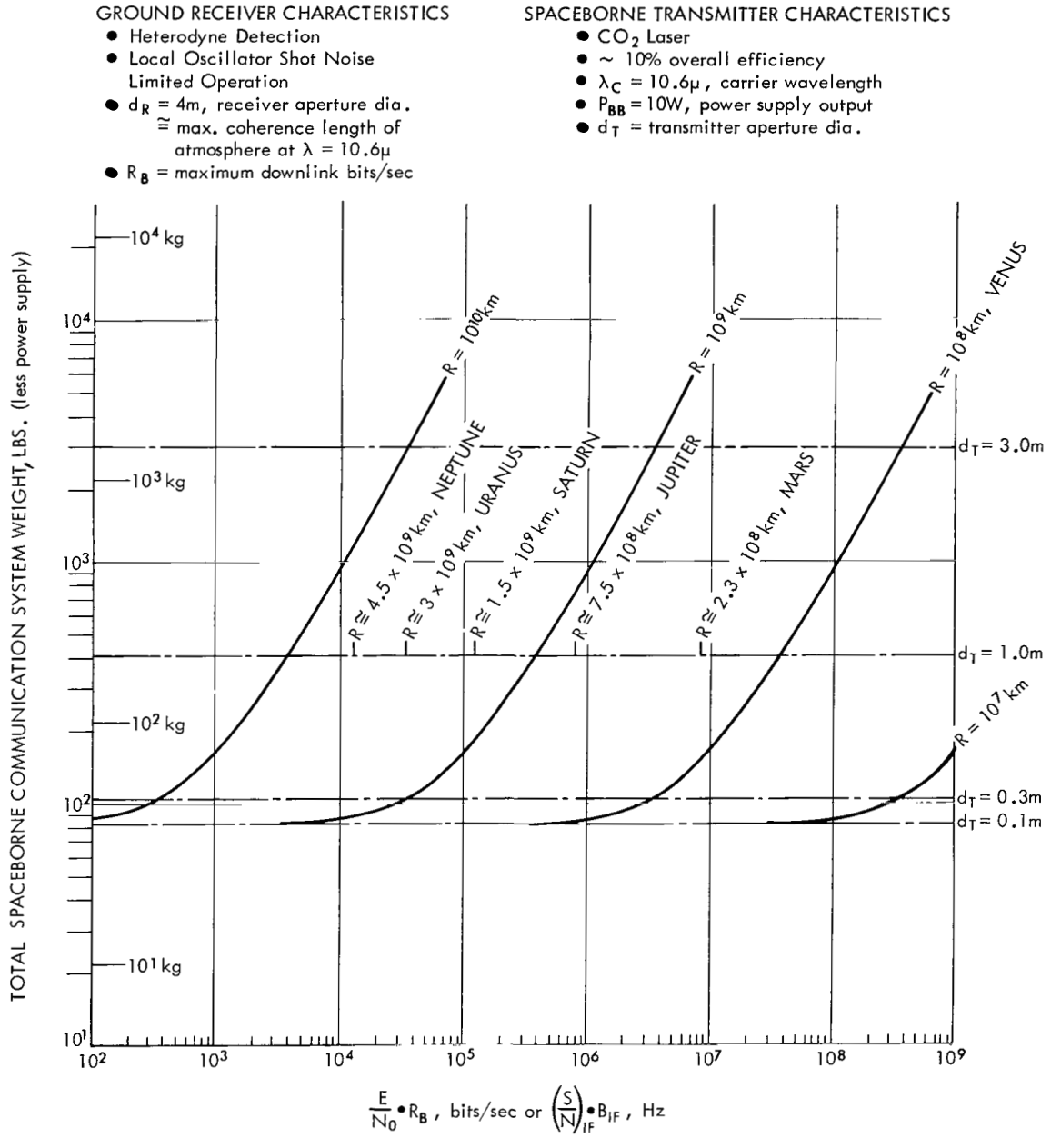

Figure 10b–Optical (IR, $\lambda = 10.6\mu$) spaceborne communication system weight versus downlink performance capability–a parametric analysis for planetary missions, for a power supply output of 10 watts.

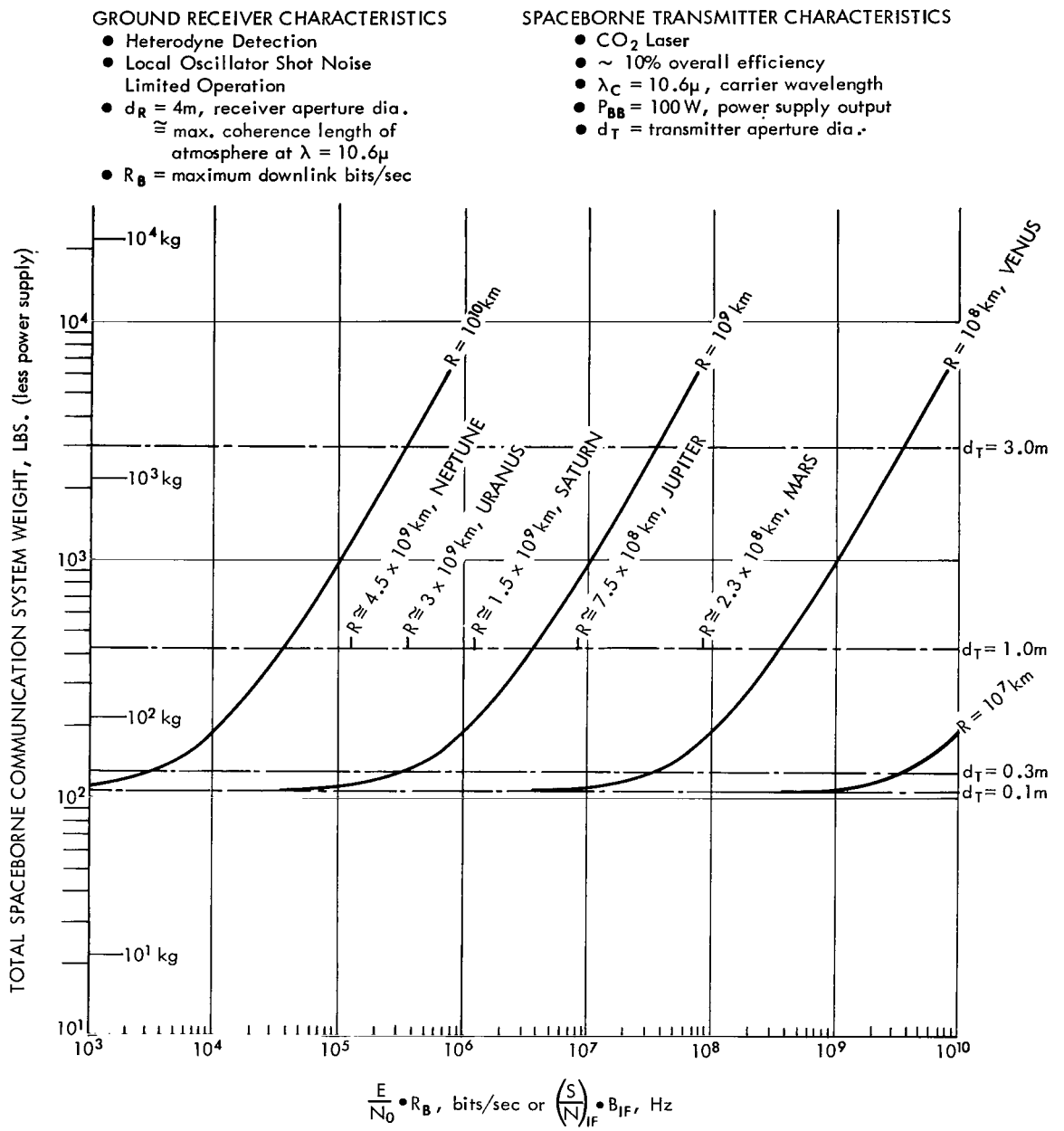

Figure 10c–Optical (IR, $\lambda = 10.6\mu$) spaceborne communication system weight versus downlink performance capability–a parametric analysis for planetary missions, for a power supply output of 100 watts.

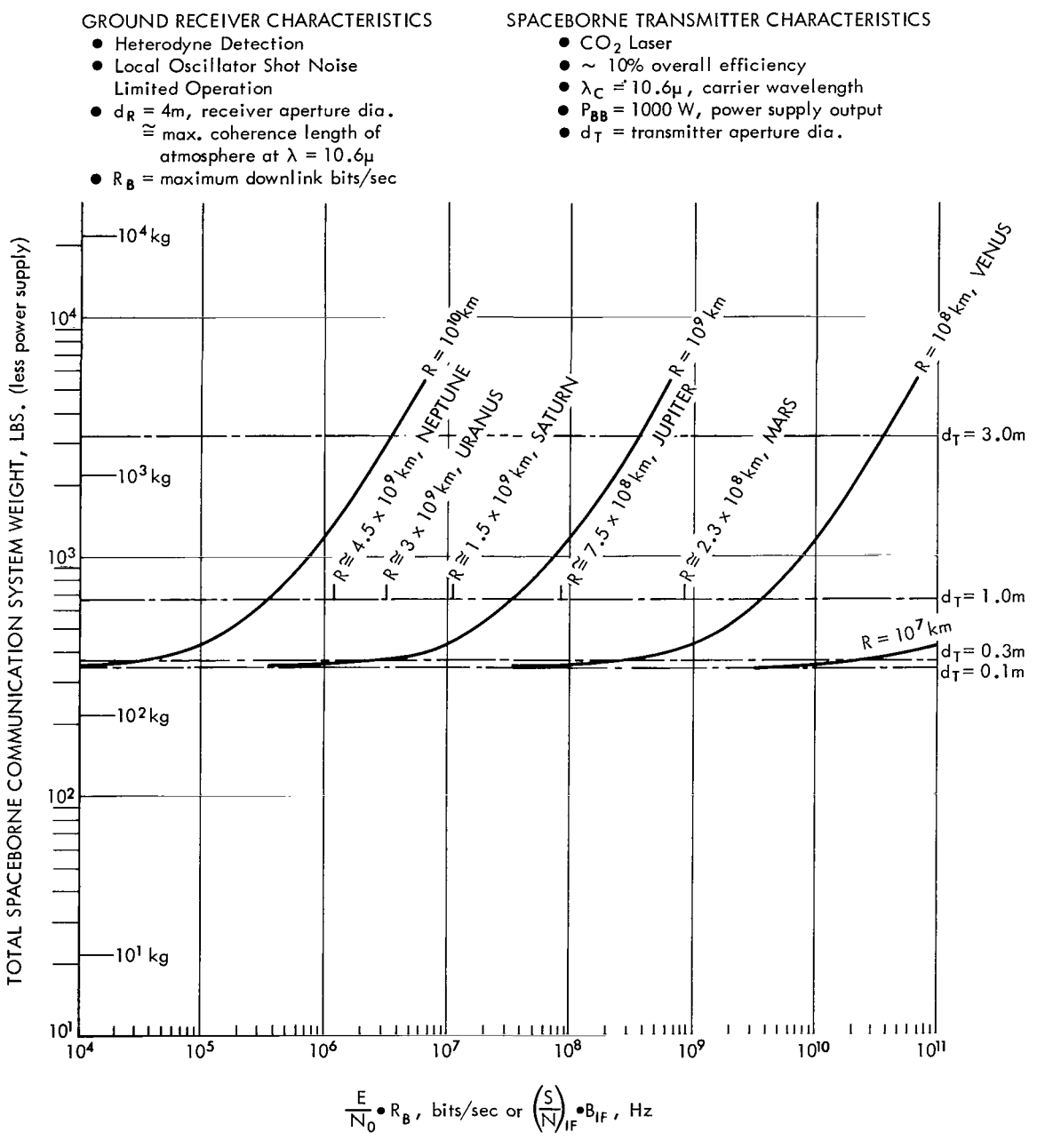

Figure 10d–Optical (IR, $\lambda = 10.6\mu$) spaceborne communication system weight versus downlink performance capability–a parametric analysis for planetary missions, for a power supply output of 1000 watts.

GROUND RECEIVER CHARACTERISTICS

- Direct Detection
- Negligible Thermal and Dark Current Noise
- d_R = 10m, effective receiver aperture diameter
- θ_R = 0.1 mrad, receiver field of view
- λ_i = 10Å (10^{-9}m), receiver optical filter bandpass, centered at 0.53μ
- $\mu_{N,B}R_B$ = 7.85 x 10^8, Ave. background noise photoelectrons/sec., ~a constant for this receiver
- $\mu_{S,B}$= ave. signal photoelectrons/bit
- R_B = downlink signal bit rate, bits/sec

SPACEBORNE TRANSMITTER CHARACTERISTICS

- Nd^{+++}YAG Laser with Lithium Niobate frequency doubler
- ~ 1% overall efficiency
- λ_C = 0.53μ, carrier wavelength
- P_{BB} = 1 W, power supply output
- d_T = transmitter aperture dia.
- R_B = downlink bit rate, bits/sec.
- These efficiencies and powers represent an extrapolation from operating units at ~1 W and have not yet been achieved in practice.

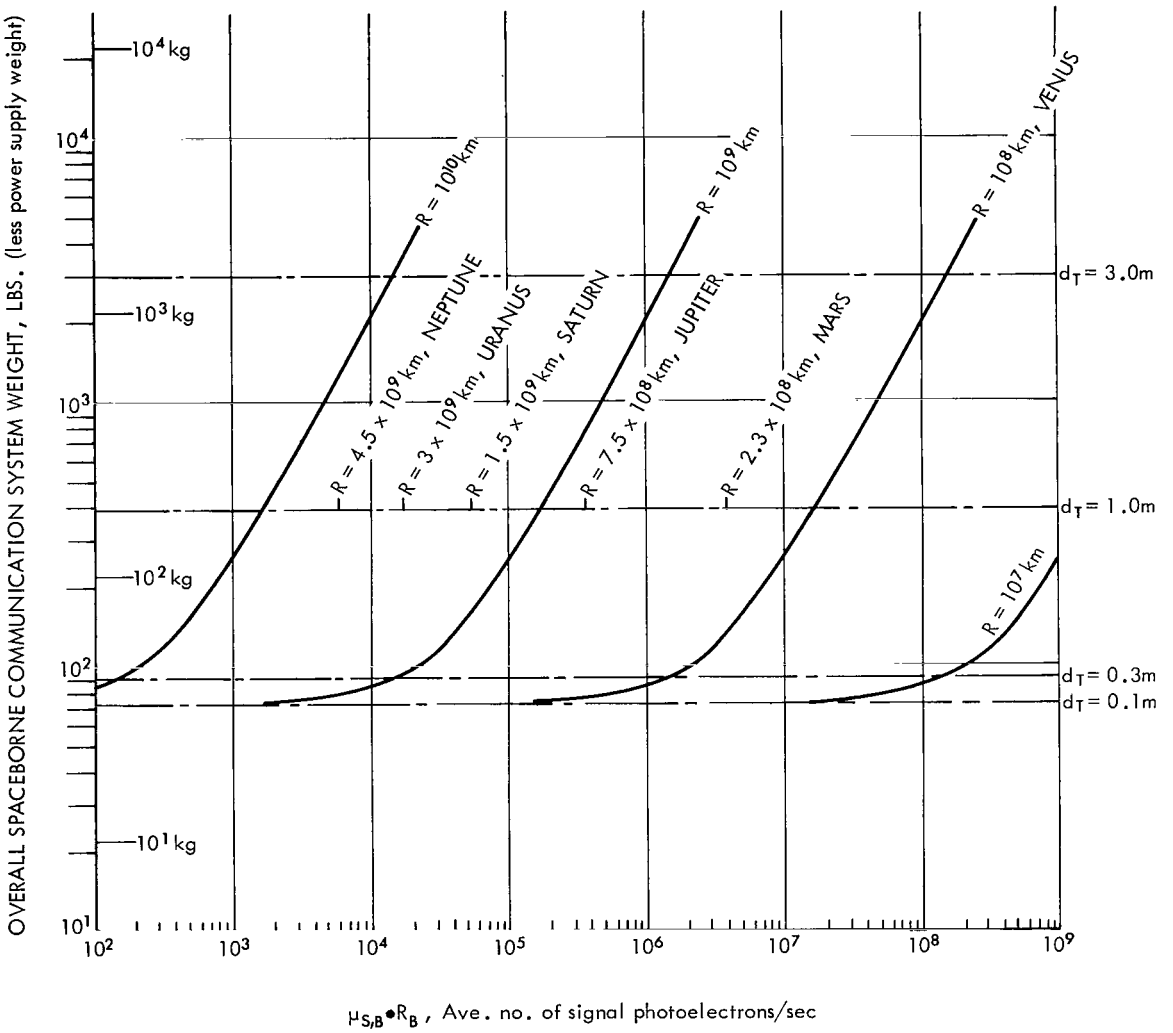

Figure 11a–Optical (visible, $\lambda = 0.53\mu$) spaceborne communication system weight versus downlink performance capability–a parametric analysis for planetary missions, for a power supply output of 1 watt.

GROUND RECEIVER CHARACTERISTICS

- Direct Detection
- Negligible Thermal and Dark Current Noise
- d_R = 10m, effective receiver aperture diameter
- θ_R = 0.1 mrad, receiver field of view
- λ_i = 10Å (10^{-9}m), receiver optical filter bandpass, centered at 0.53μ
- $\mu_{N_iB}R_B = 7.85 \times 10^8$, Ave. background noise photoelectrons/sec., ~a constant for this receiver
- μ_{S_iB}= ave. signal photoelectrons/bit
- R_B = downlink signal bit rate, bits/sec

SPACEBORNE TRANSMITTER CHARACTERISTICS

- Nd^{+++}YAG Laser with Lithium Niobate frequency doubler
- ~ 1% overall efficiency
- λ_C = 0.53μ, carrier wavelength
- P_{BB} = 10 W, power supply output
- d_T = transmitter aperture dia.
- R_B = downlink bit rate, bits/sec.
- These efficiencies and powers represent an extrapolation from operating units at ~1 W and have not yet been achieved in practice.

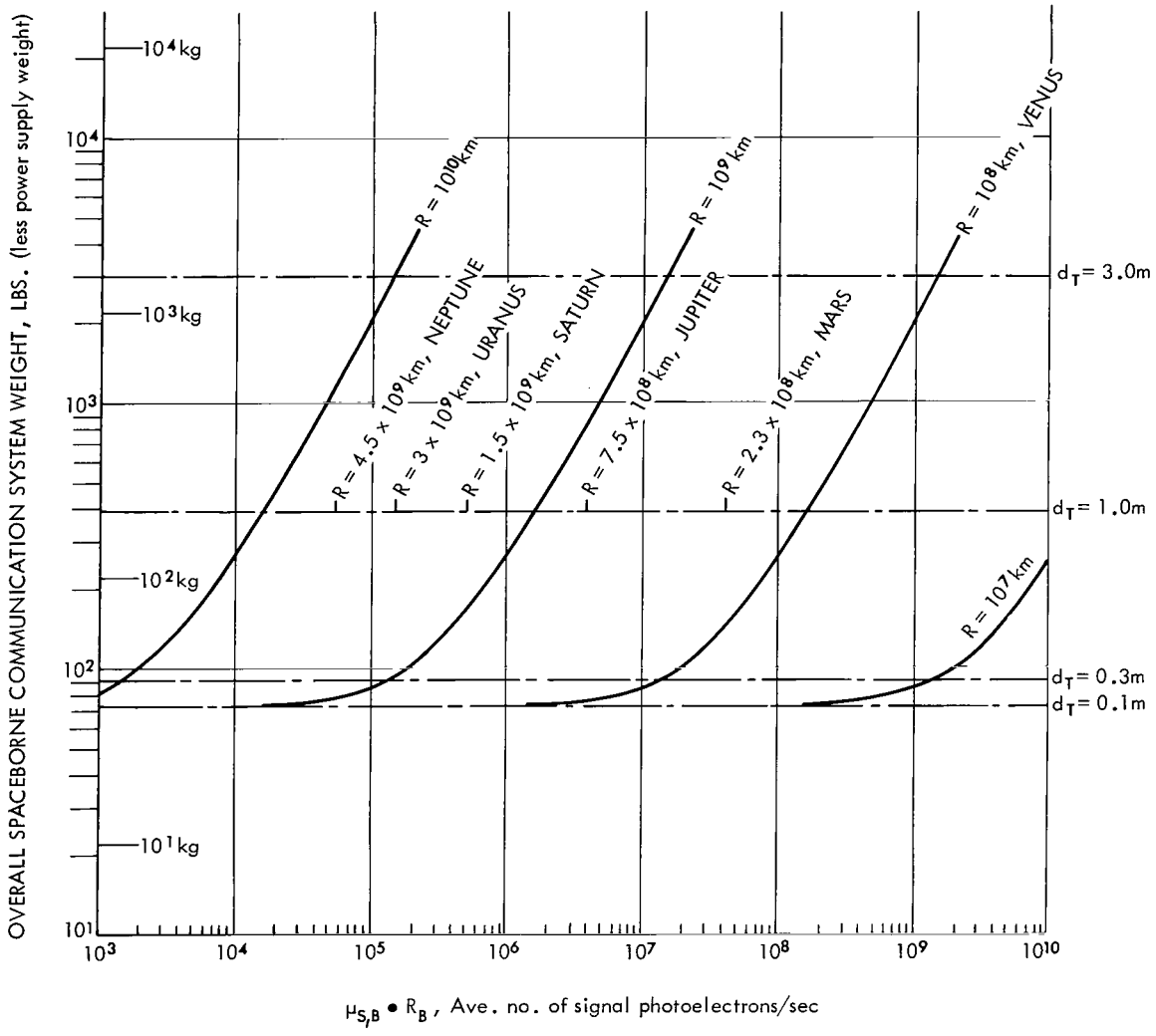

Figure 11b–Optical (visible, $\lambda = 0.53\mu$) spaceborne communication system weight versus downlink performance capability–a parametric analysis for planetary missions, for a power supply output of 10 watts.

GROUND RECEIVER CHARACTERISTICS

- Direct Detection
- Negligible Thermal and Dark Current Noise
- d_R = 10m, effective receiver aperture diameter
- θ_R = 0.1 mrad, receiver field of view
- λ_i = 10Å (10^{-9}m), receiver optical filter bandpass, centered at 0.53μ
- $\mu_{N,B}R_B = 7.85 \times 10^8$, Ave. background noise photoelectrons/sec., ~a constant for this receiver
- $\mu_{S,B}$= ave. signal photoelectrons/bit
- R_B = downlink signal bit rate, bits/sec

SPACEBORNE TRANSMITTER CHARACTERISTICS

- Nd^{+++}YAG Laser with Lithium Niobate frequency doubler
- ~ 1% overall efficiency
- λ_C = 0.53μ, carrier wavelength
- P_{BB} = 100 W, power supply output
- d_T = transmitter aperture dia.
- R_B = downlink bit rate, bits/sec.

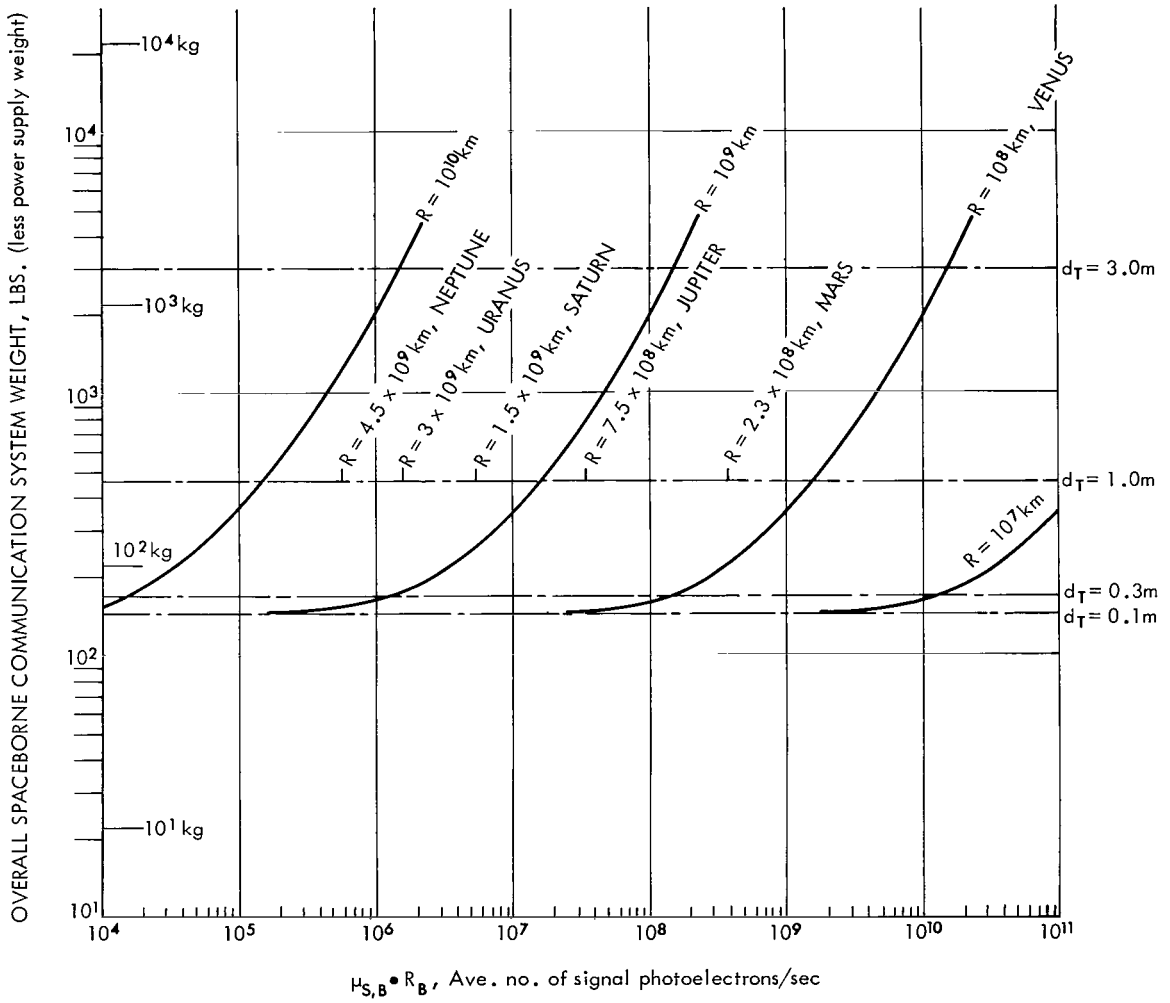

Figure 11c–Optical (visible, $\lambda = 0.53\mu$) spaceborne communication system weight versus downlink performance capability–a parametric analysis for planetary missions, for a power supply output of 100 watts.

GROUND RECEIVER CHARACTERISTICS

- Direct Detection
- Negligible Thermal and Dark Current Noise
- d_R = 10m, effective receiver aperture diameter
- θ_R = 0.1 mrad, receiver field of view
- λ_i = 10Å (10^{-9}m), receiver optical filter bandpass, centered at 0.53μ
- $\mu_{N,B}R_B = 7.85 \times 10^8$, Ave. background noise photoelectrons/sec., ~a constant for this receiver
- $\mu_{S,B}$= ave. signal photoelectrons/bit
- R_B = downlink signal bit rate, bits/sec

SPACEBORNE TRANSMITTER CHARACTERISTICS

- Nd^{+++}YAG Laser with Lithium Niobate frequency doubler
- ~ 1% overall efficiency
- λ_C = 0.53μ, carrier wavelength
- P_{BB} = 1000 W, power supply output
- d_T = transmitter aperture dia.
- R_B = downlink bit rate, bits/sec.

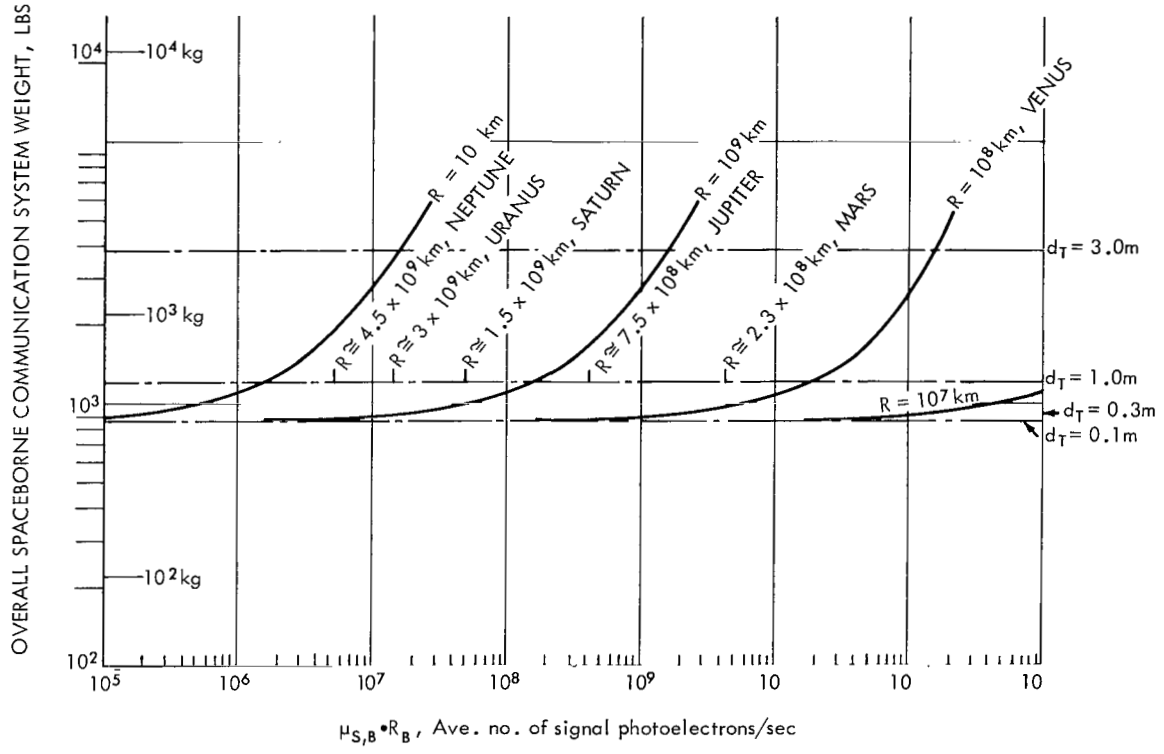

Figure 11d–Optical (visible, λ = 0.53μ) spaceborne communication system weight versus downlink performance capability–a parametric analysis for planetary missions, for a power supply output of 1000 watts.

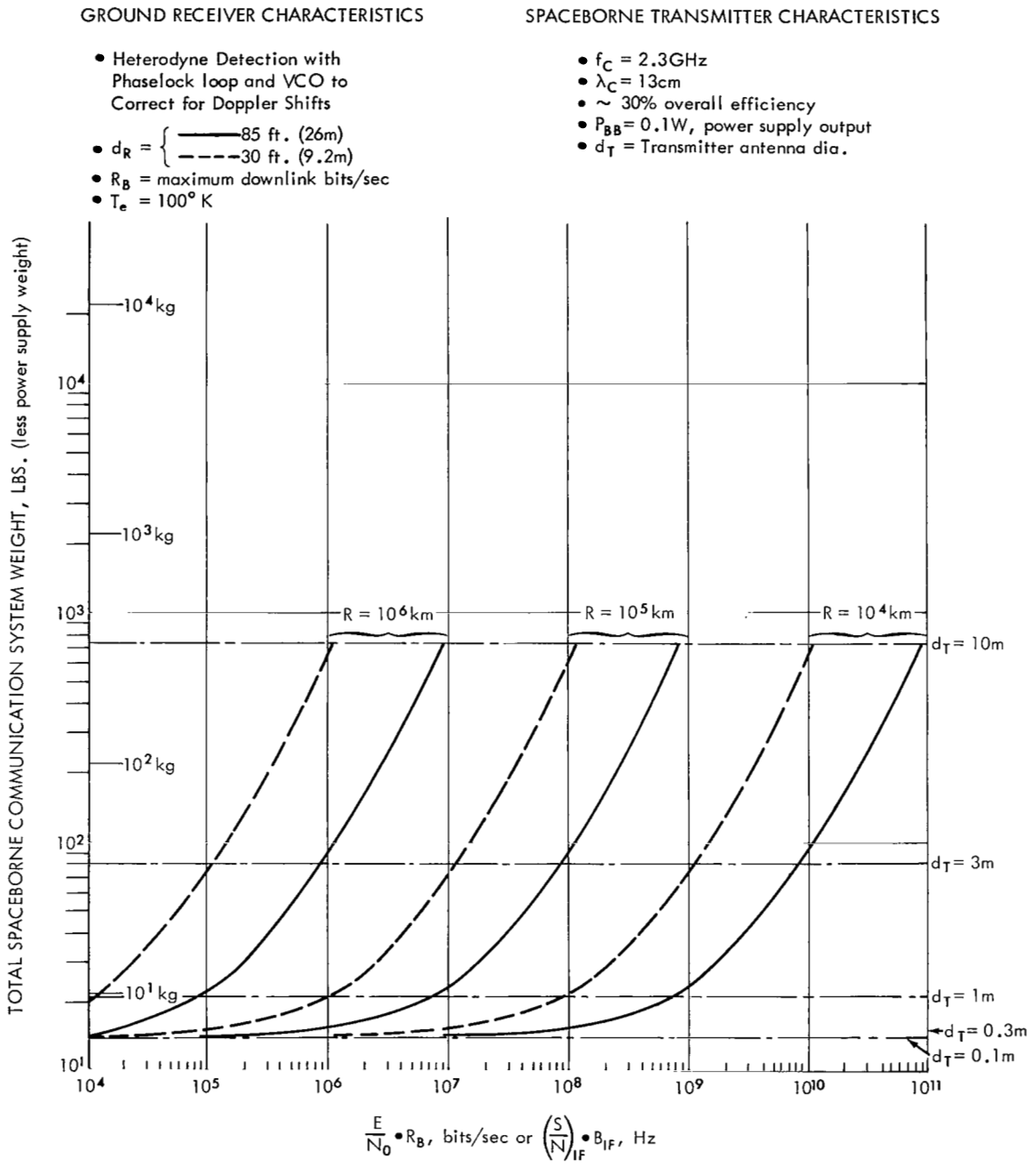

Figure 12a–S-band (f = 2.3 GHz) spaceborne communication system weight versus downlink performance capability–a parametric analysis for earth and lunar missions, for a power supply output of 0.1 watt.

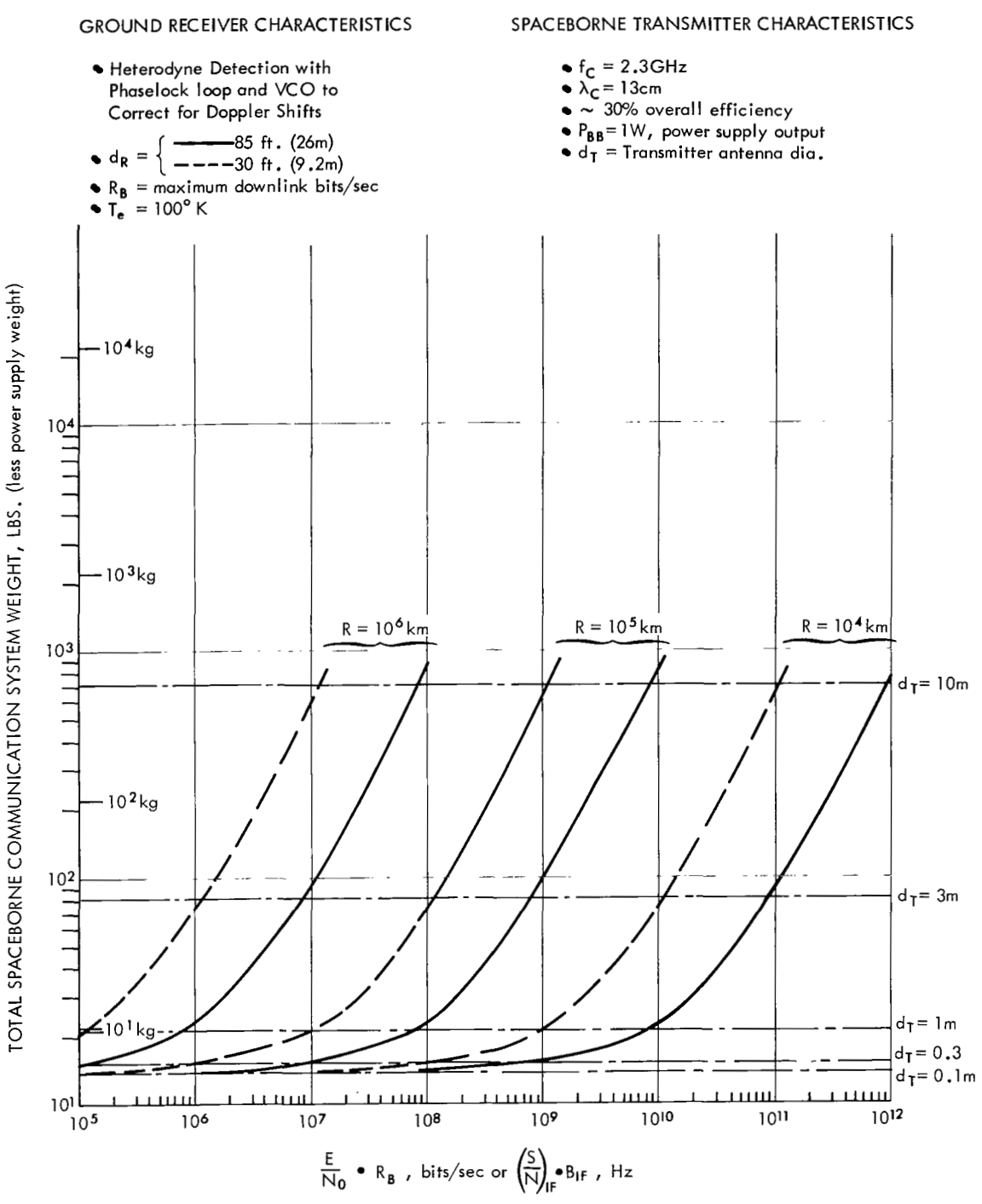

Figure 12b–S-band (f = 2.3 GHz) spaceborne communication system weight versus downlink performance capability–a parametric analysis for earth and lunar missions, for a power supply output of 1 watt.

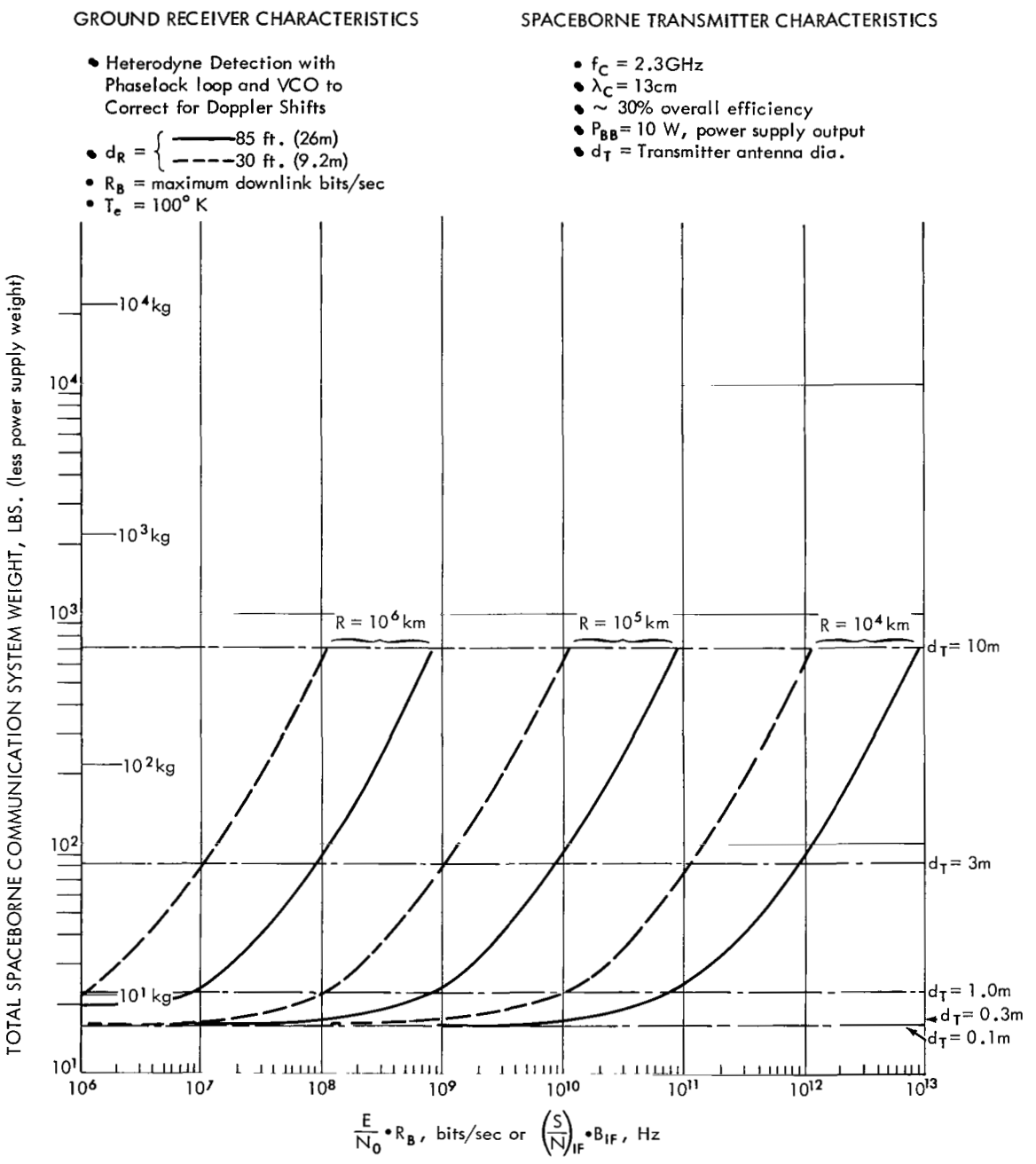

Figure 12c–S-band (f = 2.3 GHz) spaceborne communication system weight versus downlink performance capability–a parametric analysis for earth and lunar missions, for a power supply output of 10 watts.

GROUND RECEIVER CHARACTERISTICS

- Heterodyne Detection with Phaselock loop and VCO to Correct for Doppler Shifts
- d_R = ——85 ft. (26m) / – – – –30 ft. (9.2m)
- R_B = maximum downlink bits/sec
- T_e = 100° K

SPACEBORNE TRANSMITTER CHARACTERISTICS

- f_C = 2.3GHz
- λ_C = 13cm
- ~ 30% overall efficiency
- P_{BB} = 100 W, power supply output
- d_T = Transmitter antenna dia.

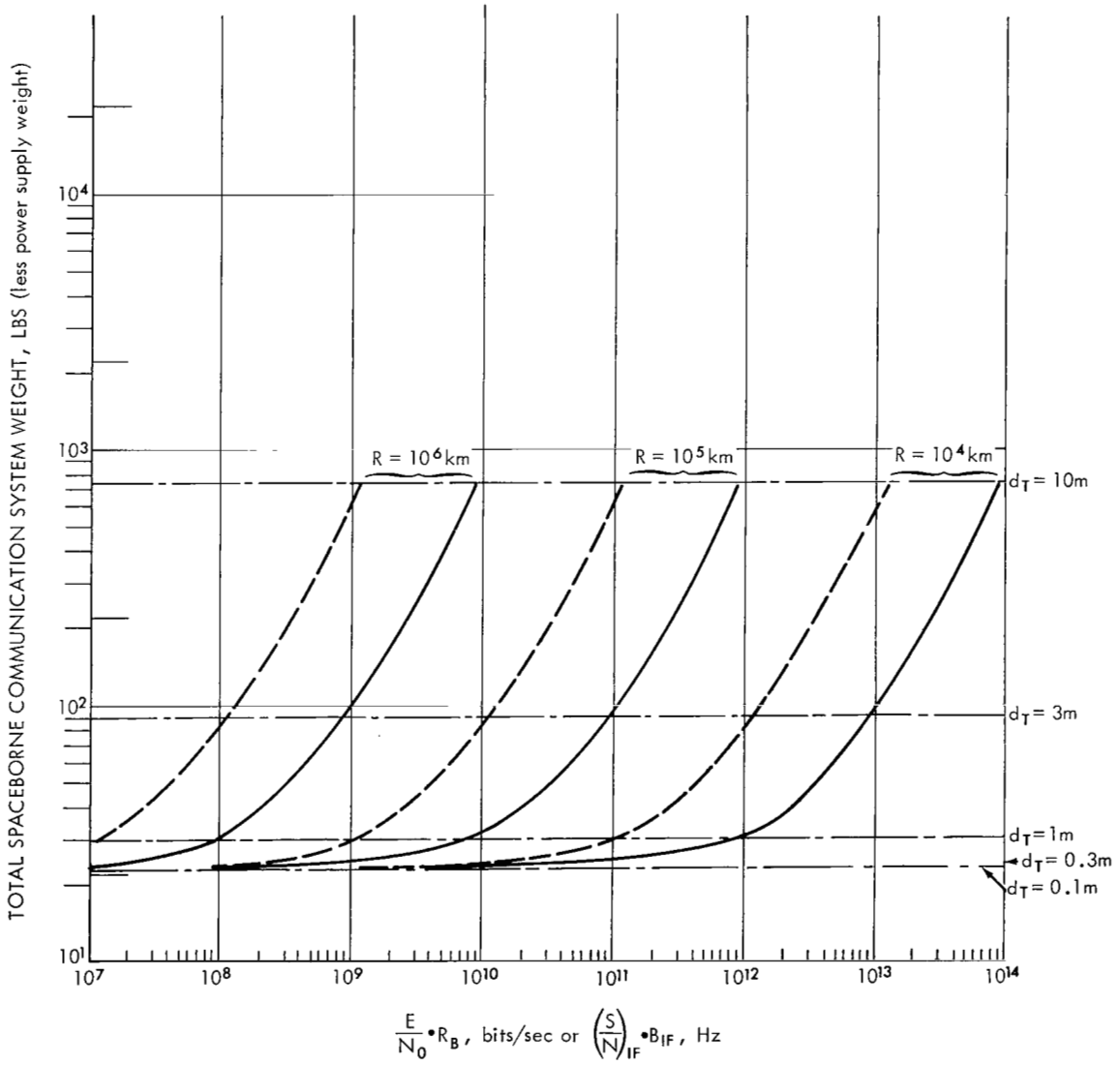

Figure 12d–S-band (f = 2.3 GHz) spaceborne communication system weight versus downlink performance capability–a parametric analysis for earth and lunar missions, for a power supply output of 100 watts.

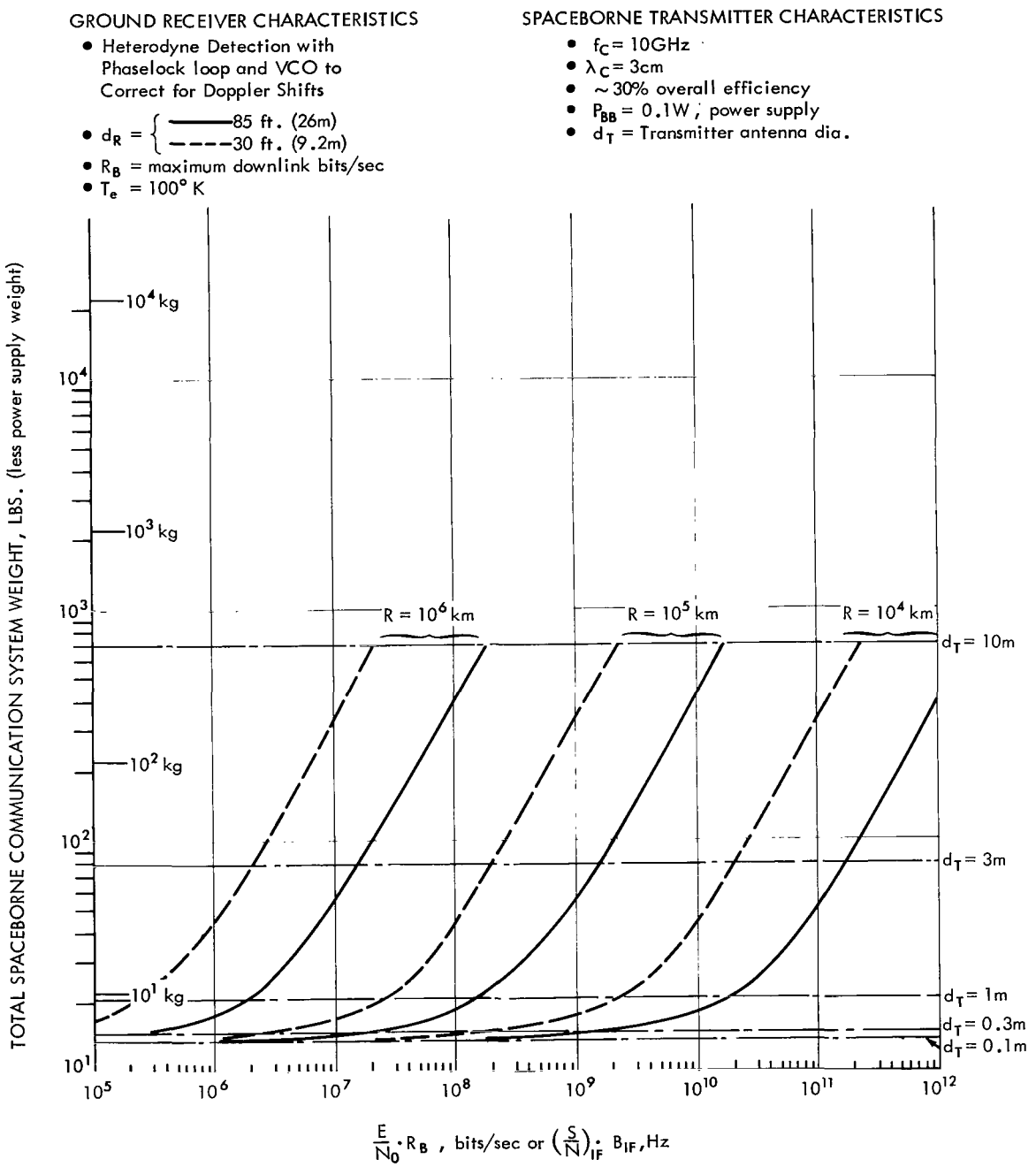

Figure 13a–X-band (f = 10 GHz) spaceborne communication system weight versus downlink performance capability–a parametric analysis for earth and lunar missions, for a power supply output of 0.1 watt.

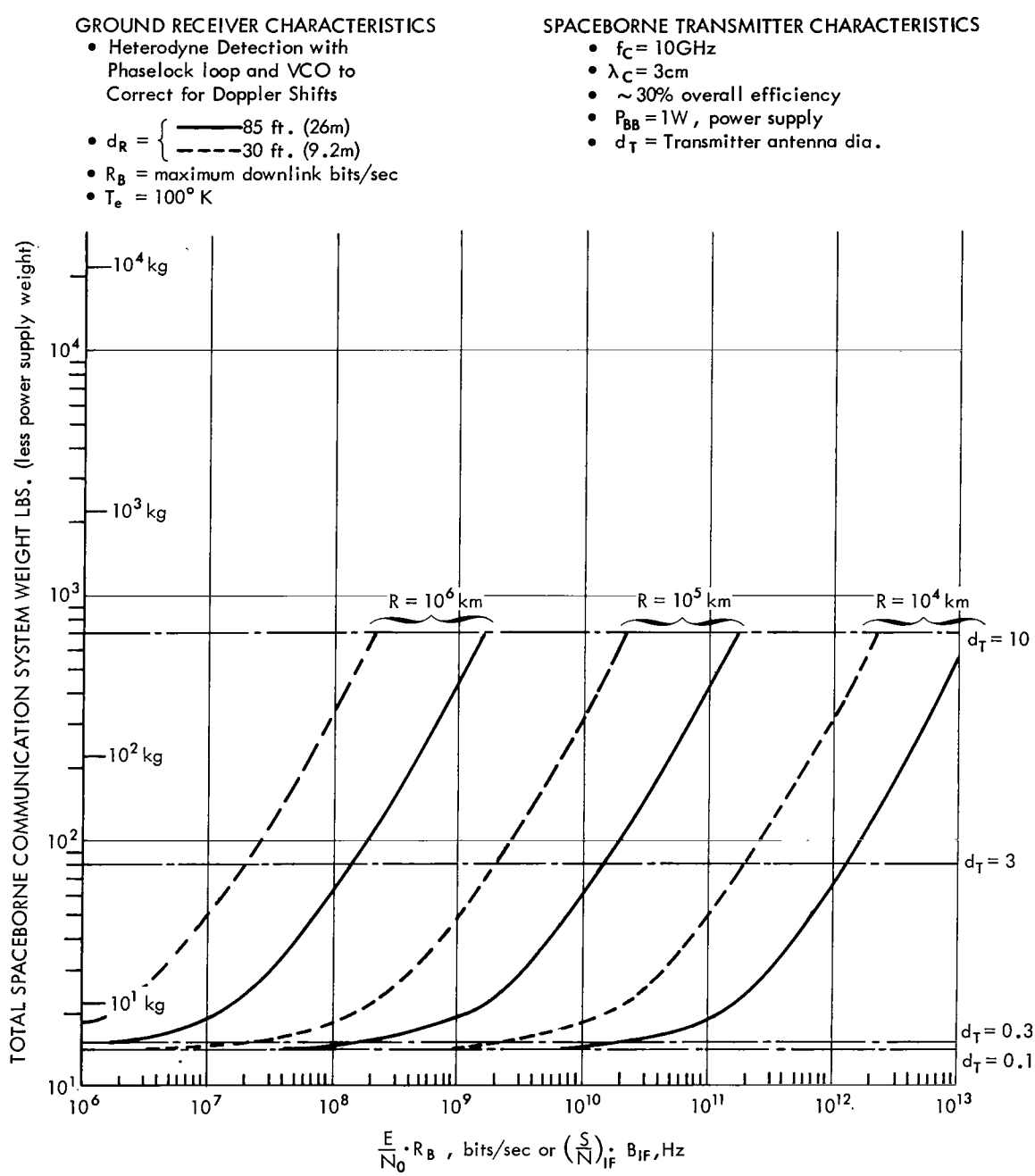

Figure 13b–X-band (f = 10 GHz) spaceborne communication system weight versus downlink performance capability–a parametric analysis for earth and lunar missions, for a power supply output of 1 watt.

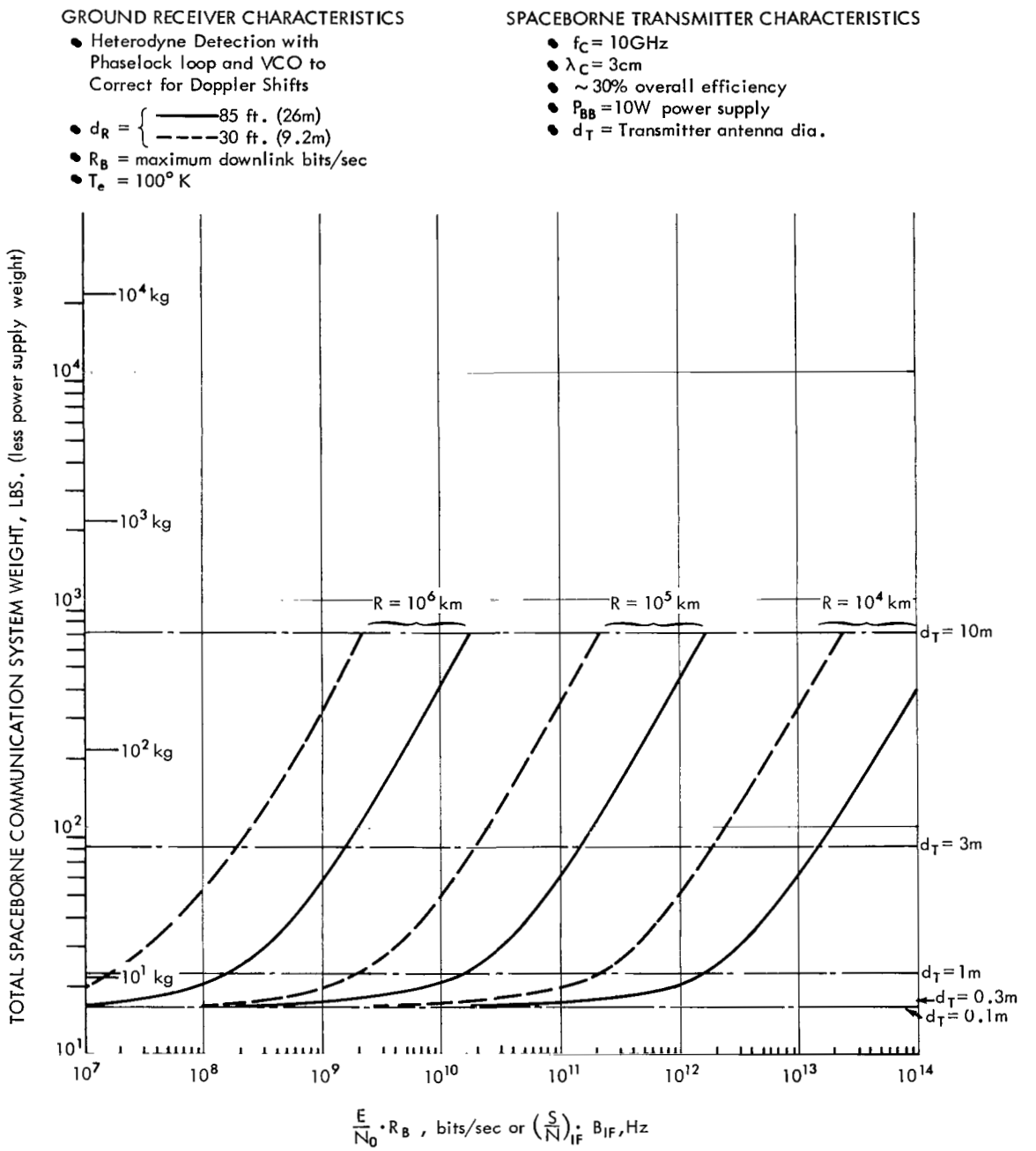

Figure 13c–X-band (f = 10 GHz) spaceborne communication system weight versus downlink performance capability–a parametric analysis for earth and lunar missions, for a power supply output of 10 watts.

GROUND RECEIVER CHARACTERISTICS

- Heterodyne Detection with Phaselock loop and VCO to Correct for Doppler Shifts
- d_R = { ——— 85 ft. (26m); – – – – 30 ft. (9.2m) }
- R_B = maximum downlink bits/sec
- T_e = 100° K

SPACEBORNE TRANSMITTER CHARACTERISTICS

- f_C = 10GHz
- λ_C = 3cm
- ~30% overall efficiency
- P_{BB} = 100W, power supply
- d_T = Transmitter antenna dia.

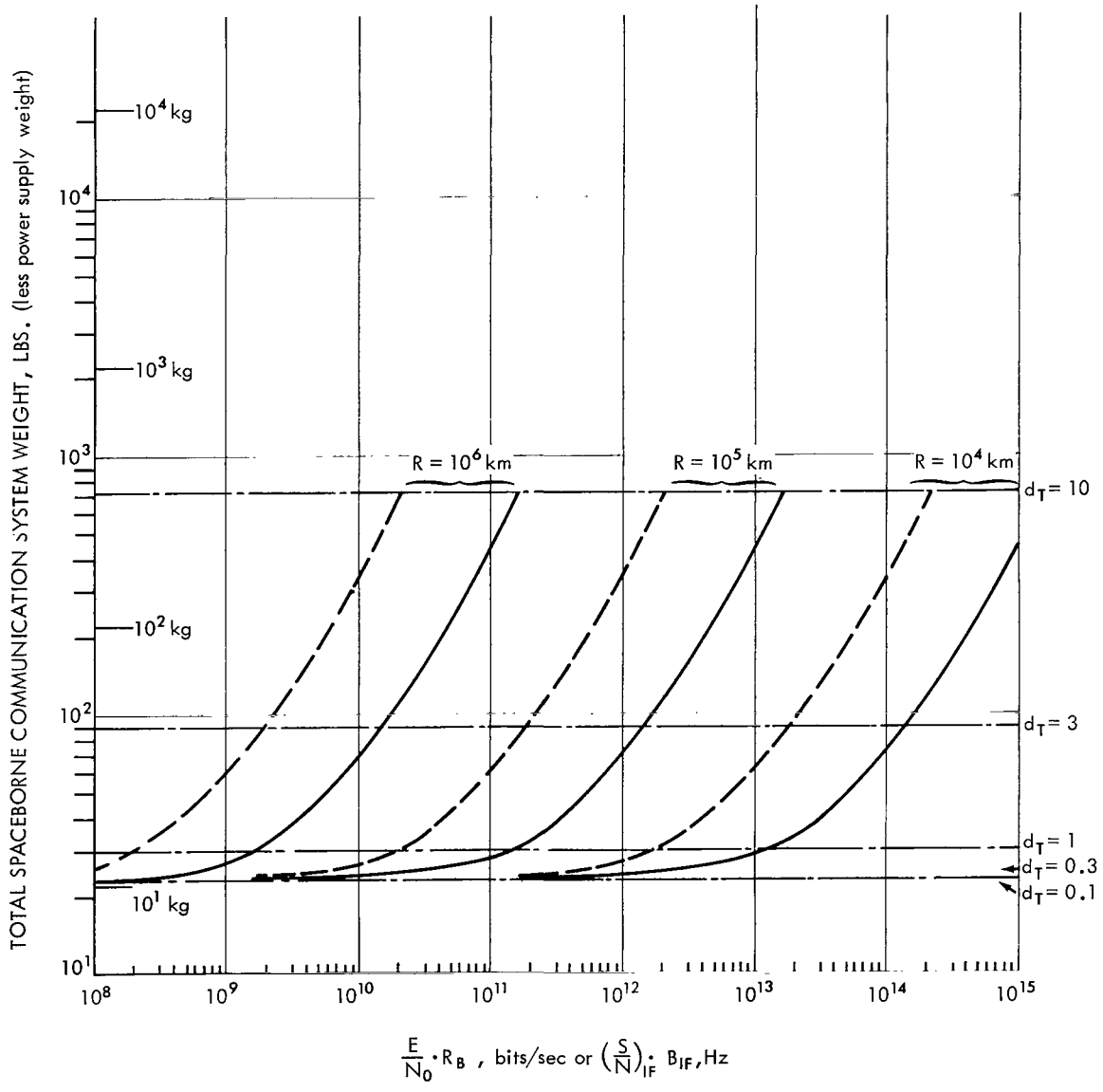

Figure 13d–X-band (f = 10 GHz) spaceborne communication system weight versus downlink performance capability–a parametric analysis for earth and lunar missions, for a power supply output of 100 watts.

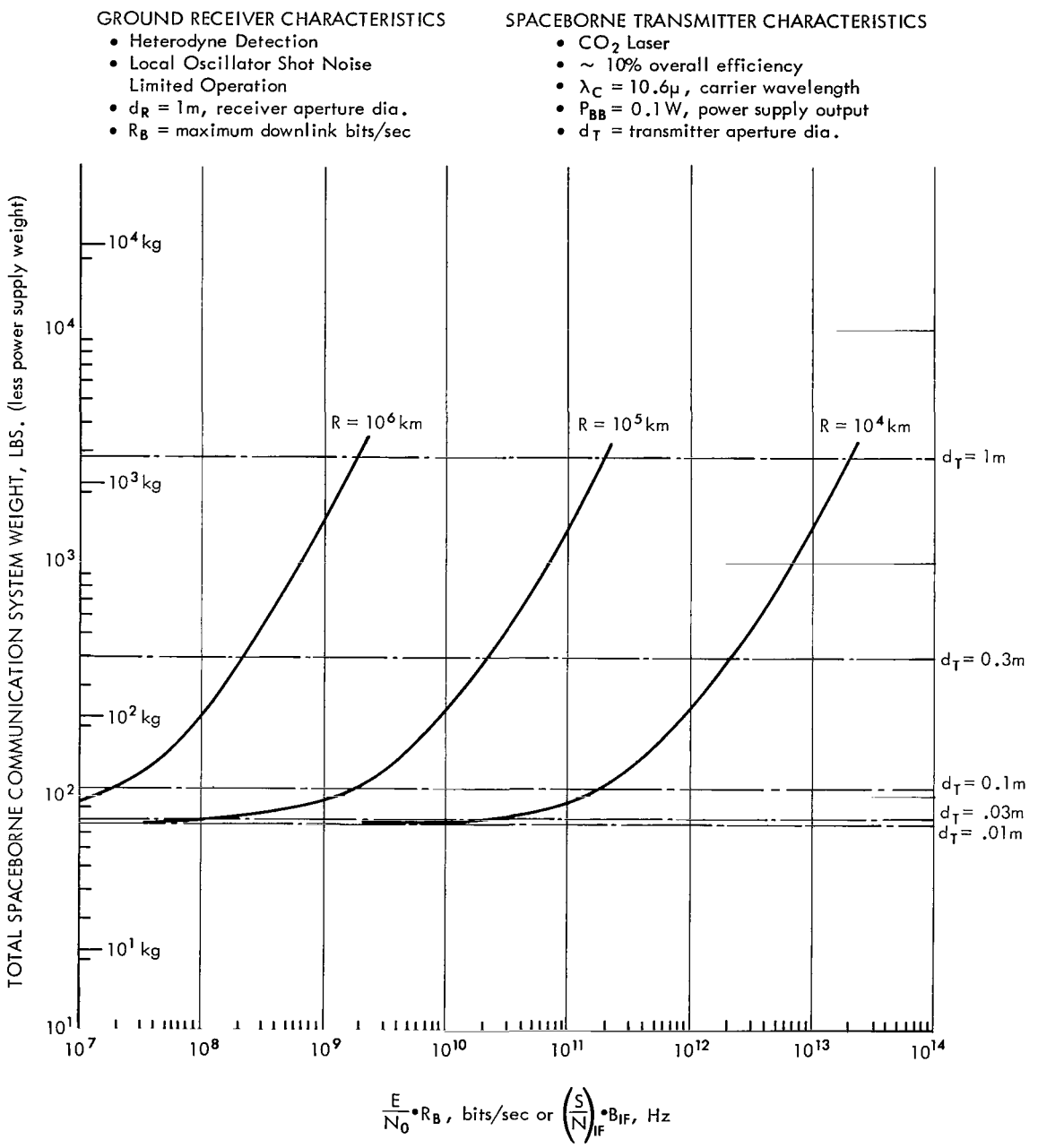

Figure 14a–Optical (IR, λ = 10.6μ) spaceborne communication system weight versus downlink performance capability–a parametric analysis for earth and lunar missions, for a power supply output of 0.1 watt.

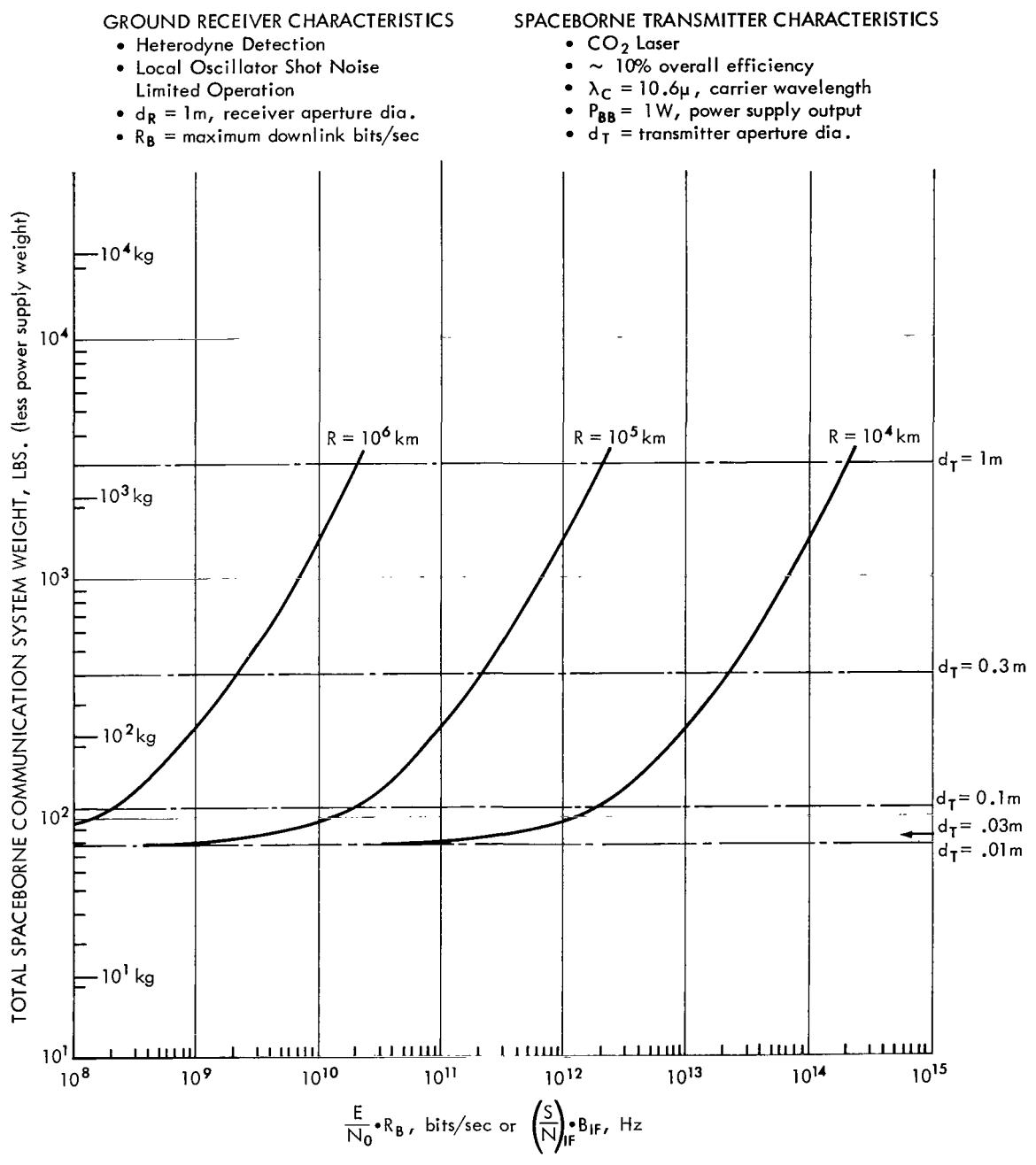

Figure 14b–Optical (IR, λ = 10.6μ) spaceborne communication system weight versus downlink performance capability–a parametric analysis for earth and lunar missions, for a power supply output of 1 watt.

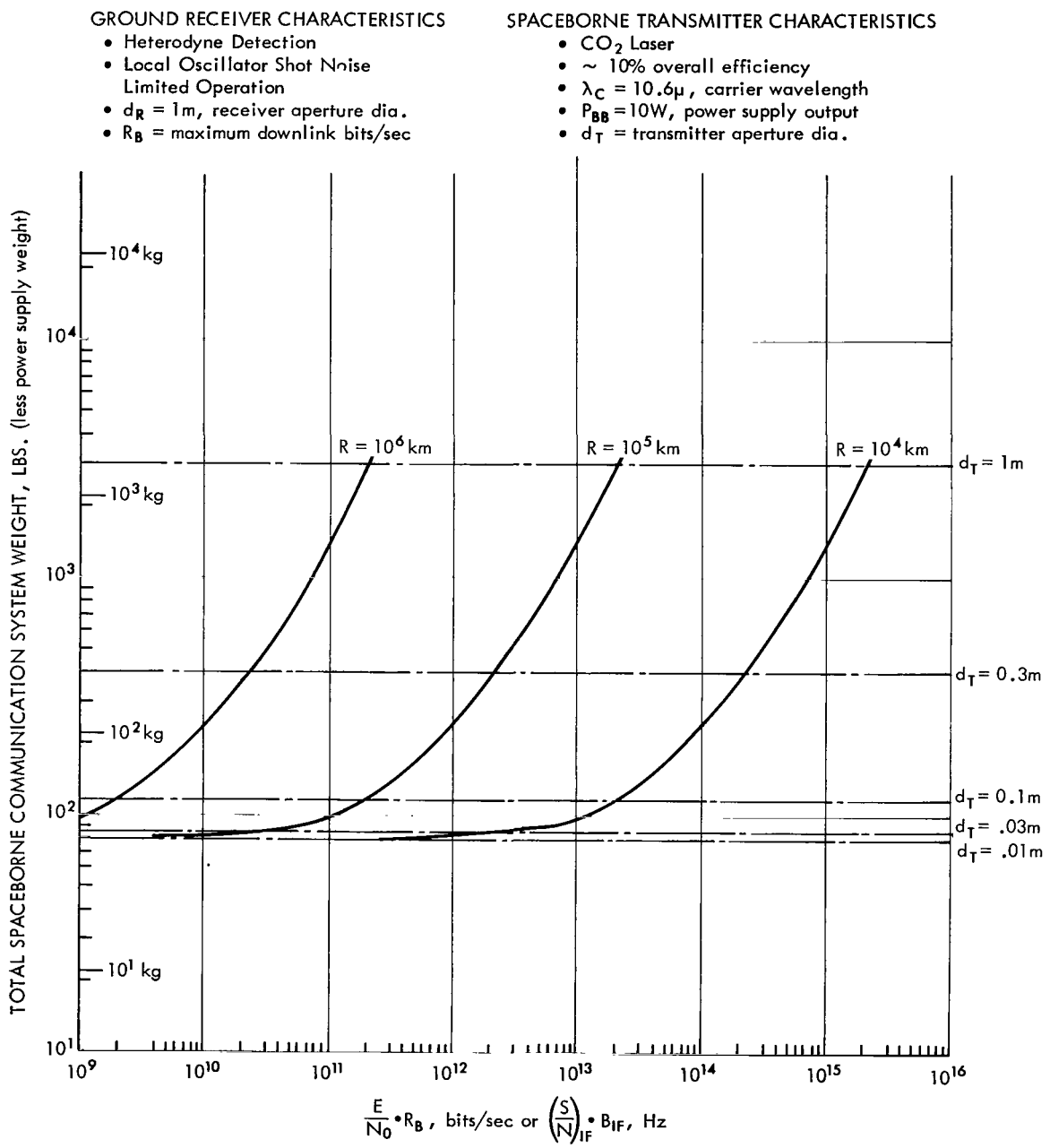

Figure 14c–Optical (IR, $\lambda = 10.6\mu$) spaceborne communication system weight versus downlink performance capability–a parametric analysis for earth and lunar missions, for a power supply output of 10 watts.

GROUND RECEIVER CHARACTERISTICS

- Heterodyne Detection
- Local Oscillator Shot Noise Limited Operation
- d_R = 1m, receiver aperture dia.
- R_B = maximum downlink bits/sec

SPACEBORNE TRANSMITTER CHARACTERISTICS

- CO_2 Laser
- ~ 10% overall efficiency
- λ_C = 10.6μ, carrier wavelength
- P_{BB} = 100 W, power supply output
- d_T = transmitter aperture dia.

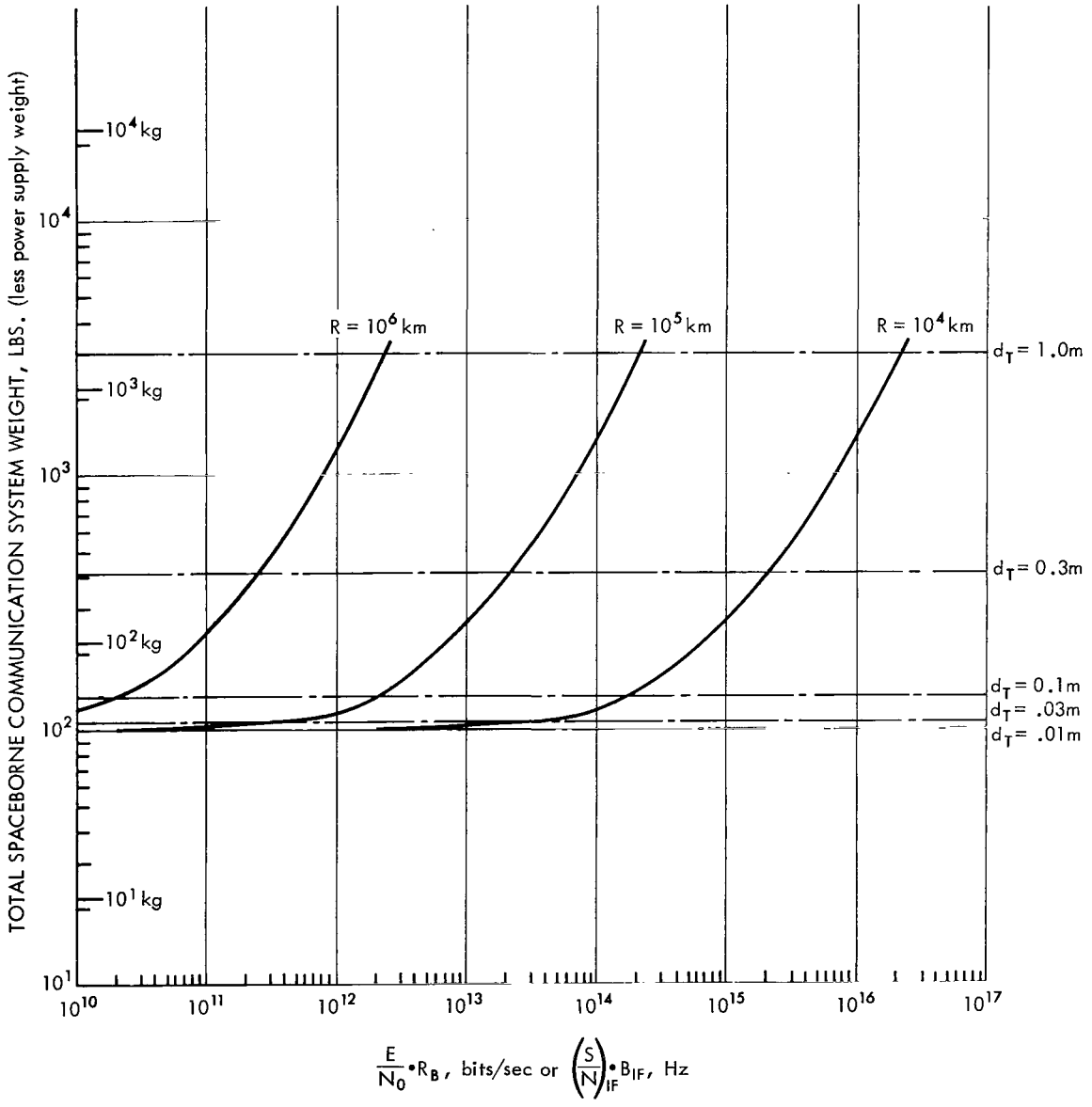

Figure 14d–Optical (IR, λ = 10.6μ) spaceborne communication system weight versus downlink performance capability–a parametric analysis for earth and lunar missions, for a power supply output of 100 watts.

GROUND RECEIVER CHARACTERISTICS

- Direct Detection
- Negligible Thermal and Dark Current Noise
- d_R = 1m, effective receiver aperture diameter
- θ_R = 0.1mrad, receiver field of view
- λ_i = 10Å (10^{-9}m), receiver optical filter bandpass, centered at 0.53μ
- $\mu_{N,B} \cdot R_B = 7.85 \times 10^8$, Ave. background noise photoelectrons/sec., ~a constant for this receiver
- R_B = max. downlink bit rate, bits/sec
- $\mu_{S,B}$= ave. signal photoelectrons/bit

SPACEBORNE TRANSMITTER CHARACTERISTICS

- Nd^{+++}YAG Laser with Lithium Niobate frequency doubler
- ~1% overall efficiency
- λ_C = 0.53 μ, carrier wavelength
- P_{BB} = 0.01W, power supply output
- d_T = transmitter aperture dia.
- These efficiencies and powers represent an extrapolation from operating units at ~1W and have not yet been achieved in practice.

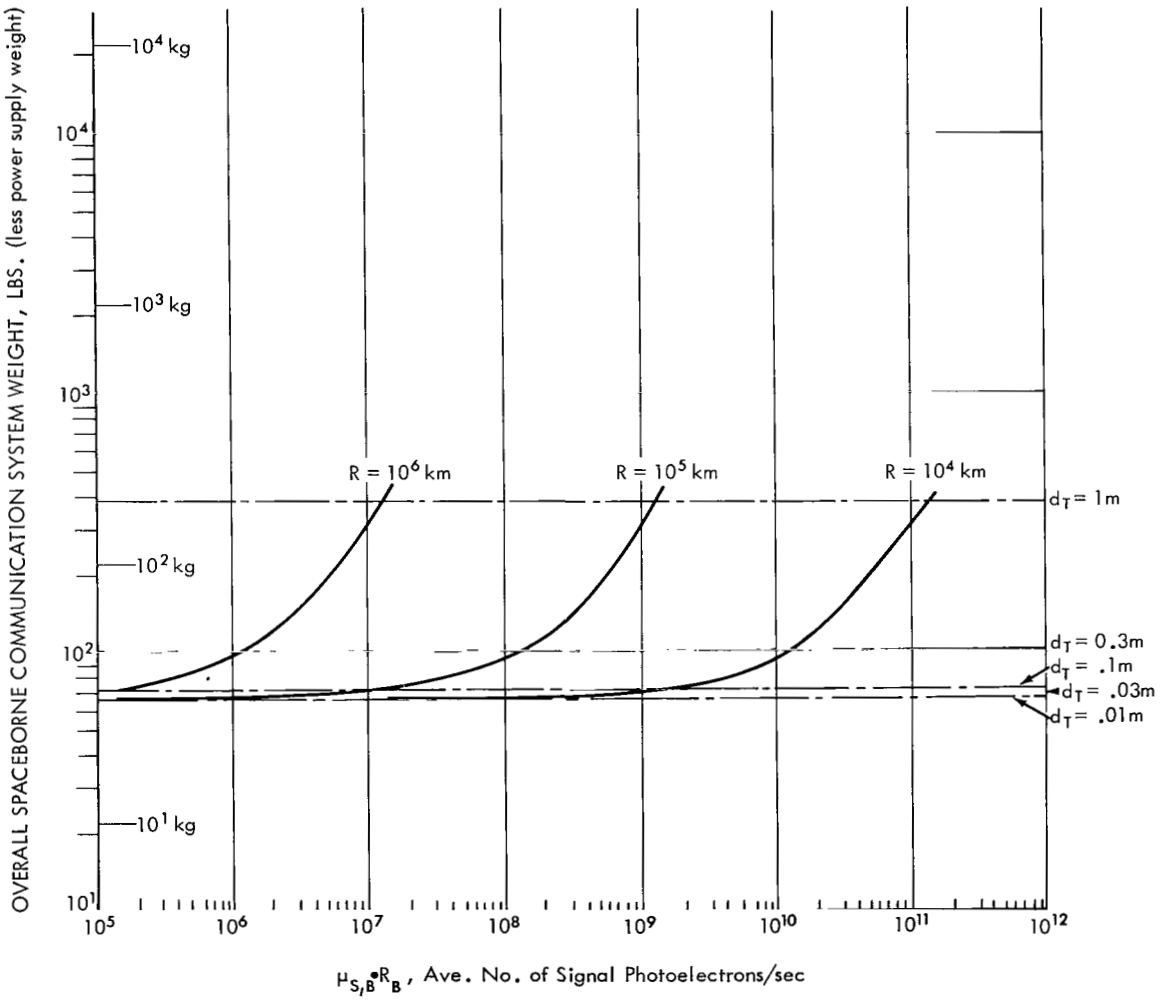

Figure 15a–Optical (visible, $\lambda = 0.53\mu$) spaceborne communication system weight versus downlink performance capability–a parametric analysis for earth and lunar missions, for a power supply output of 0.01 watt.

GROUND RECEIVER CHARACTERISTICS

- Direct Detection
- Negligible Thermal and Dark Current Noise
- d_R = 1m, effective receiver aperture diameter
- θ_R = 0.1mrad, receiver field of view
- λ_i = 10Å (10^{-9}m), receiver optical filter bandpass, centered at 0.53μ
- $\mu_{N,B} \cdot R_B$ = 7.85×10^8, Ave. background noise photoelectrons/sec., ~a constant for this receiver
- R_B = max. downlink bit rate, bits/sec
- $\mu_{S,B}$ = ave. signal photoelectrons/bit

SPACEBORNE TRANSMITTER CHARACTERISTICS

- Nd^{+++}YAG Laser with Lithium Niobate frequency doubler
- ~1% overall efficiency
- λ_C = 0.53 μ, carrier wavelength
- P_{BB} = 0.1W, power supply output
- d_T = transmitter aperture dia.
- These efficiencies and powers represent an extrapolation from operating units at ~1W and have not yet been achieved in practice.

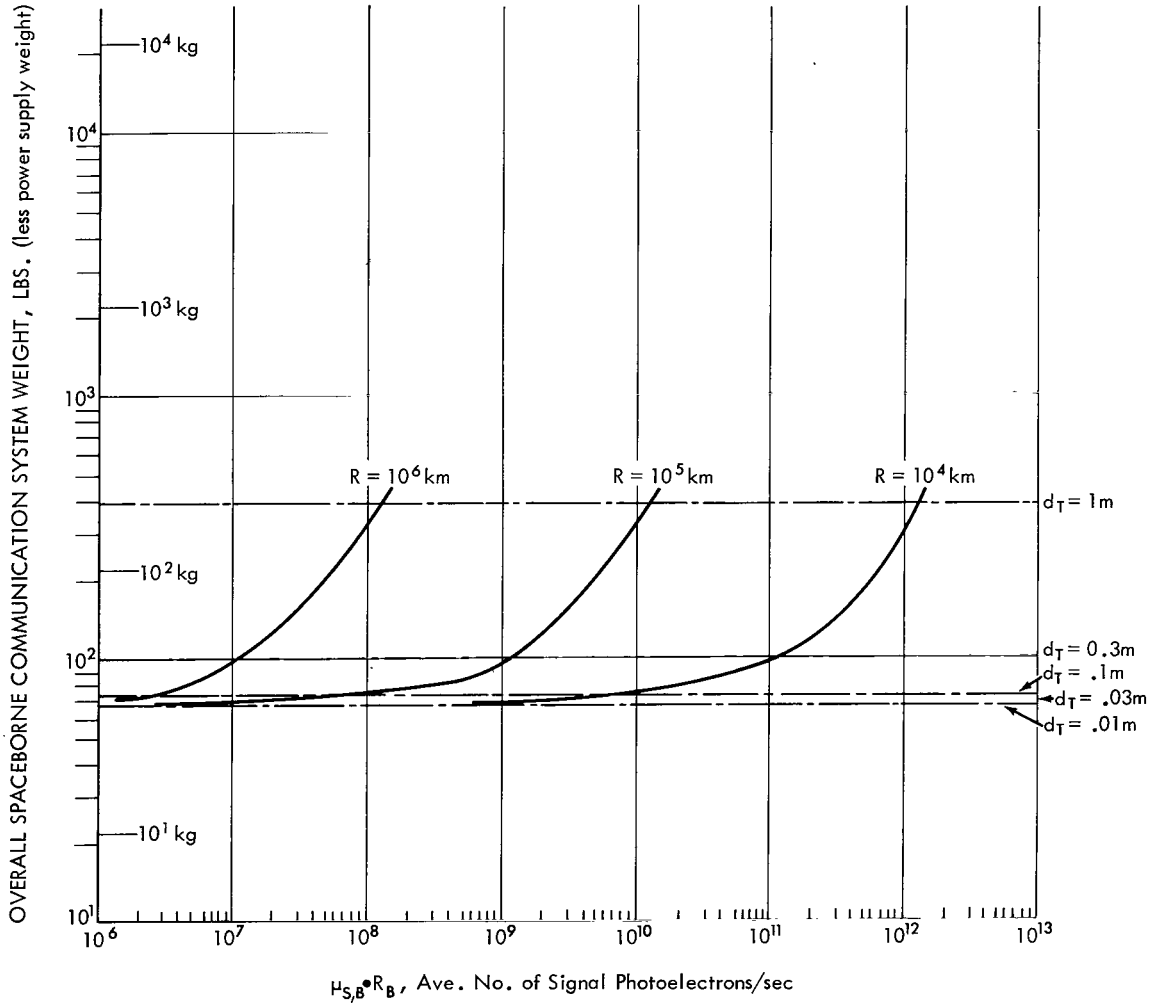

Figure 15b–Optical (visible, λ = 0.53μ) spaceborne communication system weight versus downlink performance capability–a parametric analysis for earth and lunar missions, for a power supply output of 0.1 watt.

GROUND RECEIVER CHARACTERISTICS

- Direct Detection
- Negligible Thermal and Dark Current Noise
- d_R = 1m, effective receiver aperture diameter
- θ_R = 0.1mrad, receiver field of view
- λ_i = 10Å (10^{-9}m), receiver optical filter bandpass, centered at 0.53μ
- $\mu_{N,B} \cdot R_B$ = 7.85×10^8, Ave. background noise photoelectrons/sec., ~a constant for this receiver
- R_B = max. downlink bit rate, bits/sec
- $\mu_{S,B}$ = ave. signal photoelectrons/bit

SPACEBORNE TRANSMITTER CHARACTERISTICS

- Nd^{+++}YAG Laser with Lithium Niobate frequency doubler
- ~1% overall efficiency
- λ_C = 0.53 μ, carrier wavelength
- P_{BB} = 1 W, power supply output
- d_T = transmitter aperture dia.
- These efficiencies and powers represent an extrapolation from operating units at ~1 W and have not yet been achieved in practice.

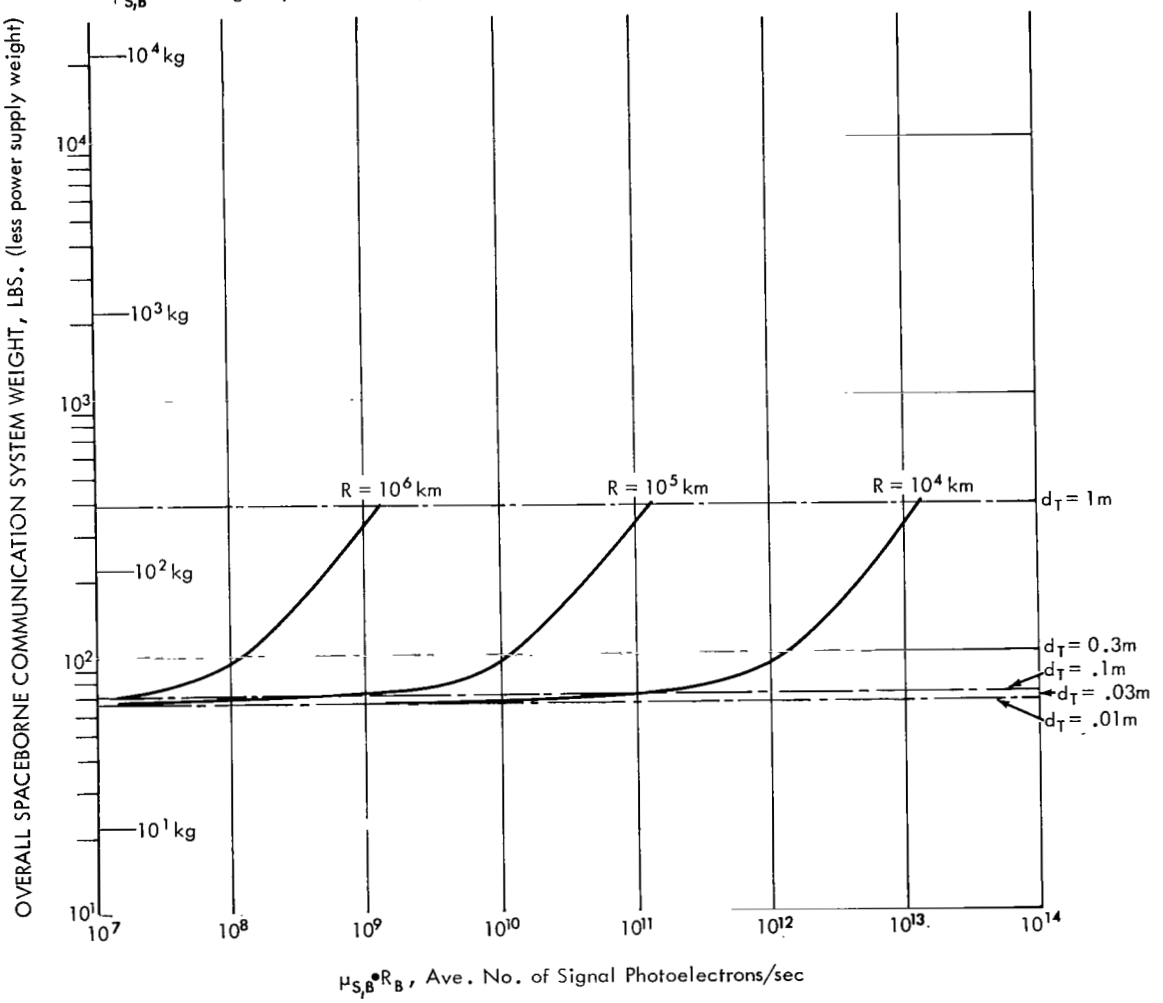

Figure 15c–Optical (visible, $\lambda = 0.53\mu$) spaceborne communication system weight versus downlink performance capability–a parametric analysis for earth and lunar missions, for a power supply output of 1 watt.

GROUND RECEIVER CHARACTERISTICS

- Direct Detection
- Negligible Thermal and Dark Current Noise
- d_R = 1m, effective receiver aperture diameter
- θ_R = 0.1mrad, receiver field of view
- λ_i = 10Å (10^{-9}m), receiver optical filter bandpass, centered at 0.53μ
- $\mu_{N,B} \cdot R_B$ = 7.85 x 10^8, Ave. background noise photoelectrons/sec., ~a constant for this receiver
- R_B = max. downlink bit rate, bits/sec
- $\mu_{S,B}$= ave. signal photoelectrons/bit

SPACEBORNE TRANSMITTER CHARACTERISTICS

- Nd^{+++}YAG Laser with Lithium Niobate frequency doubler
- ~1% overall efficiency
- λ_C = 0.53 μ, carrier wavelength
- P_{BB} =10W, power supply output
- d_T = transmitter aperture dia.
- These efficiencies and powers represent an extrapolation from operating units at ~1 W and have not yet been achieved in practice.

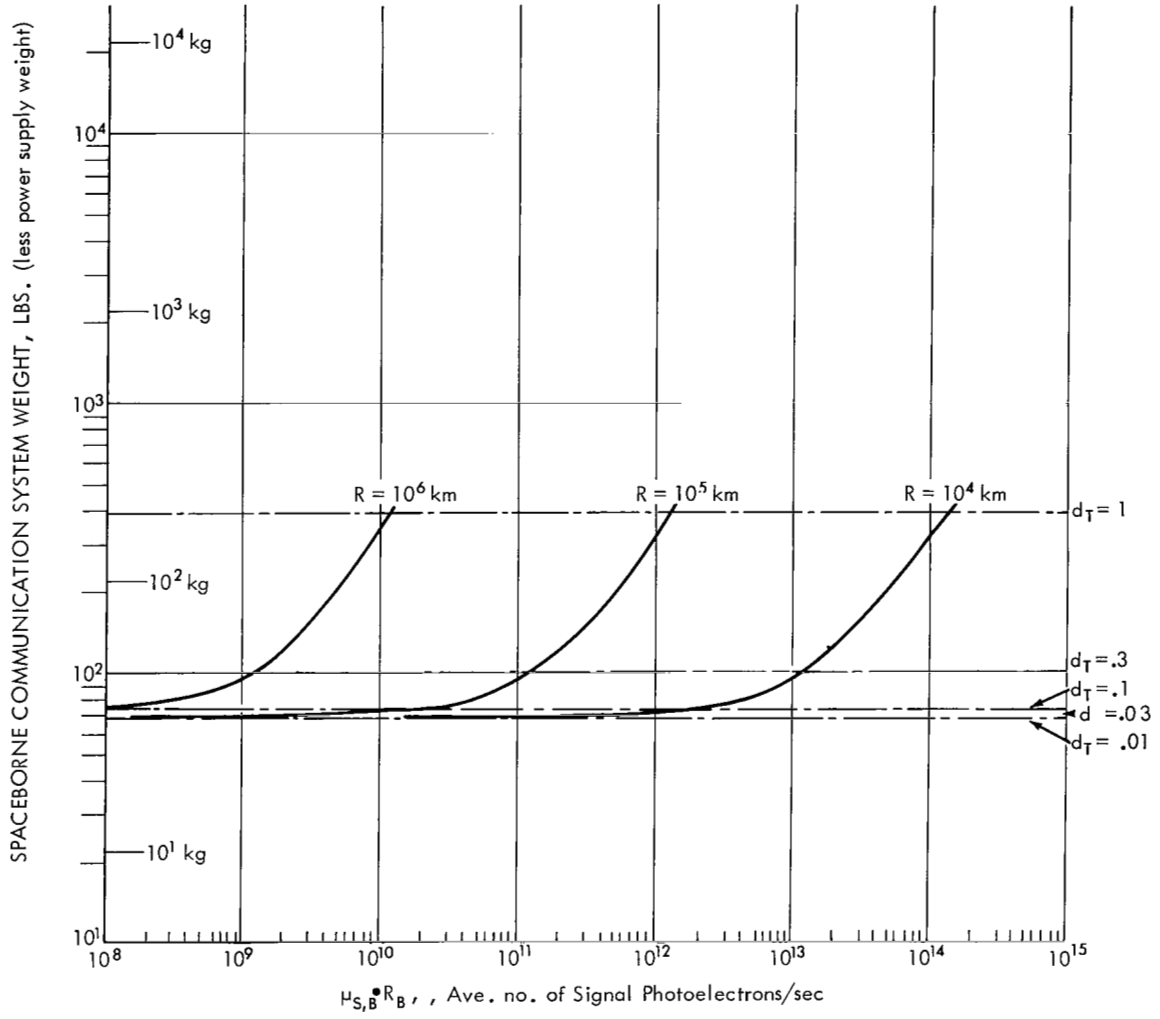

Figure 15d–Optical (visible, $\lambda = 0.53\mu$) spaceborne communication system weight versus downlink performance capability–a parametric analysis for earth and lunar missions, for a power supply output of 10 watts.

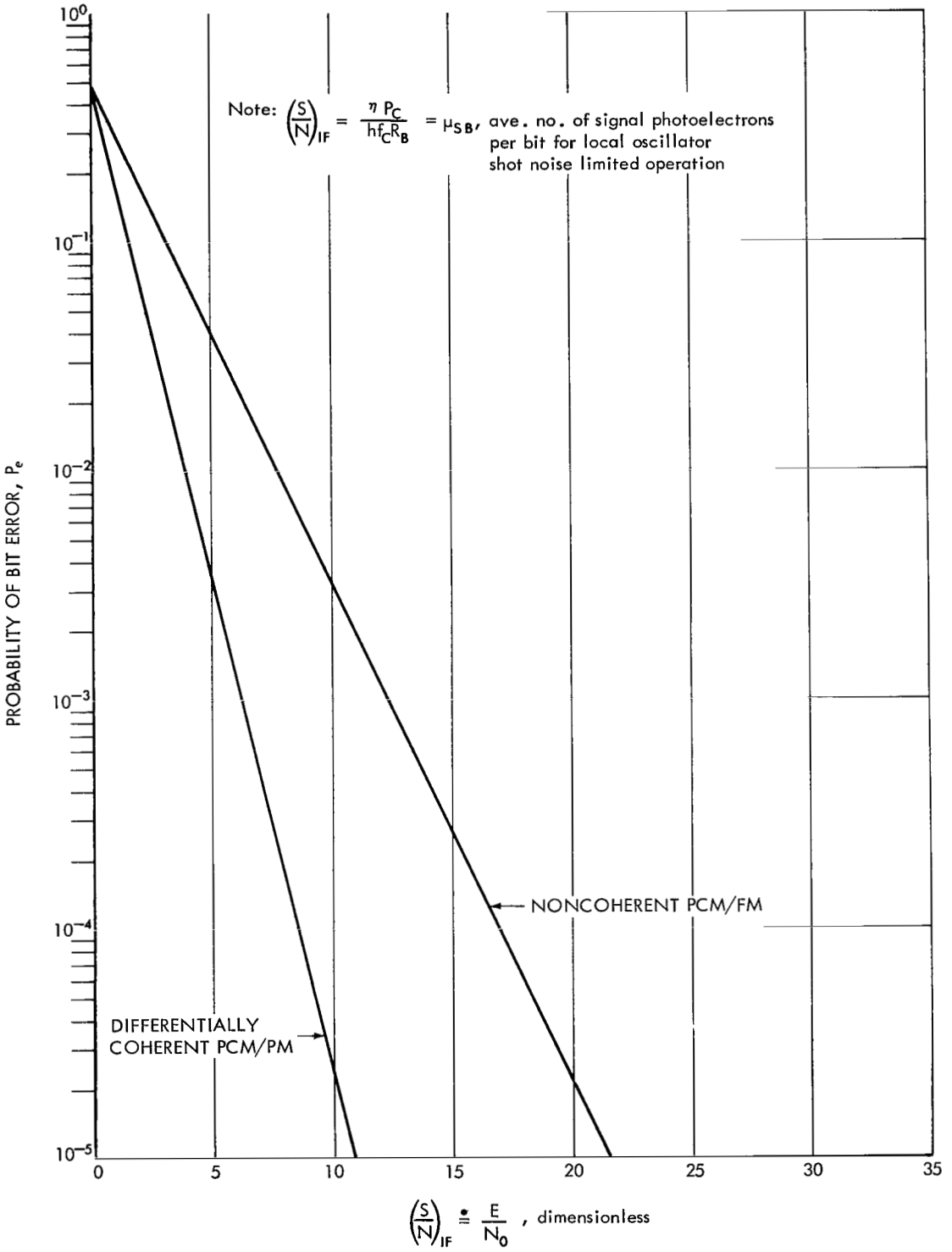

Figure 16–Probability of detection error for optical heterodyne communication with two possible types of modulation.

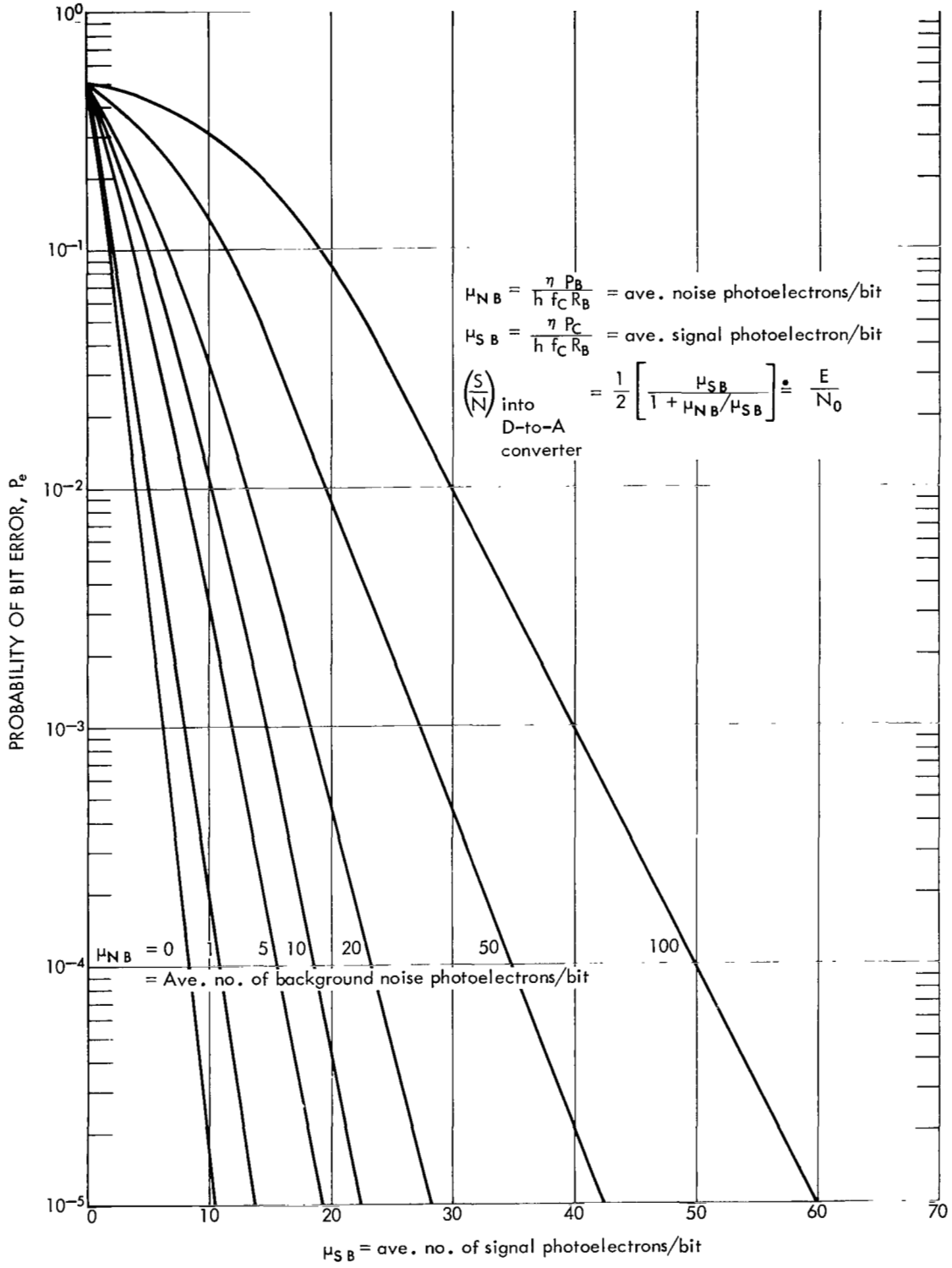

Figure 17–Probability of detection error for a PCM/PL, optical direct-detection communication system.

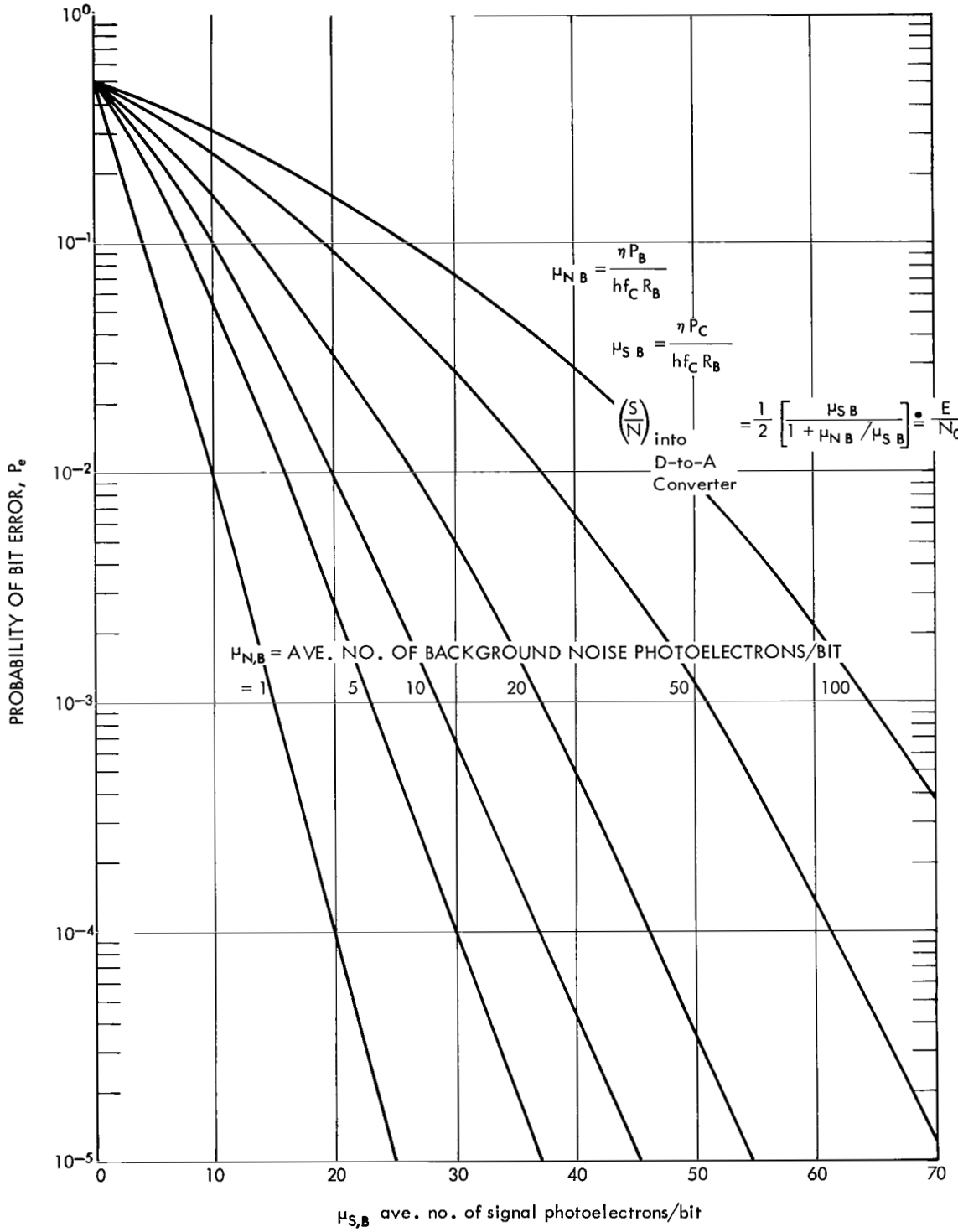

Figure 18–Probability of detection error for a PCM/IM, optical direct-detection communication system.

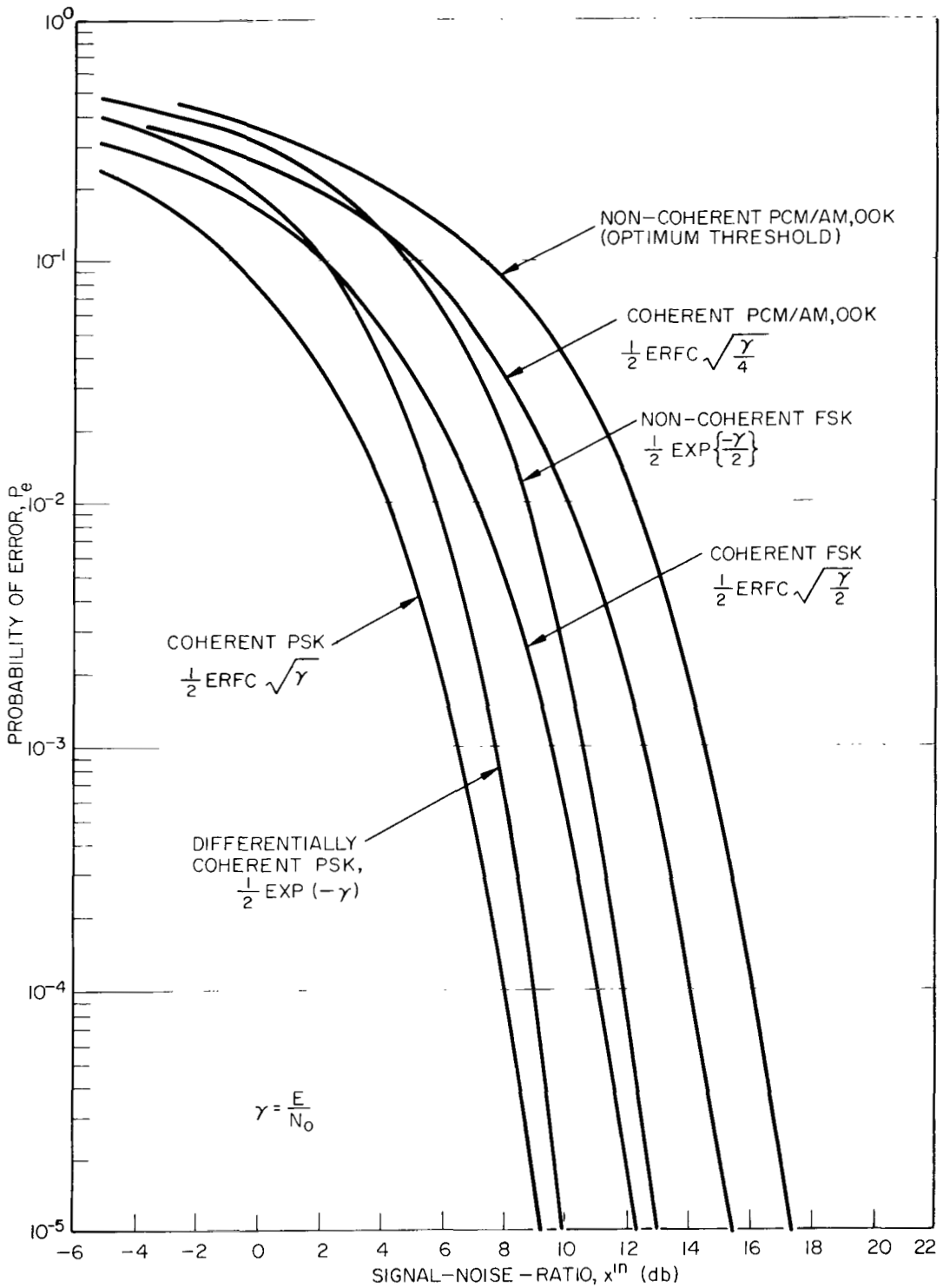

Figure 19–Probability of detection error for PCM radio communication systems.

n = number of bits per digital word, or number of bits per sample

m_f = modulation index for the wideband frequency modulation (WBFM) system

N_T = thermal noise in FM system

N_R = resultant noise in PCM system due to bit error and quantization noise

N_E = bit error noise

N_Q = quantization noise

C = total received power (carrier plus sidebands) in the channel or IF bandwidth

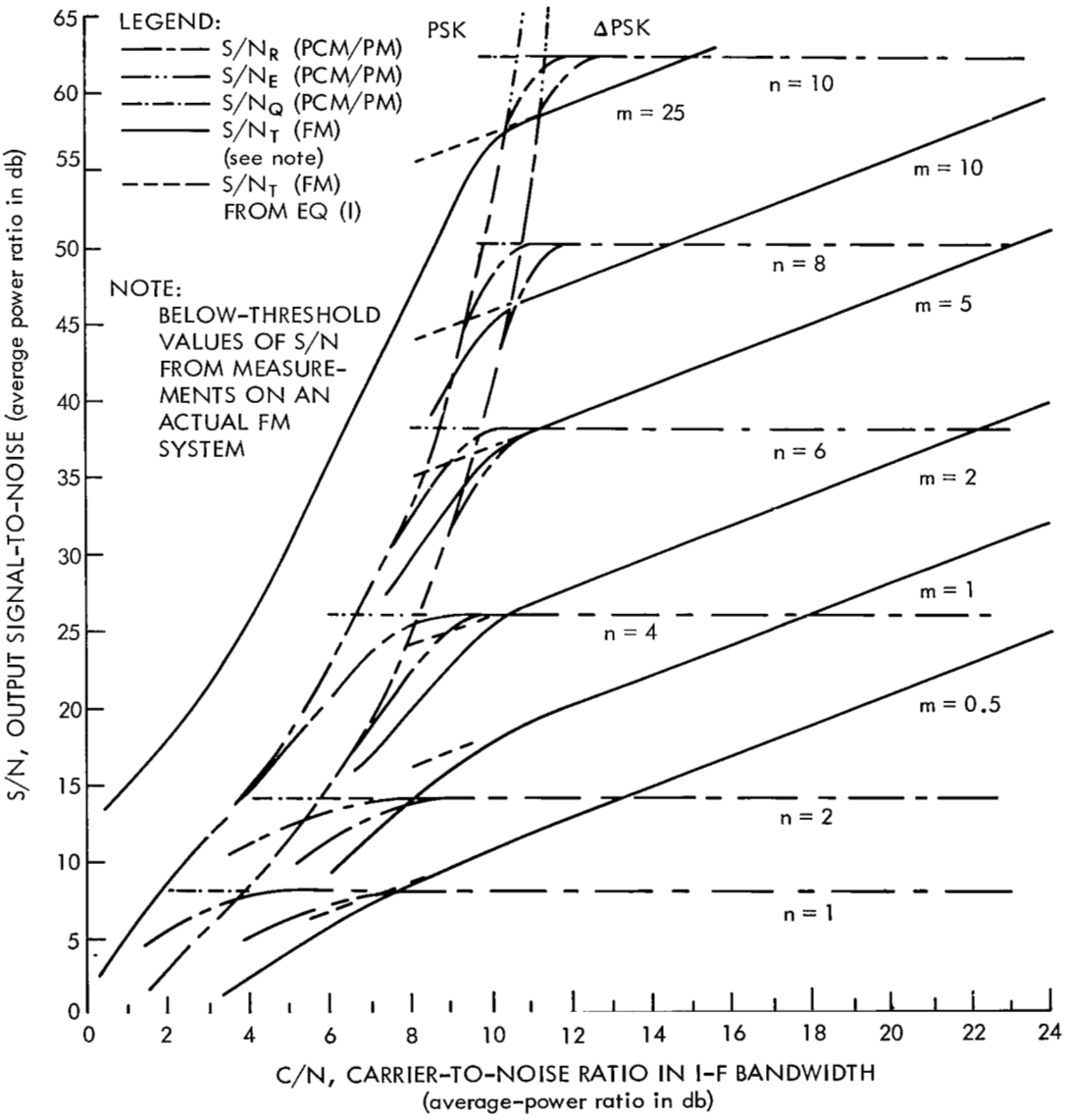

Figure 20–Output S/N ratio versus input C/N ratio (Reference 2).

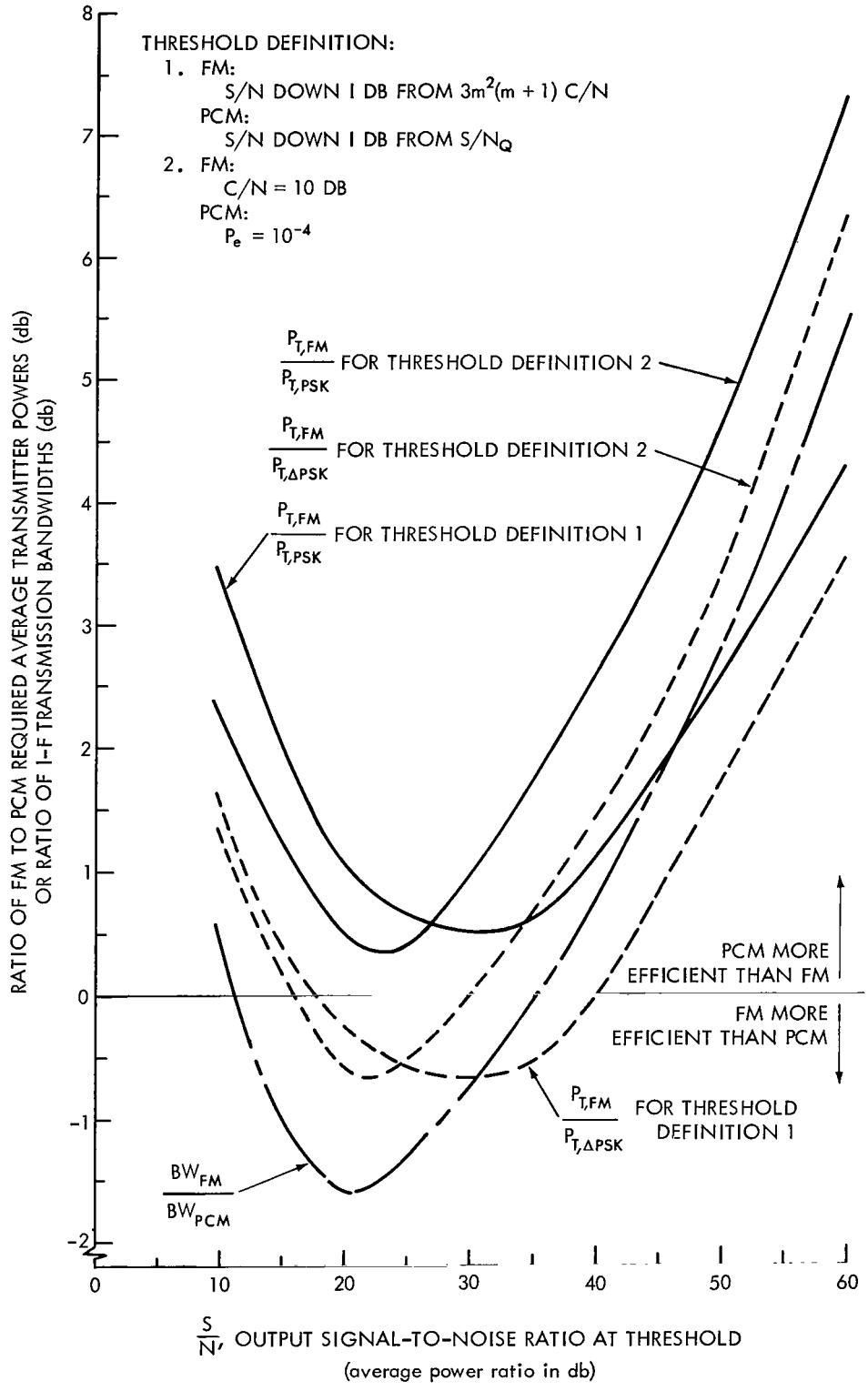

Figure 21–Relative transmitter power and IF bandwidth versus output S/N ratio at threshold, for any given baseband (f_m) (Reference 2).

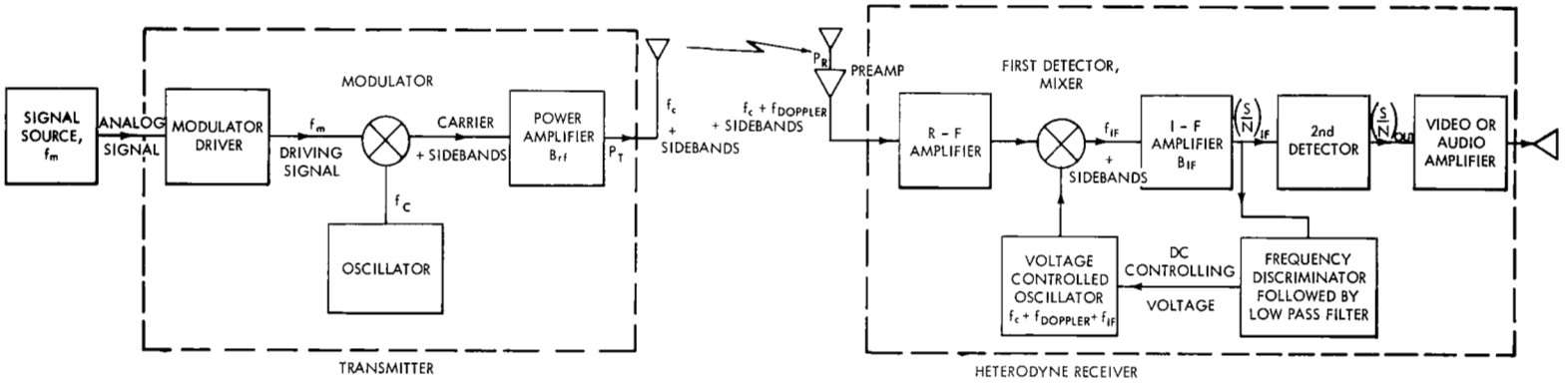

a. FUNDAMENTAL ANALOG R-F COMMUNICATION SYSTEM

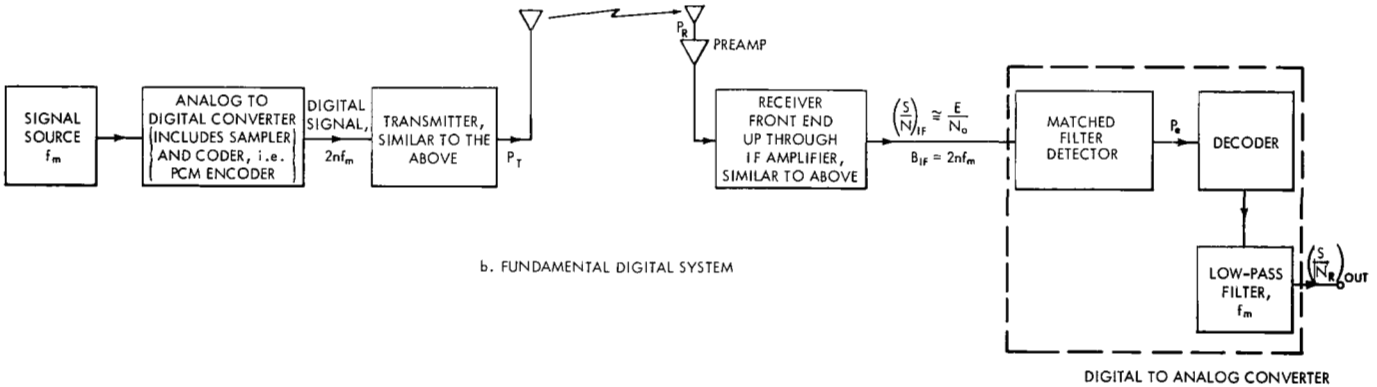

b. FUNDAMENTAL DIGITAL SYSTEM

Figure 22–Fundamental analog (RF) and digital (RF and/or optical) communication systems, block diagrams.

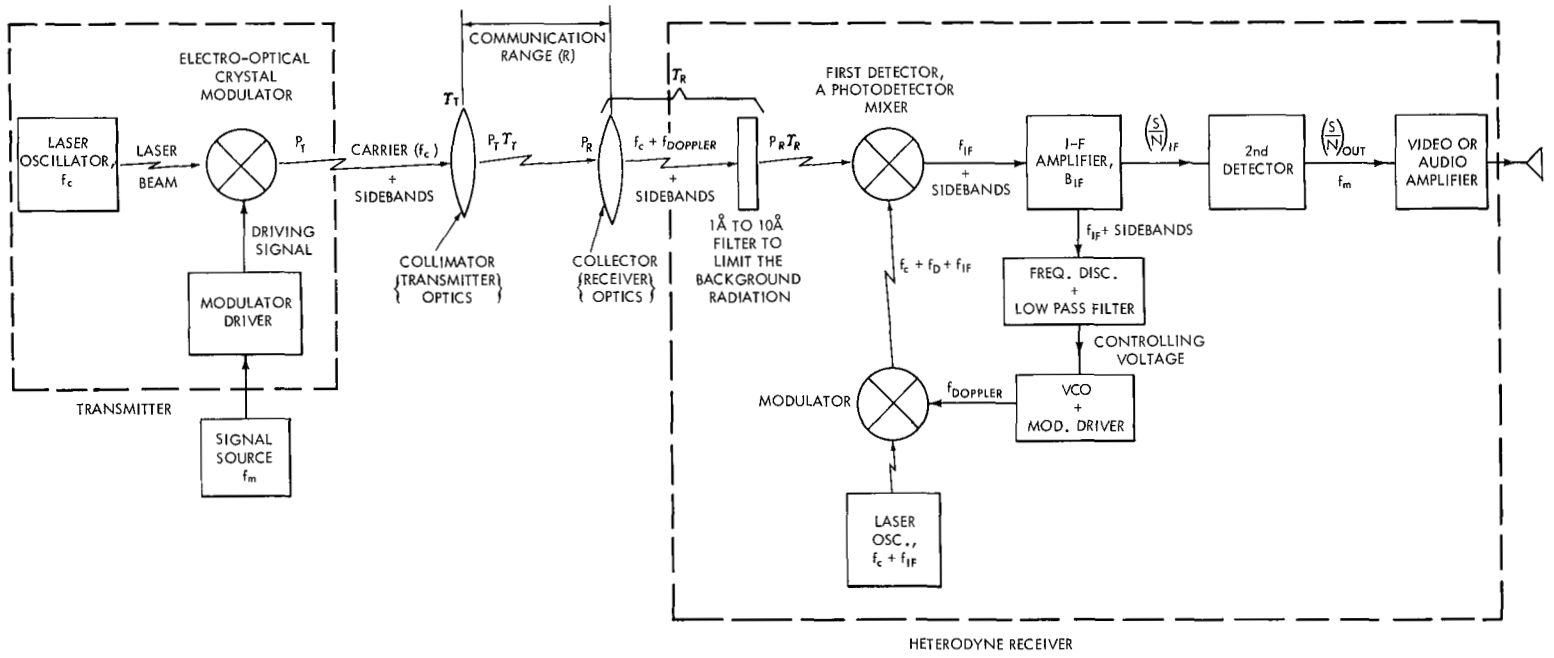

Figure 23–Fundamental optical analog communication system using heterodyne detection.

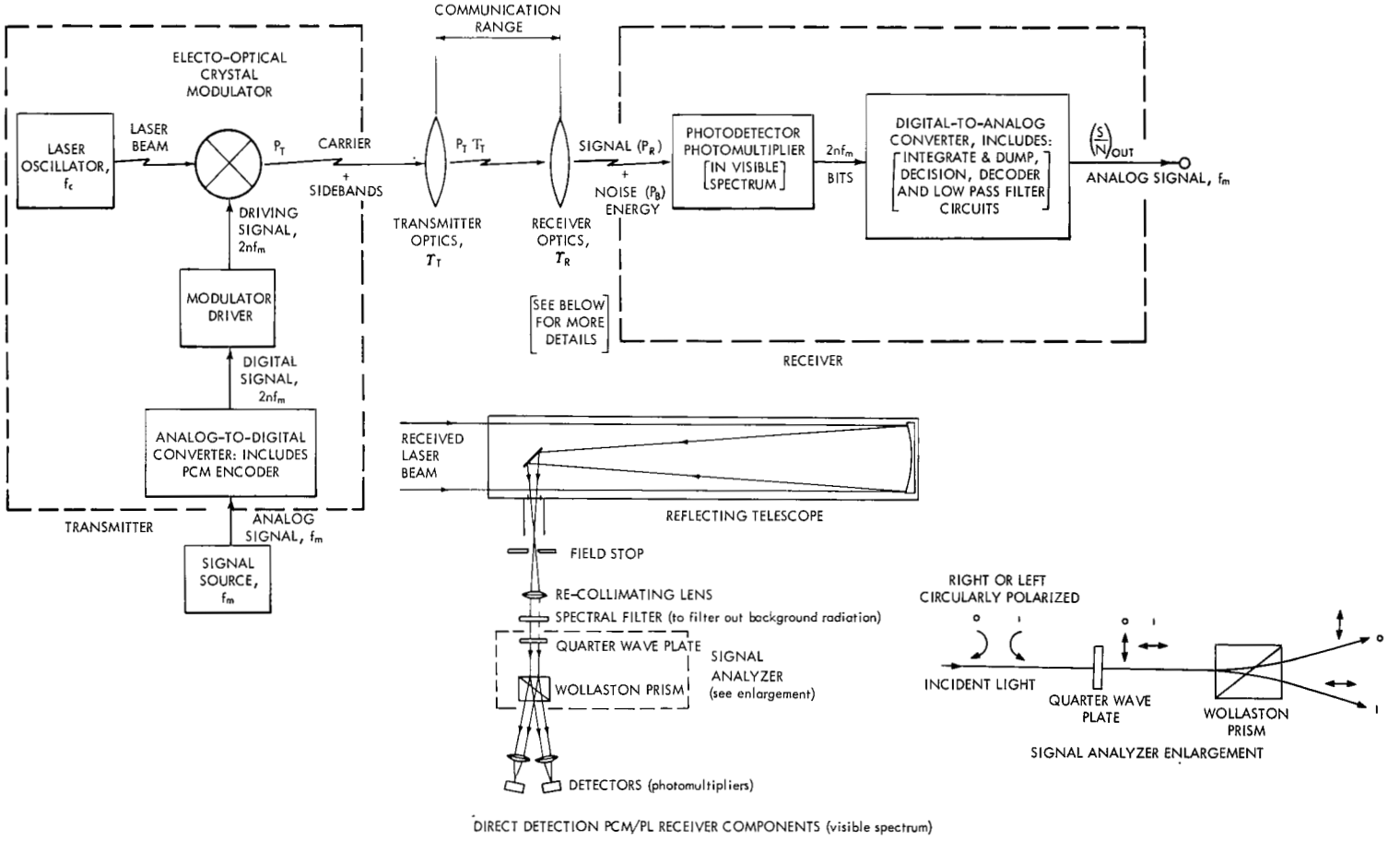

Figure 24–Optical digital communication system using direct detection.

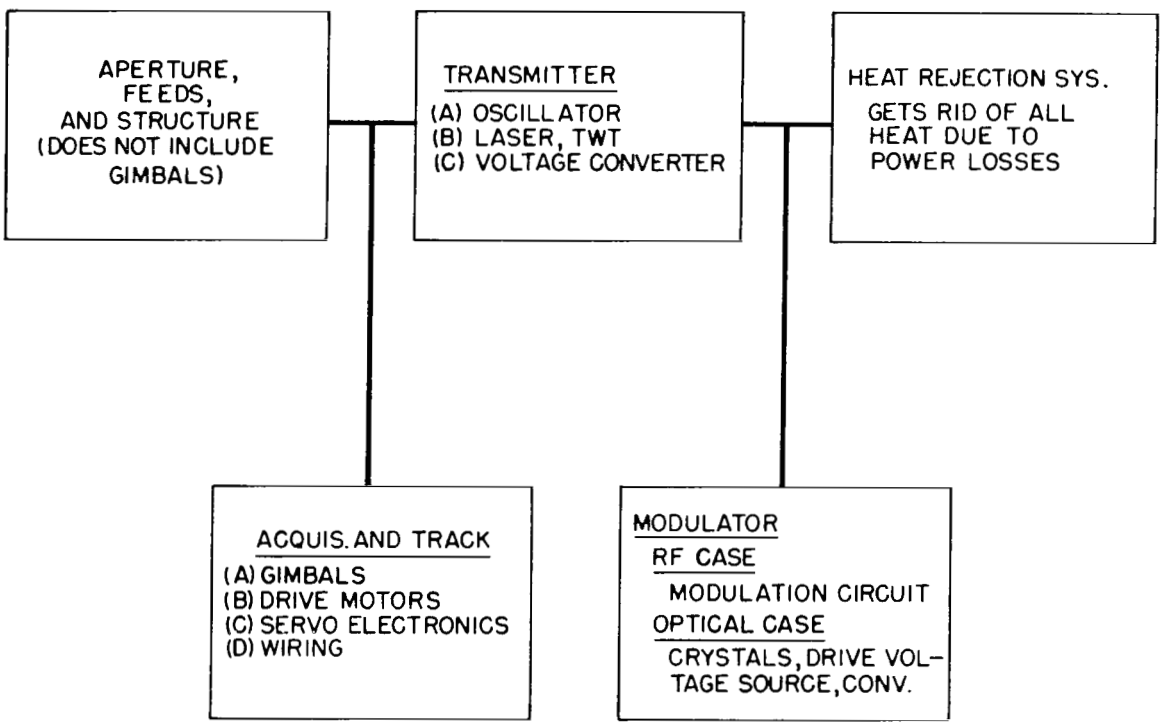

Figure B1–Block diagram showing the spacecraft communication subsystems used in the weights analysis.

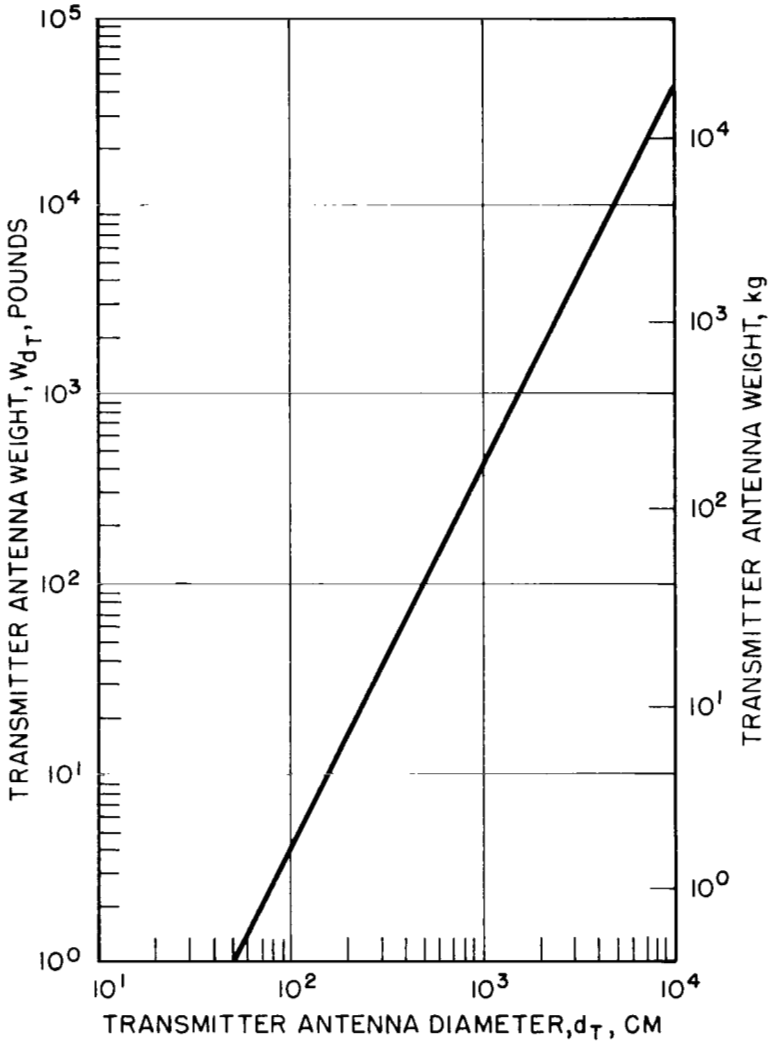

Figure B2–Spacecraft transmitter antenna weight for the 2.3- and 10-GHz systems, as a function of antenna diameter.

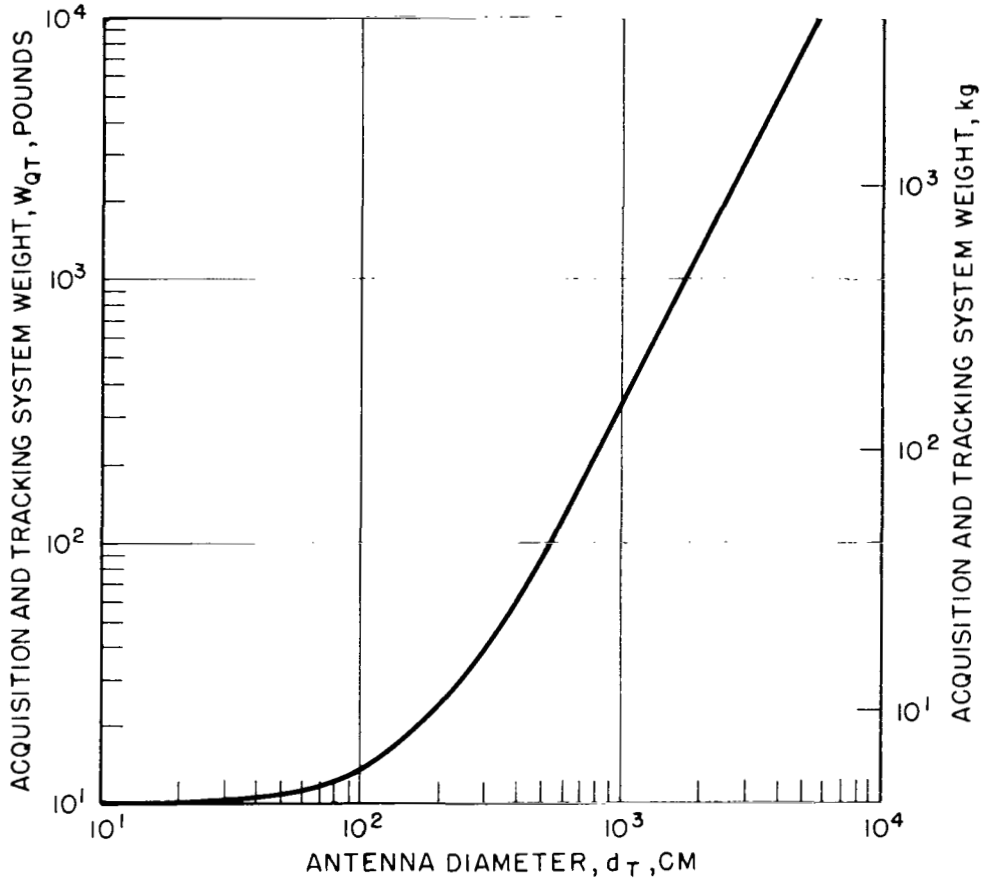

Figure B3–Spacecraft transmitter acquisition and track system weight, 2.3- and 10-GHz systems, as a function of the diameter of the transmitter antenna which it must control.

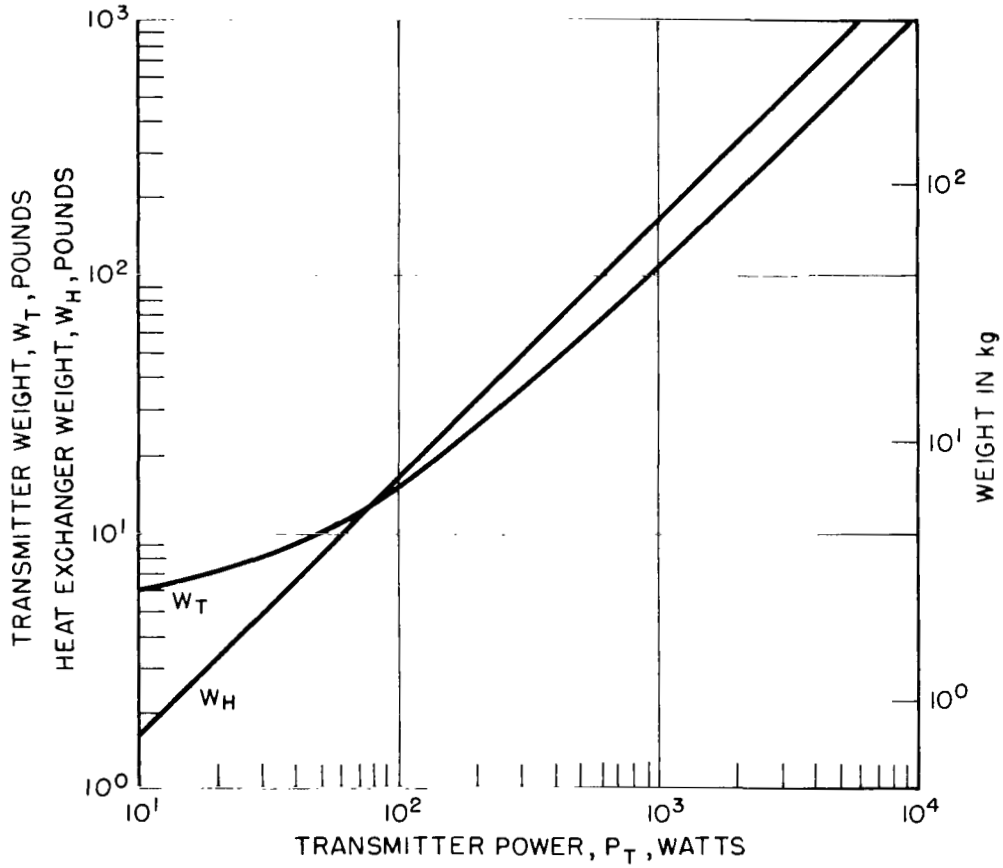

Figure B4–Weights of spacecraft transmitter (W_T) and heat dissipater (W_H), 2.3- and 10-GHz systems, as a function of transmitter power output; in the case of these microwave systems, the modulator weight is included in the W_T shown.

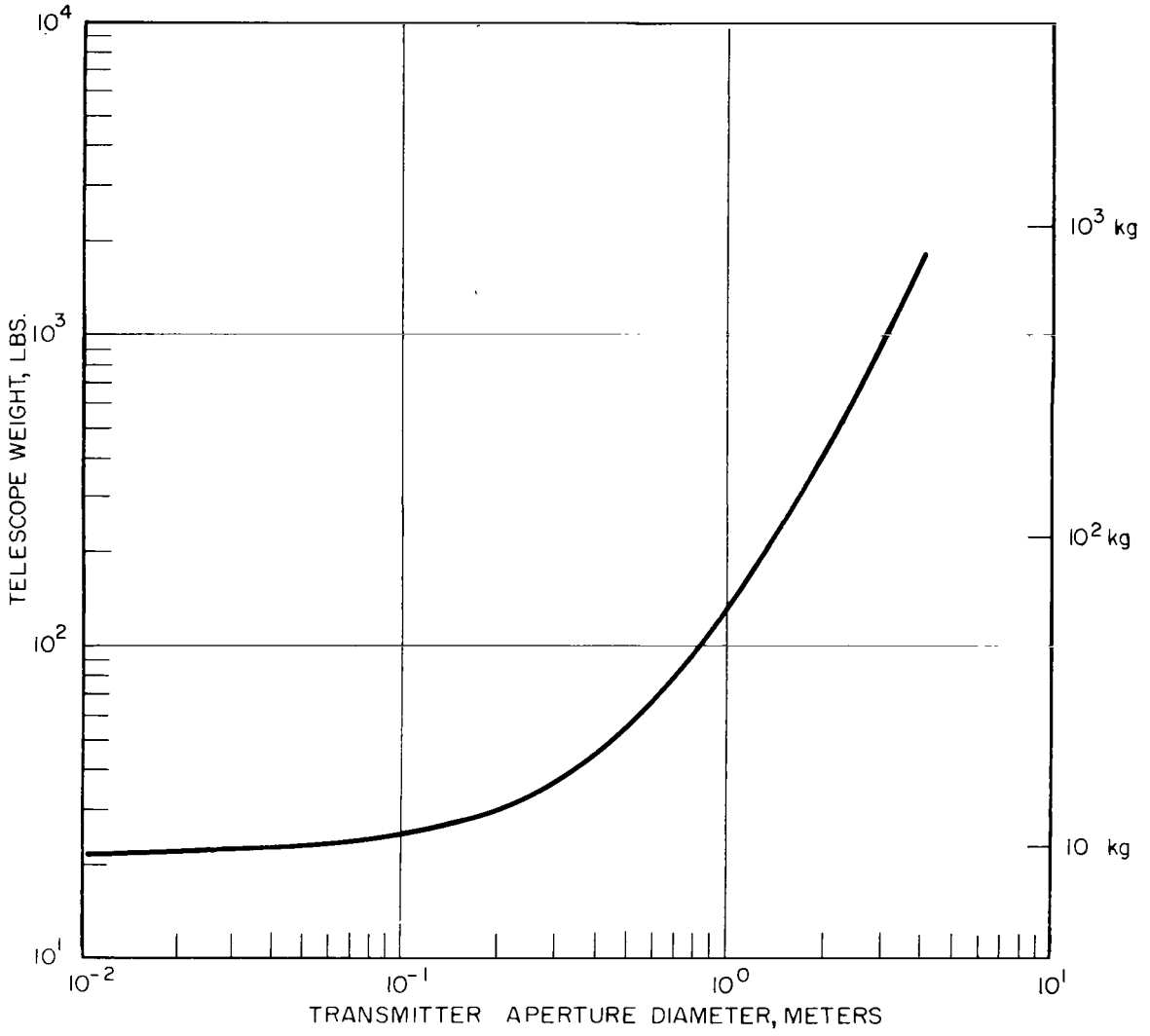

Figure B5–Spacecraft transmitter optics weight, W_{d_T} (corresponds to antenna and backup structure weight), as a function of aperture diameter.

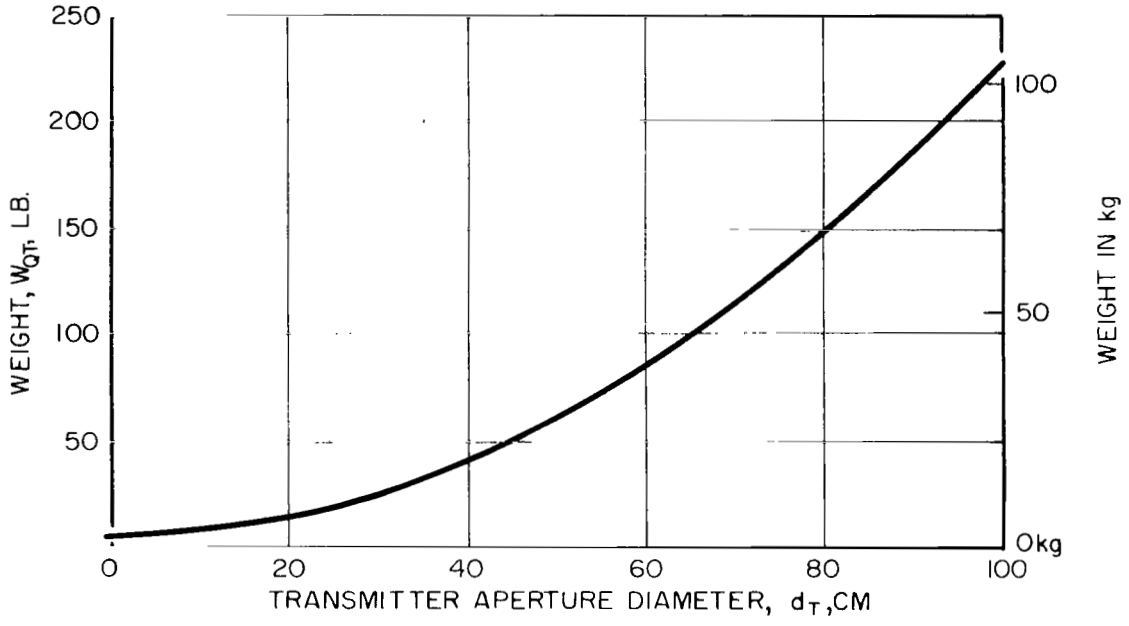

Figure B6–Weight of spacecraft optical transmitter acquisition and track system (W_{QT}), as a function of the transmitter aperture diameter which it must control.

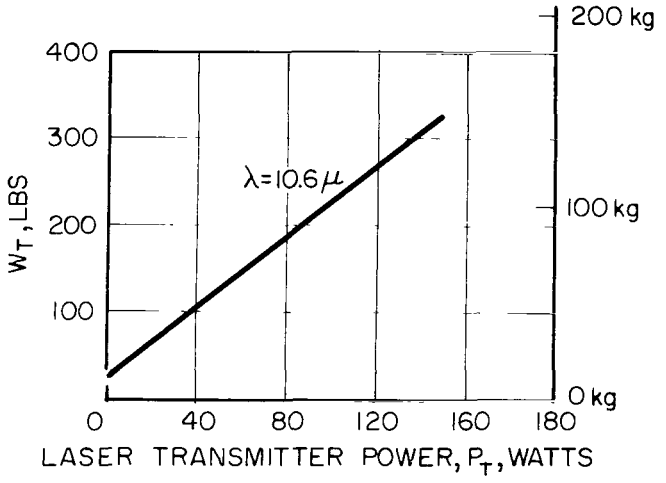

Figure B7–Weight of spaceborne CO_2 laser, W_T, as a function of transmitter output power.

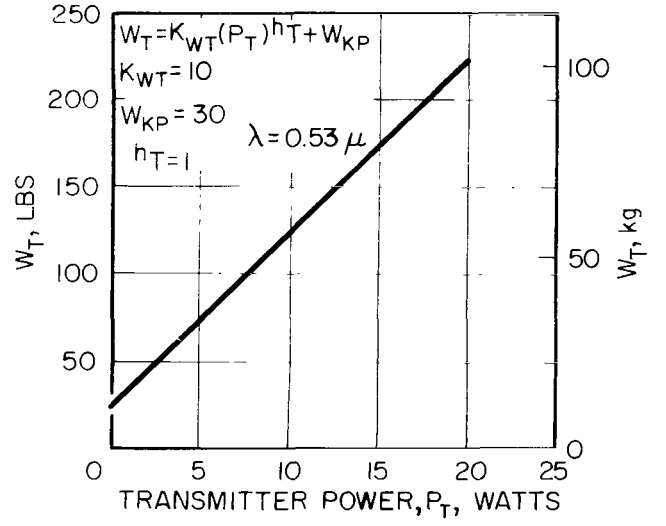

Figure B8–Weight (W_T) of spaceborne Nd^{3+} YAG laser with lithium niobate frequency doubler, as a function of transmitter power output.

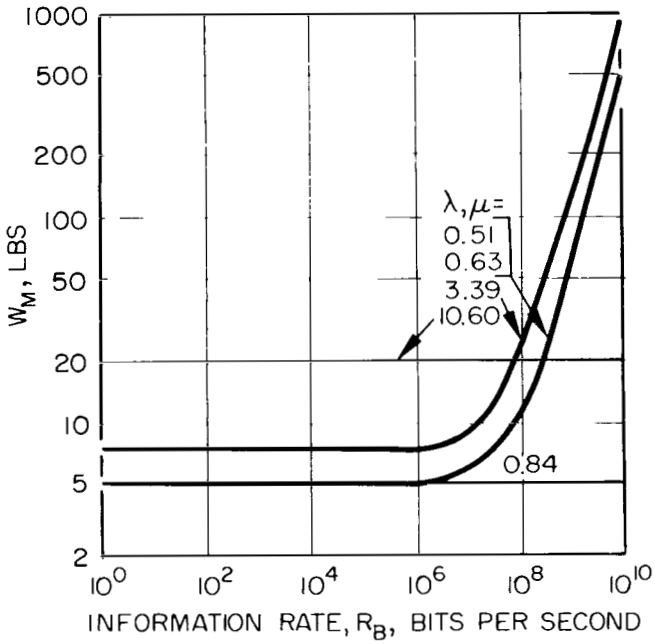

Figure B9–Spacecraft laser modulation equipment weight, W_M, as a function of information rate and carrier wavelength.

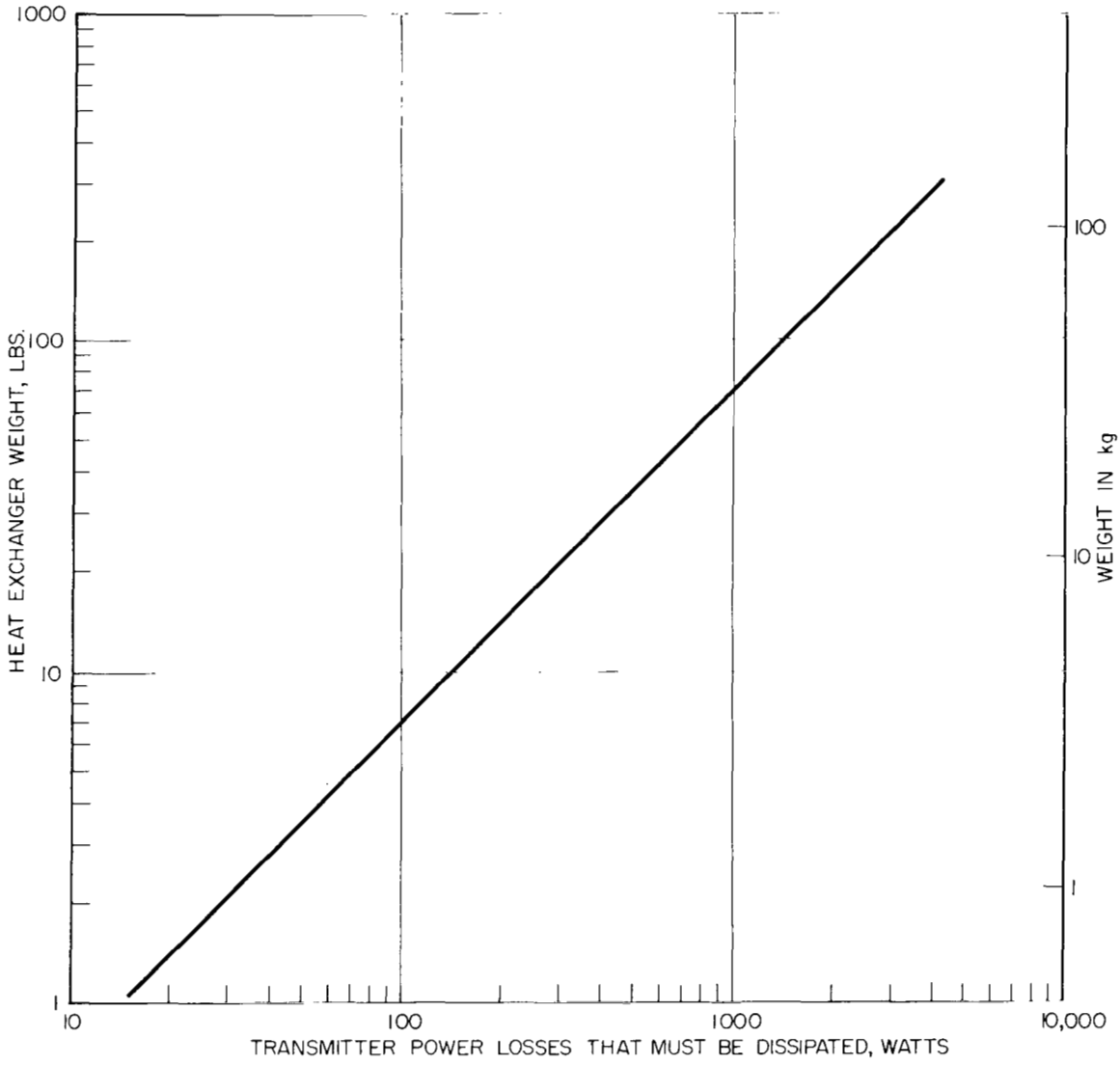

Figure B10–Heat dissipater weight as a function of wasted power.

NASA-Langley, 1969 —— 7

NATIONAL AERONAUTICS AND SPACE ADMINISTRATION
WASHINGTON, D. C. 20546

OFFICIAL BUSINESS

FIRST CLASS MAIL

POSTAGE AND FEES PAID
NATIONAL AERONAUTICS AI
SPACE ADMINISTRATION

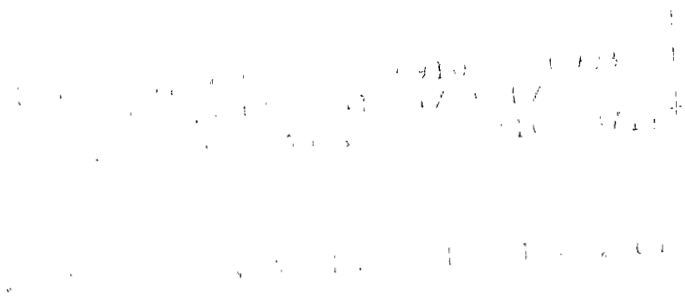

POSTMASTER: If Undeliverable (Section 15
Postal Manual) Do Not Ret

"The aeronautical and space activities of the United States shall be conducted so as to contribute . . . to the expansion of human knowledge of phenomena in the atmosphere and space. The Administration shall provide for the widest practicable and appropriate dissemination of information concerning its activities and the results thereof."

—NATIONAL AERONAUTICS AND SPACE ACT OF 1958

NASA SCIENTIFIC AND TECHNICAL PUBLICATIONS

TECHNICAL REPORTS: Scientific and technical information considered important, complete, and a lasting contribution to existing knowledge.

TECHNICAL NOTES: Information less broad in scope but nevertheless of importance as a contribution to existing knowledge.

TECHNICAL MEMORANDUMS: Information receiving limited distribution because of preliminary data, security classification, or other reasons.

CONTRACTOR REPORTS: Scientific and technical information generated under a NASA contract or grant and considered an important contribution to existing knowledge.

TECHNICAL TRANSLATIONS: Information published in a foreign language considered to merit NASA distribution in English.

SPECIAL PUBLICATIONS: Information derived from or of value to NASA activities. Publications include conference proceedings, monographs, data compilations, handbooks, sourcebooks, and special bibliographies.

TECHNOLOGY UTILIZATION PUBLICATIONS: Information on technology used by NASA that may be of particular interest in commercial and other non-aerospace applications. Publications include Tech Briefs, Technology Utilization Reports and Notes, and Technology Surveys.

Details on the availability of these publications may be obtained from:

SCIENTIFIC AND TECHNICAL INFORMATION DIVISION

NATIONAL AERONAUTICS AND SPACE ADMINISTRATION

Washington, D.C. 20546